FU JEN STUDIES

NATURAL SCIENCES

NO. 11 1977

CONTENTS

FU JEN UNIVERSITY

TAIPEI, TAIWAN, REPUBLIC OF CHINA

COMPLETE SURFACES IN E^3 WITH CONSTANT GAUSSIAN CURVATURE

YI-CHING YEN

1. INTRODUCTION

It was known and stated by Hilbert that there is no complete surface of negative constant Gaussian curvature in E^3 [1], and W. S. Massey has proved that complete surfaces of zero Gaussian curvature in E^3 are cylinders[2]. But we have no information about complete surfaces of positive constant Gaussian curvature in E^3. The purpose of this note is to show that a complete surface with positive constant Gaussian curvature is precisely a sphere, and to make some improvement on the theorem of Massey.

2. THE MAIN RESULTS

We give some lemmas which are necessary for the proofs of our theorems, and follow these with our conclusions.

Lemma 1. An orientable surface with $K = 0$ in E^3 is a torse or a plane.

Proof. If two principal curvatures k_1 and k_2 are such that $k_1 = k_2 = 0$ all over the points of the surface S, then Euler's theorem gives the normal curvature in any tangent direction as $k_n = k_1 \cos^2\vartheta + k_2 \sin^2\vartheta = 0$, where ϑ is the angle between the principal direction of k_1 and the arbitrary tangent direction we choose. Hence every curve through any point of S is asymptotic. This shows that S is a plane.

If either k_1 or k_2 is not zero, then $K = 0$ implies that $LN - M^2 = 0$ with $(L, N) \neq 0$. Thus the DE of asymptotic curves takes the form

$$(1) \qquad (\sqrt{L}du + \sqrt{N}dv)^2 = 0.$$

where u and v are parameters of S. Let the solution of the DE of (1) be $\phi(u, v) = \text{const}$. We take a system of asymptotic curves $\bar{u} = \phi(u, v)$ as a new parameter of S. Then $\bar{u} \in C^2$, and there exists

another parameter $\bar{v} = \psi(u, v) \in C^2$ of S. For such $\bar{u}$ and $\bar{v}$,

$$\bar{N} = \vec{U} \cdot \vec{x}_{\bar{v}\bar{v}} = -\vec{U}_{\bar{v}} \cdot \vec{x}_{\bar{v}} = 0. \tag{2}$$

Due to the fact that $\bar{u} = \text{const.}$ are asymptotic curves and also by $\bar{L}\bar{N} - \bar{M}^2 = 0$, we have

$$\bar{M} = \vec{U} \cdot \vec{x}_{\bar{u}\bar{v}} = -\vec{U}_{\bar{v}} \cdot \vec{x}_{\bar{u}} = 0, \tag{3}$$

where $\vec{U}$ is the unit normal vector field to S, and $\vec{x}$ is the position vector of S. Since

$$\vec{U} \cdot \vec{U}_{\bar{v}} = 0, \tag{4}$$

we get from (2), (3) and (4) that

$$\vec{U}_{\bar{v}} = \vec{0}. \tag{5}$$

Therefore

$$(\vec{x} \cdot \vec{U})_{\bar{v}} = \vec{x}_{\bar{v}} \cdot \vec{U} = 0, \tag{6}$$

or

$$\vec{x} \cdot \vec{U} = \text{const.} \tag{7}$$

along $\bar{v}$ curves. That is, $\bar{v}$ curves are the intersections of planes with S and are straight lines. Hence S is a ruled surface with $K = 0$ which is, by definition, a torse.

Now the theorem of Massey can be extended as follows.

Theorem 1. A complete orientable surface in E^3 with $K = 0$ is a plane or a torse.

Proof. By Lemma 1, surfaces with $K = 0$ are planes and torses, among which the complete surfaces are only planes and cylinders.

Lemma 2 (Hopf-Rinow)[3]. A complete surface for which the Gaussian curvature $K \geq \frac{1}{r^2}$, $r = \text{const.}$, is such that the distance of any pair of points in S is $\leq \pi r$. Hence S is compact, i.e., closed.

Lemma 3 (Liebmann)[4]. If S is a compact surface in E^3 with positive constant Gaussian curvature K, then S is a sphere of radius $1/\sqrt{K}$.

Thus a complete surface with positive Gaussian curvature $K = 1/r^2$ is, by Lemma 2, a compact surface, and, by Lemma 3, it is a sphere of radius r. Therefore we obtain the following main theorem:

Theorem 2. A complete surface S with Gaussian curvature $K = 1/r^2$, $r = \text{const.} > 0$, is a sphere of radius r.

REFERENCES

(1) Hilbert, D., Appendix of the fifth edition of the *Grundlagen der Geometrie*, Leipzig and Berlin, (1909).

(2) Massey, W.S., Surfaces of Gaussian curvature zero in Euclidean 3 space, *Tohoku Math. J.*, **14**, 73-79, (1962).

(3) Hopf, H., Rinow, W., Über den Begriff der vollständigen differentialgeometrischen Fläche, *Comm. Math. Helvetici*, **3**, 209-225, (1931).

(4) Liebmann, H., Über die Verbiegung der geschlossenen Flächen positiver Krümmung, *Math. Ann., Bd.* **53**, 81-112, (1900).

"I shall always consider the best guesser the best Prophet."

CICERO, *De Divinitate*

"Don't ever prophesy—unless you know."

JAMES RUSSEL LOWELL,
The Biglow Papers.

APPROXIMATE IDENTITIES IN NORMED ALGEBRAS

TSING-JEN HO

ABSTRACT

The notion of approximate identities has long been used in harmonic analysis and has become a basic tool in functional analysis. Some uncertainty concerning this notion still exists. To clarify this, a general definition of boundedness is introduced and it is proved that a weak approximate identity bounded in the operator norm is a strong approximate identity. The relationship, in terms of possessing approximate identities, between the closed two-sided ideals of two Banach algebras is also studied.

Throughout this paper $(A, \|\cdot\|)$ will denote a normed algebra, and $\|\cdot\|_l$ and $\|\cdot\|_r$ will denote, respectively, the left and right operator norms on A, defined by

$$\|f\|_l = \sup \{\|fg\| \mid g \in A \text{ and } \|g\| \leq 1\}$$

and

$$\|f\|_r = \sup \{\|gf\| \mid g \in A \text{ and } \|g\| \leq 1\} \qquad \forall f \in A.$$

1. APPROXIMATE IDENTITIES

Burnham[2] [Theorem 1.2] has pointed out that every proper A-Segal algebra has no bounded right weak approximate identity, and yet Reiter[4] [§8, Proposition 1] proved that every Segal algebra has a left approximate identity bounded in the L^1-norm. This suggests to us that there is needed a general notion of boundedness of (weak) approximate identities. With this tool we can generalize or improve some results obtained by Altman[1] [Lemma 2.3], Dixon[3] [Proposition 4.3], and Reiter[4] [§7, Lemmas 1, 3].

Definition 1.1. Let U be a subset of A.

(i) U is called a left (resp. right, two-sided) weak approximate identity for A if, given any $f \in A$ and $\varepsilon > 0$, $\exists\, u \in U$ such that

$$\|uf - f\| < \varepsilon \text{ (resp. } \|fu - f\| < \varepsilon, \|uf - f\| < \varepsilon \text{ and } \|fu - f\| < \varepsilon).$$

(ii) U is called a left (resp. right, two-sided) approximate identity for A if, given any finite set $F \subset A$ and $\varepsilon > 0$, $\exists\, u \in U$ such that, $\forall\, f \in F$,

$$\|uf - f\| < \varepsilon \text{ (resp. } \|fu - f\| < \varepsilon, \|uf - f\| < \varepsilon \text{ and } \|fu - f\| < \varepsilon).$$

(iii) U is called a left (resp. right, two-sided) strong approximate identity for A if, given any compact set $K \subset A$ and $\varepsilon > 0$, $\exists\, u \in U$ such that, $\forall\, f \in K$,

$$\|uf - f\| < \varepsilon \text{ (resp. } \|fu - f\| < \varepsilon, \|uf - f\| < \varepsilon \text{ and } \|fu - f\| < \varepsilon).$$

Definition 1.2. Let p and q be two non-negative functions on A.

(i) A set $U \subset A$ is said to be bounded in p if $\exists\, C > 0$ such that $p(u) \leq C \quad \forall\, u \in U$.

If $p = \|\cdot\|$, then U is simply said to be bounded.

(ii) p is said to be weaker than q, or q is said to be stronger than p if $\exists\, M > 0$ such that

$$p(f) \leq M \cdot q(f) \qquad \forall\, f \in A.$$

In symbols we write $p < q$ or $q > p$.

(iii) p and q are said to be equivalent if $p < q$ and $q < p$. In symbols we write $p \sim q$.

Lemma 1.3. If U is a left (resp. right) weak approximate identity for A which is bounded in $\|\cdot\|_l$ (resp. $\|\cdot\|_r$), then U is a left (resp. right) approximate identity for A.

Proof. Let any finite set $F \subset A$ and $\varepsilon > 0$ be given, then by Reiter[4] [§7, Lemma 1] $\exists\, v \in A$ such that

$$\|vf - f\| < \varepsilon/2\,(M+1) \qquad (f \in F),$$

where M is a constant such that

$$\|u\|_l \leq M \quad (u \in U).$$

Now choose $u \in U$ such that

$$\|uv - v\| < \varepsilon/2 \cdot \max\{\|f\| \mid f \in F\}.$$

Then $\forall f \in F$ we have

$$\begin{aligned} \|uf - f\| &\leq \|u(f - vf)\| + \|(uv - v)f\| + \|vf - f\| \\ &\leq \|u\|_l \|f - vf\| + \|uv - v\| \|f\| + \|vf - f\| \\ &< \varepsilon. \end{aligned}$$

Therefore U is a left approximate identity for A.

Lemma 1.4. Let U and V be respectively left and right approximate identities for A. If either V is bounded in $\|\cdot\|_l$ or U is bounded in $\|\cdot\|_r$, then $V \circ U$ is a two-sided approximate identity for A.

Proof. Consider e.g. V to be bounded in $\|\cdot\|_l$, i.e. $\exists\, M > 0$ such that

$$\|v\|_l \leq M \qquad (v \in V).$$

Let any finite set $F \subset A$ and $\varepsilon > 0$ be given, then $\exists\, u \in U$ such that

$$\|uf - f\| < \varepsilon/(M+1) \qquad (f \in F).$$

Now choose $v \in V$ such that

$$\|fv - f\| < \varepsilon/(\|u\| + 1) \qquad (f \in F).$$

Then $\forall f \in F$ we have

$$\begin{aligned} \|(v \circ u)f - f\| &= \|(v + u - vu)f - f\| \\ &\leq \|v(f - uf)\| + \|uf - f\| \\ &\leq \|v\|_l \|f - uf\| + \|uf - f\| \\ &< \varepsilon \end{aligned}$$

and

$$\begin{aligned} \|f(v \circ u) - f\| &\leq \|fv - f\| + \|(f - fv)u\| \\ &< \varepsilon. \end{aligned}$$

Therefore $V \circ U$ is a two-sided approximate identity for A.

Lemma 1.5. If U is a two-sided weak approximate identity for A which is bounded in $\|\cdot\|_l$ and $\|\cdot\|_r$, then U is a two-sided approximate identity for A.

Proof. It follows from Lemmas 1.3 and 1.4 that A has a two-sided approximate identity. Let any finite set $F \subset A$ and $\varepsilon > 0$ be given, then $\exists\, v \in A$ such that

$$\|vf - f\| < \varepsilon/2(M+1)$$

and

$$\|fv - f\| < \varepsilon/2(M+1) \qquad (f \in F),$$

where M is a constant such that

$$\|u\|_l \leq M \text{ and } \|u\|_r \leq M \qquad (u \in U).$$

Now choose $u \in U$ such that

$$\|uv - v\| < \varepsilon/2 \cdot \max\{\|f\| \mid f \in F\}$$

and

$$\|vu - v\| < \varepsilon/2 \cdot \max\{\|f\| \mid f \in F\}.$$

Then, by the same argument used in the proof of Lemma 1.3, $\forall f \in F$ we have

$$\|uf - f\| < \varepsilon \text{ and } \|fu - f\| < \varepsilon.$$

Therefore U is a two-sided approximate identity for A.

Theorem 1.6. If U is a left (resp. right, two-sided) weak approximate identity for A which is bounded in $\|\cdot\|_l$ (resp. $\|\cdot\|_r$, $\|\cdot\|_l$ and $\|\cdot\|_r$), then U is a left (resp. right, two-sided) strong approximate identity for A.

Proof. Let any compact set $K \subset A$ and $\varepsilon > 0$ be given. Define

$$B(f, \varepsilon/2(M+1)) = \{g \in A \mid \|g - f\| < \varepsilon/2(M+1)\} \quad (f \in A),$$

where M is a constant such that

$$\|u\|_l \leq M \quad (u \in U).$$

Since K is compact, $\exists$ finitely many elements $f_1, \ldots, f_n \in A$ such that

$$K \subset \bigcup_{i=1}^{n} B(f_i, \varepsilon/2(M+1)).$$

By Lemma 1.3 $\exists\, u \in U$ such that

$$\|uf_i - f_i\| < \varepsilon/2 \quad (i = 1, \ldots, n).$$

Then, for any given $f \in K$, $\exists$ some i $(1 \leq i \leq n)$ such that

$$f \in B(f_i, \varepsilon/2(M+1))$$

and then

$$\begin{aligned}\|uf-f\| &\leq \|u(f-f_i)\| + \|uf_i - f_i\| + \|f_i - f\| \\ &< \mathrm{M}\cdot\varepsilon/2(\mathrm{M}+1) + \varepsilon/2 + \varepsilon/2(\mathrm{M}+1) \\ &= \varepsilon.\end{aligned}$$

Thus the proof is complete.

Corollary 1.7. If U is a bounded left (resp. right, two-sided) weak approximate identity for A, then U is a left (resp. right, two-sided) strong approximate identity for A.

Proof. Since $\|\cdot\|$ is stronger than $\|\cdot\|_r$ and $\|\cdot\|_l$, our corollary follows from Theorem 1.6.

Definition 1.8. Let p be a non-negative function on A, J a closed two-sided ideal of A, and π the canonical homomorphism of A onto A/J. Define a non-negative function $\bar{p}$ on A/J by

$$\bar{p}(\pi f) = \inf\{p(f+g) \mid g\in \mathrm{J}\} \qquad (f\in \mathrm{A}).$$

Such $\bar{p}$ is called the quotient function (on A/J) of p.

If $p = \|\cdot\|$, then $\bar{p}$ is the quotient norm on A/J. It is clear that

$$p > \|\cdot\|_l \Rightarrow \bar{p} > \|\cdot\|_l^- > \text{the left operator norm on A/J.}$$

Theorem 1.9. Let p be an algebra-semi-norm on A which is stronger than $\|\cdot\|_l$ (resp. $\|\cdot\|_r$), and let J be a closed two-sided ideal of A. If J and A/J have left (resp. right) weak approximate identities bounded in p and $\bar{p}$ respectively, then A has a left (resp. right) strong approximate identity bounded in p.

Proof. Let π be the canonical homomorphism of A onto A/J and C a constant such that

$$\|fg\| \leq \mathrm{C}\cdot p(f)\cdot\|g\| \quad (f, g\in \mathrm{A}).$$

Let any $f\in$ A and $\varepsilon > 0$ be given, then $\exists\ \bar{u}\in$ A/J with $\bar{p}(\bar{u}) \leq$ M (constant) such that

$$\|\bar{u}\cdot\pi f - \pi f\| < \varepsilon.$$

By the definition of $\bar{p}$, then $\exists\ v\in$ A such that

$$\pi v = \bar{u} \text{ and } p(v) \leq \bar{p}(\bar{u}) + 1 \leq \mathrm{M}+1.$$

Since $\|\pi(vf-f)\| = \|\bar{u}\cdot\pi f - \pi f\| < \varepsilon$, $\exists\ g\in$ J such that

$$\|vf - f + g\| < \varepsilon.$$

Then $\exists\ u \in J$ with $p(u) \leq N$ (constant) such that

$$\|ug - g\| < \varepsilon.$$

with $w = u \circ v$ we have

$$\begin{aligned}\|wf - f\| &= \|(vf - f + g) - u(vf - f + g) + (ug - g)\| \\ &\leq \|vf - f + g\| + C \cdot p(u) \cdot \|vf - f + g\| + \|ug - g\| \\ &< \varepsilon + CN\varepsilon + \varepsilon = (CN + 2)\varepsilon\end{aligned}$$

and

$$\begin{aligned}p(w) = p(u + v - uv) &\leq p(u) + p(v) + p(u)\,p(v) \\ &\leq N + M + 1 + N(M + 1)\end{aligned}$$

which is a constant.

Therefore A has a left weak approximate identity bounded in p. Thus by Theorem 1.6 A has a left strong approximate identity bounded in p.

For a similar result we refer the reader to Reiter[4] [§7, Lemma 2].

Corollary 1.10. Let J be a closed two-sided ideal of A. If J and A/J have bounded left (resp. right) weak approximate identities, then A has a bounded left (resp. right) strong approximate identity.

Proof. Take $p = \|\cdot\|$ in Theorem 1.9.

2. CLASSES OF TWO-SIDED IDEALS

For convenience we introduce the following notations.

Notation 2.1.

(i) $\mathcal{J}^{lw}(A)$ (resp. $\mathcal{J}^{rw}(A)$, $\mathcal{J}^{tw}(A)$) = the set of all closed two-sided ideals of A which have left (resp. right, two-sided) weak approximate identities.

(ii) $\mathcal{J}^{l}(A)$ (resp. $\mathcal{J}^{r}(A)$, $\mathcal{J}(A)$) = the set of all closed two-sided ideals of A which have left (resp. right, two-sided) approximate identities.

(iii) $\mathcal{J}^{ls}(A)$ (resp. $\mathcal{J}^{rs}(A)$, $\mathcal{J}^{ts}(A)$) = the set of all closed two-sided ideals of A which have left (resp. right, two-sided) strong approximate identities.

Notation 2.2. Let p be a non-negative function on A.

(i) $\mathcal{G}_p^{lw}(A)$ (resp. $\mathcal{G}_p^{rw}(A)$, $\mathcal{G}_p^{tw}(A)$) = the set of all closed two-sided ideals of A which have left (resp. right, two-sided) weak approximate identities bounded in p.

(ii) $\mathcal{G}_p^{l}(A)$ (resp. $\mathcal{G}_p^{r}(A)$, $\mathcal{G}_p^{t}(A)$) = the set of all closed two-sided ideals of A which have left (resp. right, two-sided) approximate identities bounded in p.

(iii) $\mathcal{G}_p^{ls}(A)$ (resp. $\mathcal{G}_p^{rs}(A)$, $\mathcal{G}_p^{ts}(A)$) = the set of all closed two-sided ideals of A which have left (resp. right, two-sided) strong approximate identities bounded in p.

Theorem 2.3.

(i) Each class defined in Notation 2.1 contains the intersection of any finitely many closed two-sided ideals in it. The statement also holds for each class defined in Notation 2.2 if p is an algebra-semi-norm on A.

(ii) If $p > \|\cdot\|_l$, then $\mathcal{G}_p^{lw}(A) = \mathcal{G}_p^{l}(A) = \mathcal{G}_p^{ls}(A)$.

(iii) If $p > \|\cdot\|_l$ or $\|\cdot\|_r$ and p is an algebra-semi-norm on A, then $\mathcal{G}_p^{lw}(A) \cap \mathcal{G}_p^{rw}(A) = \mathcal{G}_p^{tw}(A)$ and $\mathcal{G}_p^{l}(A) \cap \mathcal{G}_p^{r}(A) = \mathcal{G}_p^{t}(A)$.

Proof. (i) Consider e. g. I_1, $I_2 \in \mathcal{G}_p^{rw}(A)$, where p is an algebra-semi-norm on A. Let $f \in I_1 \cap I_2$ and $\varepsilon > 0$ be given, then $\exists\, u_1 \in I_1$ with $p(u_1) \leq C_1$ (constant) and $u_2 \in I_2$ with $p(u_2) \leq C_2$ (constant) such that

$$\|fu_1 - f\| < \varepsilon/2 \text{ and } \|fu_2 - f\| < \varepsilon/2\,\|u_1\|.$$

With $u = u_2u_1$ we have $u \in I_1 \cap I_2$, $p(u) \leq p(u_2)\,p(u_1) \leq C_2C_1$ which is a constant, and $\|fu - f\| \leq \|fu_2 - f\|\,\|u_1\| + \|fu_1 - f\| < \varepsilon$. Therefore $I_1 \cap I_2 \in \mathcal{G}_p^{rw}(A)$. The general case now follows by induction.

(ii) If $p > \|\cdot\|_l$, then p is also stronger than the left operator norm on any subalgebra of A. Thus (ii) follows from Theorem 1.6.

(iii) By Lemma 1.4 and its analogue.

Lemma 2.4. Let A and A′ be two Banach algebras and T a bounded homomorphism of A onto A′. If a closed left (resp. right) ideal I of A has a right (resp. left) weak approximate identity bounded in $\|\cdot\|_r$ (resp. $\|\cdot\|_l$), then $I' = T(I)$ is a closed left (resp. right) ideal of A′.

Proof. Let $J = \{f \in A \mid Tf = 0\}$, then by the open mapping theorem we may assume without loss of generality that the A′-norm $\|\cdot\|'$ is defined by

$$\|Tf\|' = \inf\{\|f+g\| \mid g\in J\} \qquad (f\in A).$$

Since I' is algebraically isomorphic to $I/J\cap I$ and $I/J\cap I$ is complete under the quotient norm induced by I and $J\cap I$, I' is also complete under $\|\cdot\|''$ defined by

$$\|Tf\|'' = \inf\{\|f+g\| \mid g\in J\cap I\} \qquad (f\in I).$$

We will now show that $\|\cdot\|''\sim\|\cdot\|'$ on I' as follows:

Let $f\in I$ and $g\in J$ be given, then $\exists$ a sequence $\{u_n\}\subset I$ with $\|u_n\|_r \leq M$ (constant) such that

$$\|f-fu_n\|\to 0.$$

Noting that $gu_n\in J\cap I$, then we have

$$\begin{aligned}\|Tf\|'' &\leq \|f+gu_n\| \\ &\leq \|f-fu_n\| + \|f+g\|\,\|u_n\|_r \\ &\leq \|f-fu_n\| + M\|f+g\| \\ &\to M\|f+g\|.\end{aligned}$$

Therefore $\|Tf\|''\leq M\|f+g\|$ $(g\in J)$ and therefore $\|Tf\|''\leq M\|Tf\|'$. On the other hand it is clear that $\|Tf\|'\leq\|Tf\|''$. Therefore $\|\cdot\|''\sim\|\cdot\|'$ on I'.

Thus I' is complete under $\|\cdot\|'$, so I' is closed in A'.

Theorem 2.5. Let A and A' be two Banach algebras, T a bounded homomorphism of A onto A', and p an algebra-semi-norm on A which is stronger than $\|\cdot\|_l$. Then we have

$$I\in\mathscr{I}_p^l(A)\Rightarrow T(I)\in\mathscr{I}_{\bar{p}}^l(A'),$$

where $\bar{p}$ (cf. Definition 1.8) is defined by

$$\bar{p}(Tf) = \inf\{p(f+g) \mid g\in\ker T\} \qquad (f\in A).$$

Conversely if $\ker T\in\mathscr{I}_p^l(A)$, then we have

$$I'\in\mathscr{I}_{\bar{p}}^l(A')\Rightarrow T^{-1}(I')\in\mathscr{I}_p^l(A).$$

Proof. The first part of this theorem follows from Lemma 2.4 and the definition of $\bar{p}$. The second part follows from Theorem 1.9 and the fact: $T^{-1}(I')/\ker T\cong I'$.

Corollary 2.6. Let A, A′ be two Banach algebras and T a bounded homomorphism of A onto A′.

(i) If $I \in \mathcal{G}^l_{\|\cdot\|}(A)$, then $T(I) \in \mathcal{G}^l_{\|\cdot\|'}(A')$.

(ii) If $\ker T \in \mathcal{G}^l_{\|\cdot\|}(A)$ and $I' \in \mathcal{G}^l_{\|\cdot\|'}(A')$, then $T^{-1}(I') \in \mathcal{G}^l_{\|\cdot\|}(A)$.

Proof. Take $p = \|\cdot\|$ in Theorem 2.5 and notice that $\|\cdot\|^- \sim \|\cdot\|'$ on A.

We remark that Theorem 2.3(ii), Theorem 2.5, and Corollary 2.6 all have right-hand and two-sided versions.

REFERENCES

(1) Altman, M., Contractors, approximate identities and factorization in Banach algebras, *Pac. J. Math.* 48, 323-334, (1973).

(2) Burnham, J. T., Closed ideals in subalgebras of Banach algebra, *Proc. Amer. Math. Soc.* **32**, 551-555, (1972).

(3) Dixon, P. G., Approximate identities in Banach algebras, *Proc. London Math. Soc. 3*, **26**, 485-496, (1973).

(4) Reiter, H., *L^1-algebras and Segal Algebras, Lecture notes in Math.* V. 231, Springer-Verlag, Berlin, (1971).

AN ELECTRIC FIELD PARADOX

The electric field inside a hollow conductor is zero...or is it? When a charge is placed inside the hollow conductor, it experiences a force which draws it to the interior surface.

The resolution of this paradox underlines the necessity of mapping electric fields with vanishingly small test charges.

J. HIGBIE

STUDY OF MOLECULAR PROPERTIES THROUGH RAYLEIGH SCATTERING

FONG-JEN LIN, HSIN-CHIAO OU-YANG
HSIOU-YUNG LUE, JENN-FARN WANG

1. INTRODUCTION

The observation of molecular light scattering has been considered one of the most efficient methods for studying the characteristics of molecules. The light scattering laboratory was built up by Dr. G. Breuer of Hamburg University during his 4-year stay at Fu Jen University (1971–74). In this laboratory a laser is used as the light source, the optical path is arranged according to the "modified" compensation method, and the lock-in amplification method is employed in the electronic detecting system. Since the summer of 1975 we have worked on the techniques of determination of molecular weights, Rayleigh factors, depolarization factors and indices of refraction of gases by using the Rayleigh scattering method. The results have been satisfactory. The determination of the principal polarizabilities of molecules with low vapor pressure is difficult. A method has been developed by our group for determining the principal polarizabilities of dipolar molecules which can be dissolved in solution. At present this group is engaged in studying the properties of macromolecules such as polymers and biomacromolecules.

2. BASIC THEORY

A. Rayleigh Scattering

If we consider an isolated optically isotropic and nonabsorbing particle which is small compared with the wavelength of light falling on it, and if there are no interactions between the particles or molecules, then the scattering of light by molecules can be considered in terms of radiation by dipoles associated with molecules, which are induced by the linearly polarized incident light. The Rayleigh factor is defined as

$$R = \frac{I_s r^2}{I_0 V} = \frac{F_s}{F_0 \Omega l},$$

where I_s, I_0 are scattered and incident light intensity respectively, V is scattering volume, and r is the distance from scattering volume to detector. F_s, F_0 are scattering and incident flux respectively, l is the effective scattering length, and Ω is the solid angle of the cone of scattered light accepted by the detector. For isotropic molecules, the Rayleigh theory leads to the result[1]

$$R_{is} = \frac{16\pi^4}{\lambda^4} b^2 N_L, \tag{1}$$

where R_{is} is the isotropic Rayleigh factor measured at a scattering angle of 90°. N_L is the number of molecules per unit volume, λ is the wavelength of light in vacuum, b is the polarizability of the molecule.

The isotropic light scattering by a dense medium may be considered to be the result of inhomogeneity of the thermal fluctuation, which produces a fluctuation in the optical dielectric constant (ε) in a small volume element V of the medium. According to the theory of Einstein, if the incident light is polarized, then the isotropic part of the Rayleigh factor can be expressed as

$$R_{is} = \frac{\pi^2}{\lambda^4} V \overline{\Delta\varepsilon^2}. \tag{2}$$

We assume that $\Delta\varepsilon$ is a function of two independent thermodynamic variables, for example, ρ and T, and if we consider a solution, then it is also a function of the concentration c of its components:

$$\Delta\varepsilon(\rho, T, c) = \left(\frac{\partial\varepsilon}{\partial\rho}\right)_{T,c} \Delta\rho + \left(\frac{\partial\varepsilon}{\partial T}\right)_{\rho,c} \Delta T + \left(\frac{\partial\varepsilon}{\partial c}\right)_{T,\rho} \Delta c. \tag{3}$$

If the fluctuations of density, temperature, and concentration are statistically independent, we get

$$\overline{\Delta\varepsilon^2(\rho, T, c)} = \left(\frac{\partial\varepsilon}{\partial\rho}\right)^2_{T,c} \overline{\Delta\rho^2} + \left(\frac{\partial\varepsilon}{\partial T}\right)^2_{\rho,c} \overline{\Delta T^2} + \left(\frac{\partial\varepsilon}{\partial c}\right)^2_{T,\rho} \overline{\Delta c^2}. \tag{4}$$

The first two components in Eq.(4) characterize the isotropic scat-

tering in a pure liquid, and the last term is characteristic of a solution.

The isotropic Rayleigh factor can be obtained as follows: According to the statistical mechanical theory of fluctuation[2], we have

$$\overline{(\Delta\rho)^2} = \frac{kT\beta_T\rho^2}{V}, \qquad \overline{(\Delta T)^2} = \frac{kT^2}{c_v},$$

where c_v is the heat capacity of the scattering volume V at constant volume, and β_T is the isothermal compressibility. Then,

$$V\overline{\Delta\varepsilon^2} = kT\left(\beta_T\rho^2\left(\frac{\partial\varepsilon}{\partial\rho}\right)_T^2 + \frac{VT}{c_v}\left(\frac{\partial\varepsilon}{\partial T}\right)_\rho^2\right), \tag{5}$$

using the relation

$$\rho\left(\frac{\partial\varepsilon}{\partial\rho}\right)_T = \frac{1}{\beta_T}\left(\frac{\partial\varepsilon}{\partial P}\right)_T, \text{ and } \left(\frac{\partial\varepsilon}{\partial T}\right)_\rho = \left(\frac{\partial\varepsilon}{\partial T}\right)_P + \frac{\alpha_P}{\beta_T}\left(\frac{\partial\varepsilon}{\partial P}\right)_T,$$

and performing some thermodynamic transformations,

$$V\overline{(\Delta\varepsilon)^2} = \frac{kT}{\beta_T}\left(\frac{\partial\varepsilon}{\partial P}\right)_T^2\left(1 + \left(\frac{\beta_T}{\beta_s} - 1\right)x^2\right), \tag{6}$$

where α_P is the volume expansion coefficient and β_s is the adiabatic compressibility. In Eq. (6) we have used the abbreviation[1]

$$x = 1 + \frac{\beta_T\left(\frac{\partial\varepsilon}{\partial T}\right)_P}{\alpha_P\left(\frac{\partial\varepsilon}{\partial P}\right)_T} = 1 + \frac{\beta_T\left(\frac{\partial n}{\partial T}\right)_P}{\alpha_P\left(\frac{\partial n}{\partial P}\right)_T}.$$

Inserting Eq. (6) into Eq. (2) we obtain:

$$R_{is} = \frac{\pi^2}{\lambda^4}\frac{kT}{\beta_T}\left(\frac{\partial\varepsilon}{\partial P}\right)_T^2\left(1 + \left(\frac{\beta_T}{\beta_s} - 1\right)x^2\right). \tag{7}$$

For most liquids, the correction term $\left(\frac{\beta_T}{\beta_s} - 1\right)x^2$ in Eq. (7) is $10^{-4} - 10^{-3}$, which is completely negligible. Therefore the approximation corresponding to Eq. (6) is

$$V\overline{(\Delta\varepsilon)^2} \approx kT\beta_T\left(\rho\frac{\partial\varepsilon}{\partial\rho}\right)_T^2 = \frac{kT}{\beta_T}\left(\frac{\partial\varepsilon}{\partial P}\right)_T^2.$$

Then, the isotropic Rayleigh factor is

$$R_{is} = \frac{\pi^2}{\lambda^4} kT\beta_T \left(\rho \frac{\partial \varepsilon}{\partial \rho}\right)_T^2 . \tag{8}$$

However, molecules are generally not isotropic. The anisotropy of molecules is revealed by the depolarization of the light scattered by anisotropic molecules. The ratio of the total to the isotropic scattering is given by the factor of Cabannes:

$$f(\Delta) = \frac{R_{tot}(90°)}{R_{is}(90°)} = \frac{3 + 3\Delta_v}{3 - 4\Delta_v}, \tag{9}$$

where $\Delta_v = I_h/I_v$, the depolarization for polarized incident light, is the ratio of the scattered intensities with polarization parallel and perpendicular to the plane of observation, respectively. The Rayleigh factor is now given by Einstein-Cabannes formula:

$$R = \frac{\pi^2}{\lambda^4} \left(\rho \frac{\partial \varepsilon}{\partial \rho}\right)_T^2 \beta_T kT f(\Delta). \tag{10}$$

B. Refractivity Determination

For an ideal gas, the connection between ε and ρ is determined by Clausius-Mossotti formula:

$$\frac{\varepsilon - 1}{\varepsilon + 2} = c\rho,$$

where c is a proportionality constant and ρ is the density of the gas. Therefore

$$\left(\rho \frac{\partial \varepsilon}{\partial \rho}\right)_T \approx \varepsilon - 1 \approx 2(n-1)$$

and

$$\beta_T = -\frac{1}{V}\left(\frac{\partial V}{\partial P}\right)_T = \frac{1}{N_L}\frac{1}{kT}.$$

Hence the Rayleigh factor may be written in the alternate form

$$R = \frac{4\pi^2(n-1)^2}{\lambda^4 N_L} \frac{3 + 3\Delta_v}{3 - 4\Delta_v}. \tag{11}$$

The relationship between the refractivity and the temperature and

pressure is $n-1=(n_0-1)\frac{PT_0}{P_0T}$. Inserting this equation into Eq. (11)
we get

$$R=\frac{4\pi^2kT_0^2(n_0-1)^2f(\Delta)}{\lambda^4P_0^2T}P,$$

or

$$F_s(T_0, P)=\frac{1}{c}(n_0-1)^2f(\Delta)P, \tag{12}$$

where

$$c=\frac{\lambda^4P_0^2}{4\pi^2F_0\Omega l kT_0}.$$

If the temperature is kept constant in the experiment, there is a linear relation between scattering flux, F_s, and pressure, P. From the experimental points in Figures 3 to 6, we may use the least squares method to find the slope of the best fitting straight line passing through the points. If the experiments are performed under similar conditions in the same apparatus, then in Eq. (12), c is a constant of the apparatus which includes the solid angle and the effective scattering length. And if we treat the refractive index of argon as a standard, then the relative refractive index of other gases may be shown to be[3]

$$\frac{(n_0-1)_i^2}{(n_0-1)_{Ar}^2}=\left(\frac{3-4\Delta_v}{3+3\Delta_v}\right)_i\frac{S_i}{S_{Ar}}, \tag{13}$$

where S_i is the slope of the straight line, F_s *versus* P, of the ith gas graph. The Cabannes factor is taken to be unity for argon.

C. Molecular Weight Determination

For the computation of the intensity of light scattered by fluctuations in the concentration, we substitute in Eq. (2) only that part of $\Delta\varepsilon$ from Eq. (4) which is determined by the concentration fluctuations. On the basis of Eq. (2) and Eq. (4), we obtain

$$I_{conc}(90°)=I_0\frac{\pi^2V}{\lambda^4r^2}\left(\frac{\partial\varepsilon}{\partial c}\right)_{\rho,T}^2\frac{ckT}{\left(\frac{\partial p}{\partial c}\right)_T}f(\Delta), \tag{14}$$

where p is the osmotic pressure and c is the gram molar concentration. By the Van't Hoff equation:

$$\frac{p}{R_g T c} = 1/M + Bc + Dc^2 + \cdots,$$

where M is the molecular weight of the dissolved substance, R_g is the gas constant, B and D are the first and second virial coefficients, we get

$$K\frac{c}{R_{conc}} = 1/M + 2Bc + 3Dc^2 + \cdots, \tag{15}$$

where

$$K = \frac{\pi^2}{\lambda^4 N_A}\left(\frac{\partial \varepsilon}{\partial c}\right)^2_{\rho,T} f(\Delta) = \frac{4\pi^2}{\lambda^4 N_A} n^2 \left(\frac{\partial n}{\partial c}\right)^2_{\rho,T} f(\Delta).$$

The experimental determination of R_{conc} is obtained by subtracting R_{90} of the pure liquid from R_{90} of the solution with a given concentration, i.e., $R_{conc} = R_{sol} - R_{pure}$. Eq. (15) shows that the experimental determination of R_{90} in the solution for different concentrations, and the measurement of $\left(\frac{\partial \varepsilon}{\partial c}\right)_{\rho,T}$, suffice to find the molecular weight M. Plotting $K\frac{c}{R_{conc}}$ *versus* c in a region of low concentration gives a straight line and the intersection of the straight line with the ordinate gives the reciprocal of the molecular weight of the dissolved substance.

D. Depolarization Factor of Light Scattering in Gases

If we ignore the interactions between molecules in a gaseous system, the light scattering of the system can be considered as the sum of the scattering of each individual molecule over the scattering system. In other words, in calculating the depolarization factor of the light scattered by gases, we only have to study the behavior of an isolated molecule under the irradiation of the incident light.[1] For simplicity, we consider the case of an isolated molecule irradiated by linearly polarized light. In general, molecules are more or less anisotropic, i.e., the principal polarizabilities b_1, b_2 and b_3 are not

equal. Therefore the light scattered by such an anisotropic molecule would be depolarized. We choose the coordinate system attached to the molecule as the molecular coordinate system, and the system of coordinates fixed to the laboratory as the laboratory coordinate system. For light incident along the y-axis with its electric field oscillating along the z-axis and the observation being made along the x-axis, the depolarization factor is defined as I_y/I_z, where I_y and I_z are the intensities of the scattered light polarized along the y- and z-directions, respectively. For dipole radiation induced by incident light, the radiated intensity can be written as $I \propto (\ddot{P})^2 = w^4 P^2$, where P, the induced dipole moment in the molecule, can be written $\vec{P} = (T^{-1} b T)\,\vec{E}$. Here $\vec{E}$ is the electric field of the incident light, and T is the transformation matrix from the laboratory system to the molecular system through the three Eulerian angles θ, ψ and φ. By considering the $E = E_z$, we can calculate P_y and P_z. Without going through the elementary but cumbersome calculations, we write the final results[4]

$$\begin{aligned} P_y = [&b_1(\sin\theta \sin\psi \cos\psi \sin\varphi + \sin\theta \cos\theta \sin^2\psi \cos\varphi) \\ &+ b_2(-\sin\theta \sin\psi \cos\psi \sin\varphi \\ &+ \sin\theta \cos\theta \cos^2\psi \cos\varphi) - b_3(\sin\theta \cos\theta \cos\varphi)]\, E_z \end{aligned}$$

$$P_z = (b_1 \sin^2\theta \sin^2\psi + b_2 \sin^2\theta \cos^2\psi + b_3 \cos^2\theta)\, E_z \qquad (16)$$

In order to compare them with experimental values, P_y^2 and P_z^2 have to be averaged over the Eulerian angles θ, ψ and φ. Assuming that the orientation of the molecule in the gaseous system is randomly distributed, we can take the average as follows:

$$\begin{aligned} \overline{P_y^2} &= \frac{\int_0^{2\pi}\int_0^{2\pi}\int_0^{\pi} P_y^2 \sin\theta\, d\theta\, d\psi\, d\varphi}{\int_0^{2\pi}\int_0^{2\pi}\int_0^{\pi} \sin\theta\, d\theta\, d\psi\, d\varphi} \\ \overline{P_z^2} &= \frac{\int_0^{2\pi}\int_0^{2\pi}\int_0^{\pi} P_z^2 \sin\theta\, d\theta\, d\psi\, d\varphi}{\int_0^{2\pi}\int_0^{2\pi}\int_0^{\pi} \sin\theta\, d\theta\, d\psi\, d\varphi}. \end{aligned} \qquad (17)$$

From Eq. (17) the depolarization factor can be written as

$$\Delta_v = \frac{(b_1 - b_2)^2 + (b_2 - b_3)^2 + (b_3 - b_1)^2}{6(b_1^2 + b_2^2 + b_3^2) + 4(b_1b_2 + b_2b_3 + b_3b_1)}, \tag{18}$$

where the subscript v of Δ_v denotes that the electric field of the incident light is vertically polarized along the z-axis.

For convenience we introduce the notations

$$\gamma^2 = \frac{1}{2}((b_1 - b_2)^2 + (b_2 - b_3)^2 + (b_3 - b_1)^2)$$

$$b = \frac{1}{3}(b_1 + b_2 + b_3),$$

where $\frac{2\gamma^2}{9b^2}$ is the so-called optical anisotropy and b is the mean polarizability of the molecule. Eq. (18) can be written as

$$\Delta_v = \frac{3\gamma^2}{45b^2 + 4\gamma^2}. \tag{19}$$

From Eq. (19) we can see that the depolarization of the scattered light in gases is caused by the molecular anisotropy.

E. Determination of the principal polarizabilities of the molecule

1. *In gases*

Eq. (18) gives us a relation between the principal polarizabilities and an experimental measurable quantity Δ_v. For a molecule which does not have an axis of symmetry it is necessary to use three relations to solve the principal polarizabilities b_1, b_2 and b_3. According to R. Gans'[1] choice, the expression of the index of refraction in gases or vapors,

$$n - 1 = 2\pi N_L \frac{1}{3}(b_1 + b_2 + b_3), \tag{20}$$

is used as the first equation, the second equation is obtained from rearranging Eq. (19), i.e.,

$$\frac{10\Delta_v}{3 - 4\Delta_v} = \frac{(b_1 - b_2)^2 + (b_2 - b_3)^2 + (b_3 - b_1)^2}{(b_1 + b_2 + b_3)^2}, \tag{21}$$

and the Kerr effect provides the third equation,

$$2b_3 - b_2 - b_1 = \frac{45k^2T^2K}{3\pi N_L \mu^2}, \tag{22}$$

where K is the Kerr constant and μ is the dipole moment of a plane molecule.

Eqs. (21) and (22) are related to two independent experiments. We find that a third equation can also be obtained from experimental observation of the Rayleigh scattering.[4] That is, the third relation, Eq. (22), can be replaced by a relation of the dependence of the depolarization factor upon an applied d.c. electric field. According to the viewpoint of Langevin for the explanation of the Kerr effect, the anisotropic molecules, which originally are randomly oriented, so arrange themselves in an electric field that they take the state of minimum potential energy. At the same time, because of thermal motion, there is a preferential equilibrium orientation, which depends on the temperature. If the axes of the molecule in the absence of a field are randomly oriented, when the electric field is applied, assuming that thermal equilibrium has been attained, dN molecules will have a definite orientation[1]

$$dN = Ce^{-U/kT} \sin\theta \; d\theta \, d\psi \, d\varphi, \tag{23}$$

where U is the potential energy of the molecule in the electric field.

Therefore the calculation of the depolarization factor of the scattered light of a gaseous system under an applied d.c. electric field is similar to the derivation in Sec. D, except that the weighting factor $e^{-U/kT}$ must be applied to the integrands, i.e., the averages must be expressed as

$$\overline{P_y^2} = \frac{\int_0^{2\pi}\int_0^{2\pi}\int_0^{\pi} P_y^2 e^{-U/kT} \sin\theta \, d\theta \, d\psi \, d\varphi}{\int_0^{2\pi}\int_0^{2\pi}\int_0^{\pi} e^{-U/kT} \sin\theta \, d\theta \, d\psi \, d\varphi}$$

and

$$\overline{P_z^2} = \frac{\int_0^{2\pi}\int_0^{2\pi}\int_0^{\pi} P_z^2 e^{-U/kT} \sin\theta \, d\theta \, d\psi \, d\varphi}{\int_0^{2\pi}\int_0^{2\pi}\int_0^{\pi} e^{-U/kT} \sin\theta \, d\theta \, d\psi \, d\varphi}, \tag{24}$$

where the potential energy U can be written as

$$U = -\left(A_1 E_{0z} + \frac{1}{2} A_2 E_{0z}^2\right) \tag{25}$$

for a d.c. electric field E_{0z} applied along the z-axis, and

$$A_1 = \mu_1 \sin\theta \sin\psi + \mu_2 \sin\theta \cos\psi + \mu_3 \cos\theta \tag{26}$$

$$A_2 = a_1 \sin^2\theta \sin^2\psi + a_2 \sin^2\theta \cos^2\psi + a_3 \cos^2\theta\,, \tag{27}$$

for a molecule with permanent dipole moment μ_i and induced dipole moment a_i corresponding to its axes x', y' and z', respectively. In examining Eq. (24), it should be noted that if the energy of the molecule in the external electric field is small in comparison with the energy of the thermal motion, there is no need of computing Eq. (24) exactly. Sufficient accuracy is obtained if we expand the exponent under the integral in powers of U/kT and keep terms to the second order in E_{0z}, inclusively. Then

$$e^{-U/kT} = 1 + \frac{A_1}{kT} E_{0z} + \frac{A_z}{2kT} E_{0z}^2 + \frac{A_1^2}{2(kT)^2} E_{0z}^2 + \cdots . \tag{28}$$

In this case the final results of Eq. (24) can be written as

$$\overline{P_y^2} = \frac{1}{30}\left[[(b_1 - b_2)^2 + (b_2 - b_3)^2 + (b_3 - b_1)^2 + \frac{1}{14}(\theta_1 + \theta_2)E_{0z}^2\right] E_z^2$$

$$\overline{P_z^2} = \frac{1}{15}\left[3(b_1^2 + b_2^2 + b_3^2) + 2(b_1b_2 + b_2b_3 + b_3b_1) + \frac{1}{14}(\theta_3 + \theta_4)E_{0z}^2\right] E_z^2, \tag{29}$$

where

$$\theta_1 = \frac{1}{kT}[(b_1 - b_2)^2(3a_1 + 3a_2 + a_3) + (b_2 - b_3)^2(a_1 + 3a_2 + 3a_3) + (b_3 - b_1)^2(3a_1 + a_2 + 3a_3)]$$

$$\theta_2 = \frac{1}{k^2T^2}[(b_1 - b_2)^2(3\mu_1^2 + 3\mu_2^2 + \mu_3^2) + (b_2 - b_3)^2(\mu_1^2 + 3\mu_2^2 + 3\mu_3^2) + (b_3 - b_1)^2(3\mu_1^2 + \mu_2^2 + 3\mu_3^2)]$$

$$\theta_3 = \frac{1}{kT}[3(a_1 + a_2 + a_3)(b_1 + b_2 + b_3)^2 + 12(a_1b_1^2 + a_2b_2^2 + a_3b_3^2) - 4(b_1b_2a_3 + b_2b_3a_1 + b_3b_1a_2)]$$

$$\theta_4 = \frac{1}{k^2T^2}[3(\mu_1^2 + \mu_2^2 + \mu_3^2)(b_1 + b_2 + b_3)^2 + 12(\mu_1^2b_1^2 + \mu_2^2b_2^2 + \mu_3^2b_3^2) - 4(b_1b_2\mu_3^2 + b_2b_3\mu_1^2 + b_3b_1\mu_2^2)].$$

The corresponding depolarization factor, by definition, is

$$\Delta_v = \frac{\overline{P_y^2}}{\overline{P_z^2}}, \tag{30}$$

where the $\overline{P_y^2}$ and $\overline{P_z^2}$ are calculated in Eq. (29).

Thus Eqs. (29) and (30) can be used to replace Eq. (22). But we will not use Eqs. (29) and (30) directly, due to their complexity. Because $\overline{P_y^2}$ and $\overline{P_z^2}$, corresponding to I_y and I_z, can be measured separately, $\overline{P_z^2}$ is considered under a zero d.c. electric field while $\overline{P_y^2}$ is considered under a variable value of an applied d.c. electric field. For simplicity, we consider the molecule with a permanent dipole moment along one of the principal axes, say $\mu_1 = \mu_2 = 0$, $\mu_3 \neq 0$. For dipolar molecules $\theta_2 \gg \theta_1$ can always be used and θ_1 can be neglected. In this case $\overline{P_y^2}$ and $\overline{P_z^2}$ are written as

$$\overline{P_y^2} = \frac{1}{30}\Big[[(b_1-b_2)^2+(b_2-b_3)^2+(b_3-b_1)^2 + \frac{1}{14}((b_1-b_2)^2+3(b_2-b_3)^2+3(b_3-b_1)^2)\frac{\mu_3^2}{k^2T^2}E_{0z}^2\Big]E_z^2$$

$$\overline{P_z^2} = \frac{1}{15}[3(b_1^2+b_2^2+b_3^2)+2(b_1b_2+b_2b_3+b_3b_1)]E_z^2. \tag{31}$$

From Eq. (31), we can obtain the relation

$$\frac{(b_1-b_2)^2+3(b_2-b_3)^2+3(b_3-b_1)^2}{6(b_1^2+b_2^2+b_3^2)+4(b_1b_2+b_2b_3+b_3b_1)} = S, \tag{32}$$

which can be obtained experimentally as the slope of a straight line of $\overline{P_y^2}(E_{0z})/\overline{P_z^2}$ *versus* $\mu_3^2E_{0z}^2/(14k^2T^2)$. Furthermore, from Eqs. (18) and (32), we can obtain

$$\frac{(b_1-b_2)^2+3(b_2-b_3)^2+3(b_3-b_1)^2}{(b_1-b_2)^2+(b_2-b_3)^2+(b_3-b_1)^2} = \frac{S}{\Delta_v} = C. \tag{33}$$

Thus, we can compute all three principal polarizabilites b_1, b_2 and b_3 from Eqs. (20), (21) and (33).

Actually, we get from Eq. (20)

$$b_1+b_2+b_3 = \frac{3(n-1)}{2\pi N_L} = A, \tag{34}$$

from Eq. (21)

$$(b_1 - b_2)^2 + (b_2 - b_3)^2 + (b_3 - b_1)^2 = \frac{90\Delta_v}{3 - 4\Delta_v} \left(\frac{n-1}{2\pi N_L}\right)^2 = B \quad (35)$$

and from Eq. (33)

$$(b_1 - b_2)^2 + 3(b_2 - b_3)^2 + 3(b_3 - b_1)^2 = CB. \quad (36)$$

Solving the last equations, the principal polarizabilities are represented as follows:

$$b_1 = \frac{A}{3} + 3\left(\frac{3-C}{2}B\right)^{1/2} \pm \left(\frac{3C-7}{2}B\right)^{1/2}$$

$$b_2 = \frac{A}{3} - 3\left(\frac{3-C}{2}B\right)^{1/2} \pm \left(\frac{3C-7}{2}B\right)^{1/2}$$

$$b_3 = \frac{A}{3} \mp \left(\frac{3C-7}{2}B\right)^{1/2}. \quad (37)$$

2. ***In dilute solutions***

In gases the principal polarizabilities of the molecule can be determined from the above calculations. But many samples exist as liquids or solids at room temperature with rather low vapor pressures even at very high temperature. Therefore it is very difficult to perform the scattering experiment for such samples in the vapor phase.

In the liquid phase the calculations of the depolarization factor are nearly impossible. The chief difficulties are the necessity of considering the internal field acting on the scattering molecule and of finding the distribution function of the scattering molecules in liquids, since in the liquids the internal fields and the distribution function are still unknown.

The work of D. J. Coumou *et al.*[5] gives us a way to determine the principal polarizabilities from the experimental data of light scattering in dilute solutions. In their work they used the anisotropic molecule as a solute which is dissolved in the solvent of isotropic molecules and found that at infinite dilution the anisotropic part of the Rayleigh scattering by the solute is fairly independent of the solvent. They obtained an empirical formula

$$R^0_{an,m} = R^v_{an,m}\left(\frac{n_s^2+2}{3}\right)^2, \tag{38}$$

where n_s is the index of refraction of the solution at infinite dilution and $R^0_{an,m}$ and $R^v_{an,m}$ represent the anisotropic scattering of the solute molecule at infinite dilution and in vapor phase, respectively. The results of their work implies that at infinite dilution the local anisotropies scatter like free solute molecules subject to an electric field vector E_i given by the Lorentz relation.[6]

Thus the molar anisotropic scattering factor $R^v_{an,m}$ of a vapor can be determined from the molar scattering factor $R^0_{an,m}$ of anisotropic molecules in dilute solutions in a solvent consisting of nearly isotropic molecules. In gases or vapors the molecular anisotropic scattering factor can be related to the molecular principal polarizabilities by the relation

$$(b_1-b_2)^2+(b_2-b_3)^2+(b_3-b_1)^2 = \frac{45R^v_{an,m}}{56N_A}\left(\frac{\lambda}{\pi}\right)^4, \tag{39}$$

where N_A is Avogadro's number. In this case we can assume that under an applied d.c. electric field the solute molecules will arrange themselves in the dilute solution as in the vapor phase, while the solvent molecule is isotropic and will not be influenced by the applied d.c. field.[4] The arrangement of the solute molecule caused by the d.c. field will induce a change in the values of $\overline{P_y^2}$ and $\overline{P_z^2}$ as calculated in Eq. (29). For simplicity, we consider again the molecule with a permanent dipole moment directed along one of the principal axes, i.e., $\mu_1 = \mu_2 = 0$, $\mu_3 \neq 0$, $\theta_2 \gg \theta_1$ and $\theta_4 \gg \theta_3$. Therefore $\overline{P_y^2}$ and $\overline{P_z^2}$ can be written as

$$\overline{P_y^2} = \frac{1}{30}\Big\{(b_1-b_2)^2+(b_2-b_3)^2+(b_3-b_1)^2$$

$$+\frac{\mu_3^2E_{0z}^2}{14k^2T^2}[(b_1-b_2)^2+3(b_2-b_3)^2+3(b_3-b_1)^2]\Big\}E_z^2$$

$$\overline{P_z^2} = \frac{1}{15}\Big\{3(b_1^2 + b_2^2 + b_3^2) + 2(b_1b_2 + b_2b_3 + b_3b_1)$$

$$+ \frac{\mu_3^2 E_{0z}^2}{14k^2T^2}[(b_1 + b_2 + b_3)^2 + 12b_3^2 - 4b_1b_2]\Big\}E_z^2, \qquad (40)$$

and therefore

$$\frac{(b_1 - b_2)^2 + 3(b_2 - b_3)^2 + 3(b_3 - b_1)^2}{2[(b_1 + b_2 + b_3)^2 + 12b_3^2 - 4b_1b_2]} = \left(\frac{dI_y/dE_{0z}^2}{dI_z/dE_{0z}^2}\right)_{x_2 = 0}, \qquad (41)$$

where the I_y and I_z refer to light scattered by the solution at infinite dilution for various intensities of the applied d.c. electric field and x_2 refers to the molar fraction of the anisotropic component.

Thus the three relations, Eq. (20), Eq. (39) and Eq. (41), can be used to determine b_1, b_2 and b_3. Although it seems difficult to express b_1, b_2 and b_3 explicitly, they can always be obtained numerically.

3. EXPERIMENTAL METHOD

The complete setup of the optical path and the electronic detecting system is shown in Fig. 1. The arrangement of the optical path is based on the modified compensation method.[4] With this arrangement we can eliminate the influence of the instability of the intensity of the laser light source by taking the ratio of the scattering signal to a monitoring signal which indicates the intensity level of the source. In Fig. 1 the scattering signal is detected by the photomultiplier PM_1, while the monitoring signal is reflected by the beam splitter BS and detected by PM_2. Therefore all the quantities measured from the scattered light are independent of the intensity of the source at that instant.

Because the scattering signals are very small and almost always buried in noise, the S/N ratio cannot be improved by a simple multistage amplification. We use the recently developed lock-in amplification method[7] or the phase sensitive detection method, for the enhancement of the S/N ratio of the scattering signal. This method takes advantage of the fact that, while the signal can be modulated, amplified and demodulated at a fixed frequency and phase, the fre-

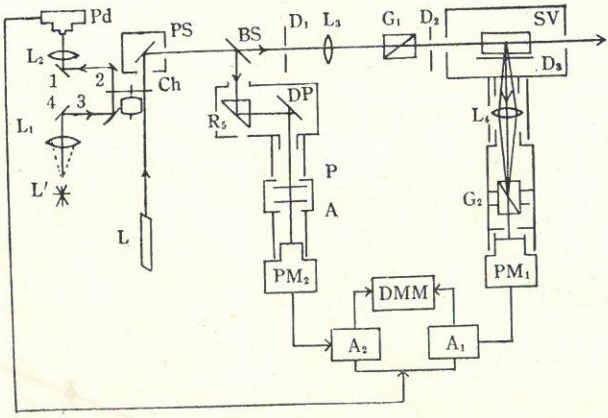

Fig. 1. Optical arrangement for the photoelectric measurement of the depolarization factor according to the modified compensation method.

L: He-Ne laser (4 mW)
Ch: mechanical chopper
PS: prism system
D_1, D_2, D_3: diaphragms
L_1, L_2, L_3, L_4: lenses
R_1, R_2, R_3, R_4, R_5: reflecting mirrors
BS: beam splitter
DP: diffuse paper
PM_1: XP 1117, Philips
PM_2: 150 AVP, Philips
A_1: phase-sensitive detector (lock-in amplifier), Brookdeal Co.
A_2: lock-in amplifier (home-made)
P, A: polaroids
G_1, G_2: Glan-Thompson prisms
Pd: photodiode
PM_1, PM_2: photomultipliers
SV: sample vessel
DMM: digital multimeter
L': lamp

quencies and phases of noise are random. Modulation is carried out by the mechanical chopper Ch, with a chopping frequency being chosen to avoid the $1/f$ and the 60 Hz noises. Then signals detected by PM_1 and PM_2 are selectively amplified by tuned amplifiers with a bandpass sufficient to pass the carrier signals and their signal sidebands, if any, where the $1/f$ noise, the interference noise, 60 Hz noise and most of the white noise are rejected. After amplification the signals are demodulated by a reference signal generated by photodiode Pd, which transforms the chopped optical signal to an electrical signal with the same frequency and a fixed phase with respect to the modulated signal. Then the demodulated signals are passed through a low pass filter and subjected to a conventional d.c. integration. Finally, the integrated signals are fed into a digital

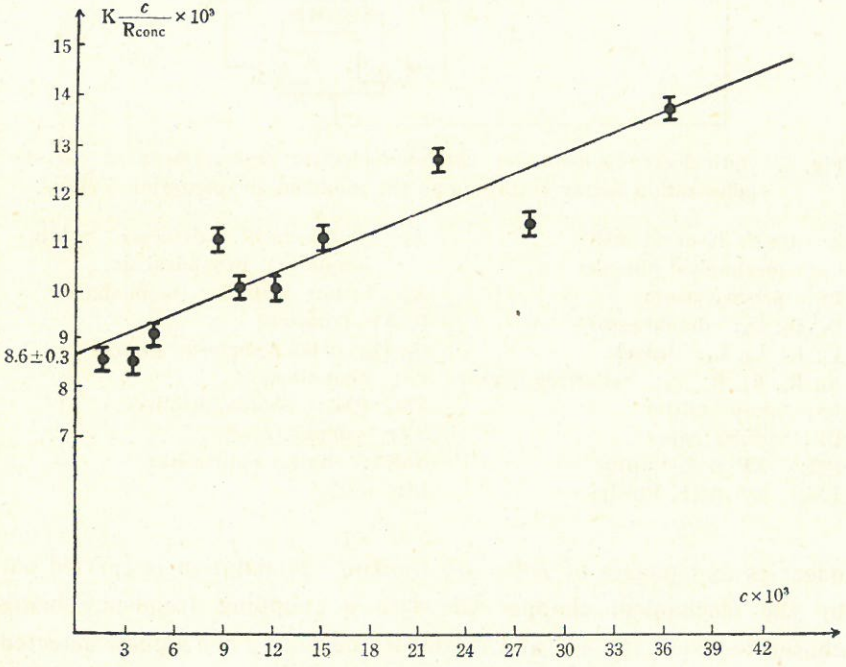

Fig. 2. Concentration effect on the Rayleigh scattering for *n*-Octane in Benzene at t=25°C

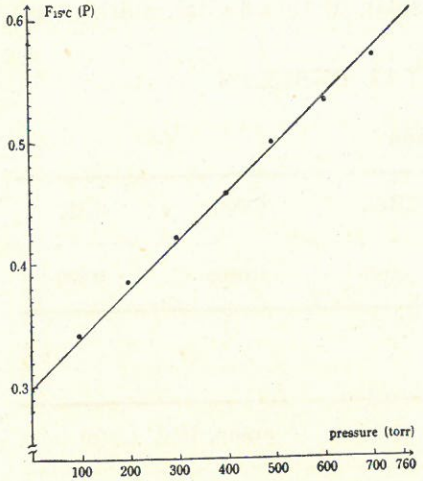

Fig. 3. Pressure effect on the Rayleigh scattering for argon at t=15°C

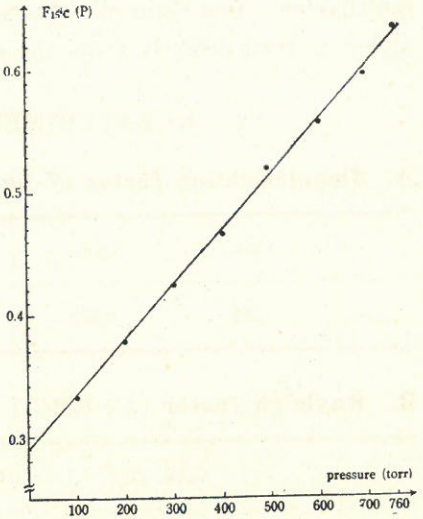

Fig. 4. Pressure effect on the Rayleigh scattering for air at t=15°C

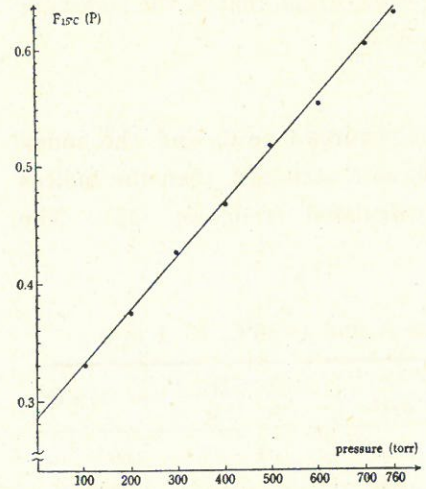

Fig. 5. Pressure effect on the Rayleigh scattering for N_2 at t=15°C

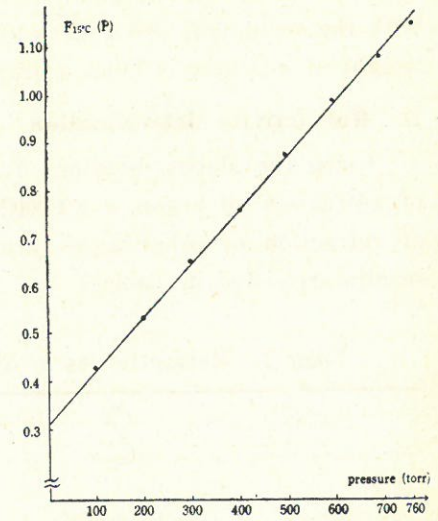

Fig. 6. Pressure effect on the Rayleigh scattering for CO_2 at t=15°C

multimeter. The ratio of the scattering signal to the monitoring signal is read directly from the display of this digital multimeter.

4. EXPERIMENTAL RESULTS

A. Depolarization factor of liquids

	C_6H_6	CCl_4	$CHCl_3$	CH_3Cl	C_7H_8
Δ_v	0.269	0.213	0.075	0.0966	0.320

B. Rayleigh factor ($\lambda = 6328$Å)

	C_6H_6, 26°C	CCl_4, 26°C	argon, 15°C, 1 atm
$R_{90}(cm^{-1})$	1.254×10^{-5}	6.13×10^{-6}	5.8×10^{-9}

C. Molecular weight determination

From Fig. 2, $K\frac{c}{R_{conc}}$ *versus* c, (cf. Eq. 15), the intersection with the ordinate is $(8.6 \pm 0.3)\times10^{-3}$ mole/gram, that is, the molecular weight of *n*-Octane is 116 ± 4 gram/mole.

D. Refractivity determination

Using the slopes, obtained from figures 3 to 6, and the index of refraction of argon, $n = 1.000266$, as a standard, then the indices of refraction of other gases are calculated from Eq. (13). The results are listed in Table 1.

Table 1. Refractivities at 6328 Å and t=15°C, P=1 atm

GAS	$\frac{S_i}{S_{Ar}}$	$\frac{f(\Delta)_i}{f(\Delta)_{Ar}}$	$\frac{(n_0-1)_i}{(n_0-1)_{Ar}}$	$(n_0-1)\times10^4$
argon	1	1	1	2.66
nitrogen	1.14±1.5%	1.031	1.051	2.79±0.04
air	1.12±1.7%	1.039	1.038	2.76±0.04
carbon dioxide	2.77±1.5%	1.103	1.580	4.20±0.06

5. DISCUSSION

A. In the determination of the absolute Rayleigh factor, there are several corrections which must be considered:
   1. Fresnel correction: consider reflection at an interface of two different indices n_1 and n_2.
   2. Correction of the index of refraction: consider the change of light path at interfaces of different media.

B. The dust and the stray light accompanying the scattered light is always a problem in light scattering experiments. So the reduction of stray light and of dust particles in the fluid were among the principal experimental problems in the work, and relate strongly to the accuracy of the measurements.

C. Figures 3 to 6 show that the intensity of the scattered light is linearly related to pressure. From such a linear relationship, we conclude that intermolecular interactions are negligible within the range of the experimental error. In other words the gases studied in this experiment may be considered as ideal gases under our experimental conditions.

D. In the determination of the molecular weight, the dimensions of the molecules and particles are small compared to the wavelength of the light. If the molecules or particles are comparable in size to the wavelength of the light, then interference plays an important role in the light scattered by a single molecule. In this case the form factor of the molecules should be taken into consideration and the molecular weight can be determined from the Zimm plot.

E. According to the calculation for the nitrobenzene molecule (dipole moment = 4.22 Debye) under an applied d.c. electric field of the order of 10^4V/cm, the expected change of the scattered light intensity is about 0.002% with respect to the case without the applied d.c. field. It is nearly impossible to detect this small effect with our experimental arrangement. In order to make the effect of the applied d.c. electric field upon the intensity of the scattered light large enough for our experimental observation,

we need a molecule with larger dipole moment. Molecules with dipole moments of the order of 10^2–10^3 Debye can be easily found among the biomolecules. The intensity change is proportional to the square of the dipole moment, so for a dipole of the order of 10^2 Debye a change of about 20% in the intensity of the scattered light is expected for a d.c. field intensity of 10^4V/cm.

6. PLANS FOR FUTURE WORK

As a natural extension of our developed model for determining the principal polarizabilities, we should apply it to molecules with large dipole moments (say, 10^2 Debye). We hope to study tobacco mosaic viruses (TMV), which possess a permanent dipole moment of 4.1×10^4 Debye. This dipole moment is large enough. However, our model should be revised to make it applicable to biomolecules, which are usually macromolecules with molecular weight of the order of 10^8 and size of about 10^3 Angstroms. In the case of molecules whose size is comparable to the wavelength of light, waves scattered from different parts are not independent. Therefore the form factors of such molecules have to be taken into consideration.

Since biomolecules are of such current interest, we also plan to investigate other physical properties of them such as molecular weight, shape, size, and their dynamics. We hope to learn about the response of biomolecules in different solutions by studying their dynamic behavior in solution.

ACKNOWLEDGEMENTS

We are grateful to the Graduate School of Physics for financial support for our study in light scattering. We would like to thank Dr. J.C. Hill for reading the manuscript thoroughly and giving us many valuable suggestions.

REFERENCES

(1) Fabelinskii, I.L. *Molecular Scattering of Light*, Plenum Press, New York, (1968).

(2) Landau, L.D. and E.M. Lifshitz, *Statistical Physics*, Addison-Wesley Publishing Company, Inc., (1974).
(3) Gill, P. and D.W.O. Heddle, *J. Opt. Soc. Amer.* **53**, 847 (1963).
(4) Ou-Yang Hsin-Chiao, M.S. thesis, Fu Jen University, (1977).
(5) Coumou, D.J., E.L. Mackor and J. Hijmans, *Trans. Faraday Soc.* **60**, 2244. (1964).
(6) Fröhlich, H., *Theory of Dielectrics*, Oxford (1958).
(7) Malmstadt, H.V., C.G. Enke and S.R. Crouch, *Electronic Measurements for Scientists*, W.A. Benjamin, Inc., (1974).

"In our machine, these atoms last forever",
Professor Kleppner said.

" 'Forever' for an atom is a millisecond",
he added.

THE EQUATORIAL EVENING MINIMUM IN THE TOTAL ELECTRON CONTENT OF THE IONOSPHERE AND ITS ROLE IN EQUATORIAL SCINTILLATION

JOHN R. KOSTER, SVD

ABSTRACT

A minimum in the total electron content of the equatorial ionosphere frequently appears shorty after sunset in measurements of Faraday rotation made at Legon, Ghana (latitude 5.63°N, longitude -0.19°E, magnetic dip 8°S). This paper describes the phenomenon and investigates its occurrence characteristics over a period of six years. It concludes that the effect is due to a transport phenomenon described as a "circulation cell" which follows the sunset line. This circulation is not considered to be the primary cause of the production of irregularities in the nighttime F region, but the mechanism is thought to contribute both to the intensity and the resulting scintillation.

1. INTRODUCTION

Soon after synchronous satellites bearing radio beacons became available for observation at Legon, and Faraday rotation measurements began, it became obvious that something unusual was happening in the equatorial ionosphere in the period following sunset, and attention was called to this in a number of publications (Koster, 1971; Koster, 1972; Yeboah-Amankwah and Koster, 1972; Koster, 1973). Several internal research reports gave further information about the phenomenon (Koster, Korfker and Yeboah-Amankwah (1970), Koster and Beer (1972), Koster (1973b)). The phenomenon in question is the rapid disappearance of ionospheric ionization shortly after sunset, evidenced by a sharp drop in the value of the Faraday rotation angle. After passing through a minimum, the value of the angle often recovers again quite quickly, leading to a maximum an hour or two later before the angle decays to its diurnal minimum around the time of sunrise. Sometimes the

behaviour is more irregular, and several maxima can appear. Typically, severe scintillation sets in during the precipitous decline. Initially the large amplitude variations in signal strength characteristic of scintillation made accurate polarimeter readings somewhat difficult to obtain. The problem was overcome to a large extent by modifications in the Legon equipment in 1969, and good records have been obtained since that time. Further improvements were made in the equipment early in 1972, and a large collection of reliable data is now on hand.

In previous articles we have referred to this phenomenon as the Equatorial Evening Minimum (EEM), and we shall use the same nomenclature in this paper.

The motivation for a further study of the phenomenon is twofold. The EEM is an interesting occurrence in its own right. But it is also closely associated with the onset of severe equatorial scintillation. This latter phenomenon has been known and studied for nearly four decades, and a full explanation of the mechanisms responsible for its occurrence is still awaited. It is felt that some useful clues to the nature of this mechanism can be found in a further investigation of the EEM.

2. A BRIEF DESCRIPTION OF THE PHENOMENON

Quite a number of plots of total electron content (TEC) versus time have appeared in the literature. We here reproduce only one figure to illustrate the general characteristics of the equatorial evening minimum. Fig. 1 shows a plot of TEC as a function of time as observed at Legon on seven consecutive days in October, 1972. Electron content is normally at its daily minimum at sunrise, so the plots commence at 6 a.m. local time on the days in question and continue till 6 a.m. on the following day. The vertical scale of the plots, in terms of TEC per unit distance, is shown on the figure. The outstanding feature in the curves is the sharp decline in TEC after ionospheric sunset, leading to a minimum around 21 hours local time. The considerable variability of this feature from day to day is well illustrated in the figure. The periods during

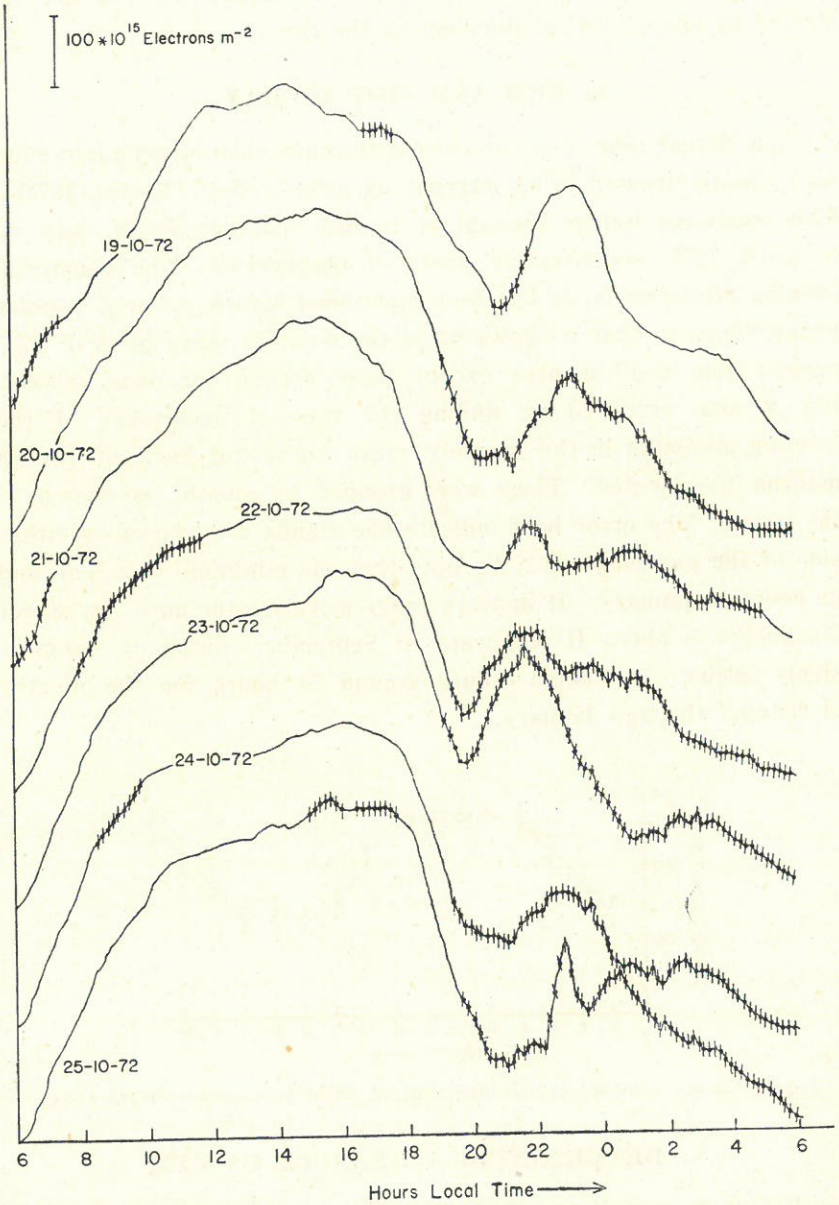

Fig. 1. Plots of TEC as a function of time for seven successive days in October, 1972. Vertical lines across the curve indicate the presence of scintillation.

which severe amplitude variations (scintillations) occurred are indicated by short vertical lines across the curve.

3. EEM AND TIME OF DAY

The actual time of occurrence of the equatorial evening minimum was initially treated in an internal scientific report (Koster, 1973b). This treatment is here brought up to date, making use of data up to April, 1977 – six effective years of observation. The equatorial evening minimum is, as has been mentioned before, a fairly regular phenomenon, in that it shows up in the monthly mean plots of TEC against time in all months except those around the June solstice. Fig. 2. was produced by finding the time of occurrence of the evening minimum in the monthly mean curve for each of the 68 months investigated. These were grouped by month, as shown in the figure. The error bars indicate one standard deviation on either side of the plotted point. We note that the minimum occurs around 21 hours in January. It appears progressively later until the effect disappears in May. It reappears in September, becoming progressively earlier till it again occurs around 21 hours for the months of October through January.

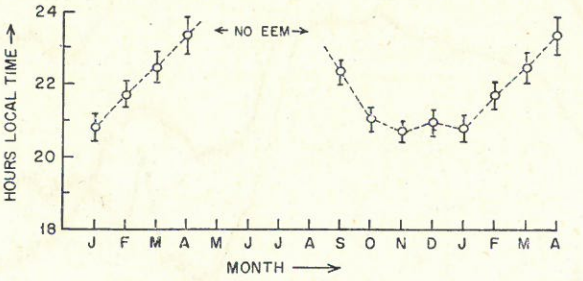

Fig. 2. Mean monthly occurrence time of EEM averaged over six years.

4. DETERMINING A MEASURE OF EEM

Before we can discuss EEM in quantitative terms, we must define some (preferably simple) way of measuring it. A number of different definitions have been used over the years—each with its advantages

and limitations. For the purposes of this paper, we shall adopt a measure that is simple in itself, and easy to implement.

We use TEC values, taken at 10 minute intervals between 18 hours and 06 hours local time (72 points in all). EEM for a given day is then defined as:

$$EEM = \frac{\sum_{I=1}^{71} |TEC(I) - TEC(I+1)| - |TEC(1) - TEC(72)|}{|TEC(1) - TEC(72)|} \times 100.$$

On days on which TEC decreases monotonically from sunset to zero, EEM will be equal to zero. Days of progressively larger rises and falls in the value of TEC during that interval will have progressively larger values of EEM. The division by the absolute difference of the first and last value of TEC is included in order to make our EEM a measure of the fractional rises and falls, rather than of their absolute values. Any definition that uses absolute values will almost certainly produce equinoctial maxima in the annual curve since TEC has maxima at that time (Koster, 1972). It will also produce a solar cycle maximum around sunspot maximum, since TEC is well known to be largest at that time in the solar cycle.

One of the limitations of our definition is the fact that it does not respond to cases where the plot of TEC as a function of time shows a rapid fall, followed by a plateau where the TEC remains relatively constant, then falls more rapidly again. While this limitation is recognized, it is not felt that this will materially affect the conclusions of this paper. The main result of the limitation is that the minimum at the June solstice is somewhat broader than it would be if a more sophisticated measure of EEM were adopted.

5. THE ANNUAL BEHAVIOUR OF EEM

To investigate the variation of EEM with season, weekly means were taken for each of the 295 weeks covered by the data. Means were determined for each of the 52 weeks of the year. They are plotted in Fig. 3. Fourier analysis of the data yielded the Fourier components shown in Table 1.

Table 1. Fourier components of the annual variation of EEM

j	0	1	2	3	4	5	6
A_j	16.54	9.98	-2.24	-2.62	1.77	0.39	-2.04
B_j	0.00	-7.52	0.50	1.12	0.45	-1.35	0.45

The curve described by the constant and the first three harmonics is sketched into Fig. 3.

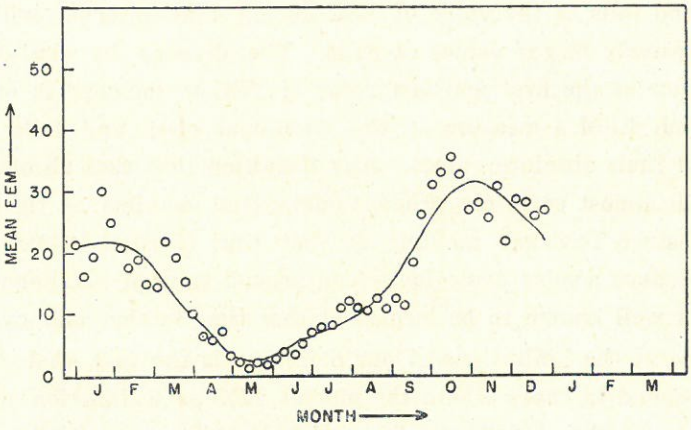

Fig. 3. The seasonal variation of EEM. Weekly means over six consecutive years. The curve is a plot of the constant term and the first three Fourier terms.

We note that the annual term predominates. The amplitude of the third harmonic is down by a factor of 4.4, and all other harmonics have values less than this. The maximum occurs in October, and the minimum in May-June.

We stress again the fact that the measure of EEM is relative. Any measure that uses the absolute changes in the value of TEC rather than the relative changes will almost certainly show a secondary peak around February-March, with a shallow minimum between. The large May minimum would remain essentially unchanged.

6. THE VARIATION OF EEM WITH SUNSPOT CYCLE

Fig. 4. is a plot of the mean value of EEM for each 4 week period (13 points annually) from September 1971 until April 1977 inclusive.

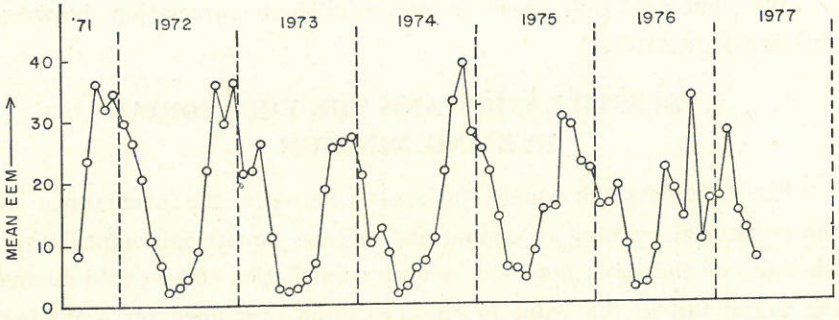

Fig. 4. The sunspot cycle dependence of EEM. The mean EEM for 28 day periods (13 per year) are shown over six years.

We note that the same general shape repeats itself annually with essentially the same amplitude over the nearly six years covered. Since this extends from near sunspot maximum to sunspot minimum, we conclude that there is no appreciable sunspot cycle variation in the phenomenon. We must mention again, however, that it is the relative change in TEC that remains constant. The actual increase in electron content, after the first minimum, is undoubtedly much larger near sunspot maximum.

7. THE VARIATION OF EEM DURING MAGNETIC STORMS

To determine this variation, continuous periods of 200 days were taken, extending from 16 September to 3 April, on each of four consecutive years. This procedure was resorted to in order to avoid including the time of year during which the value of EEM is exceedingly small. Values of EEM for each of the 200 days were correlated with the corresponding sums of the daily K_p values. The correlation coefficients turned out to be:

YEAR	CORRELATION COEFFICIENT (CC)
1971/72	0.021
1972/73	−0.109
1973/74	0.077
1974/75	0.020
MEAN CC	0.007±0.078

We conclude that there is no significant correlation between the two parameters.

8. SCINTILLATION AND THE EQUATORIAL EVENING MINIMUM

Fig. 1 depicts the usual relationship between the occurrence of the equatorial evening minimum and severe equatorial scintillation. On most of the days depicted, severe scintillation commenced during the initial fall in the value of the TEC, and continued for a number of hours thereafter—often throughout the night. On the very first day, however, (19 October, 1972), a rather large magnetic storm ($\sum K_p = 33$) occurred. On that day, although the value of EEM was relatively large (56.9), the value of TEC at the time of the evening minimum remained high (above 300×10^{15} electrons m^{-2}). When this occurs, scintillation at Legon is normally absent or greatly reduced (Koster, 1957). As Fig. 1 shows, scintillation occurred for only an hour on this day, and the value of the scintillation index remained modest. On all the other days, the scintillation was severe, both in regards to intensity (as evidenced by the scintillation index) and to duration.

Here we wish to note two things:

(a) The onset of scintillation normally coincides in time with the occurrence of EEM on days on which EEM is present.

(b) Scintillation is normally severe when EEM is large unless the TEC value remains abnormally high, as it does frequently during severe magnetic disturbances.

9. EEM AND SATELLITE ELEVATION

The results reported above were made from the analysis of

records obtained from the observation of the satellite ATS-3 during the 6 year period in which it was kept on station at 70 degrees west longitude. The elevation angle from Legon was 12°. Observations at higher elevation angles were also desired, and observations were made on IS2F3 from March 1973 through April 1974, during which time the satellite was at an elevation of approximately 65°. A number of difficulties accompanied this venture.

(a) At Legon, as a synchronous satellite moves to high elevations, the M values become progressively smaller. Should the satellite also have an inclined orbit (IS2F3 had an inclination of between 4° and 5° at this time) the value of M becomes even smaller when the satellite moves to negative latitudes. Eventually the value of M becomes so small that the quasi-longitudinal (QL) approximation on which most of the Faraday rotation reductions depend becomes inapplicable. Because of this problem, only March/April records of 1973/74 had sufficiently large values of M throughout the night to make their use reliable.

Table 2. Mean values of EEM for simultaneous observations of two satellites at different elevation angles.

ELEVATION	65°	12°
SATELLITE	IS2F3	ATS-3
PERIOD	MEAN EEM	
Mar/Apr '73	38.5±3.0	16.3±2.5
Mar '74	33.6±3.8	13.1±2.1
Apr '74	13.1±1.7	5.7±2.3

(b) For a period of around 6 weeks around the equinoxes, a sychronous satellite is eclipsed each night at an hour that depends on its longitude. This eclipse is of just over an hour's duration at its maximum. During an eclipse, there is likely to be a considerable temperature change in the satellite, with corresponding frequency

drifts on the part of its oscillator. A loss of power from its solar cells normally leads to a drop in signal intensity as well unless on-board batteries are able to provide energy during the eclipse time. Hence, care must be taken in utilizing results obtained around the equinoxes from a synchronous satellite.

In spite of the above, records of good quality were obtained during March and April of both years. Values of EEM for these periods are summarized in Table 2.

We conclude from the above that one observes larger values of EEM when looking at a high elevation satellite than when simultaneously observing a low elevation one. We would further like to remark that the correlation between the pairs of day to day values of EEM is relatively low. The significance of these observations will be commented on below.

A further observation of interest comes from plotting the pairs of curves on a common graph, so that size and occurrence time of common features can be readily seen. For the two satellites under discussion, the ray paths traverse the ionosphere (assumed to be at 420 km) at points separated by nearly one thousand kilometers. Hence, one has a simultaneous record of occurrences separated by this distance. There is a considerable day to day variability in the plots, but normally the minimum on the high elevation (easterly) satellite occurs before that of the low elevation (westerly) one. Hence, the occurrence of the TEC minimum follows local time; i.e., it moves westward with a velocity nearly that of the sunset line ($495\ ms^{-1}$). Only occasionally is there a feature that indicates a possible eastward velocity, occurring first on the record of the low elevation (westerly) satellite, then on the higher (easterly) one. This observation is significant for our later interpretation.

10. SUMMARY OF FINDINGS

We here summarize the findings thus far made concerning the behaviour of the EEM:

(a) EEM has a seasonally variable occurrence time, appearing around 21 hours from October through January. It occurs

progressively later from February through April, and disappears entirely from the monthly means from May through August. It reappears at 23 hours in September, and moves forward to 21 hours again in October.

(b) The amplitude of EEM has a predominant annual component. There is a broad minimum around the June solstice, and a maximum in October.

(c) The relative measure of EEM adopted in this paper shows no dependence on the sunspot cycle.

(d) The amplitude of EEM is uncorrelated with magnetic disturbances.

(e) EEM is greater for high elevation satellites than for low ones.

(f) EEM occurrence times generally follow the sunset line appearing first on an easterly satellite, later on a westerly one. The time difference corresponds to the velocity of the sunset line (ca 495 ms^{-1} at 420 km).

11. DISCUSSION OF FINDINGS

Our purpose in this paper is to investigate the behaviour of the equatorial evening minimum with a view to understanding the physical mechanism which gives rise to it. We specifically wish to see whether we can throw any new light on the mechanism giving rise to equatorial scintillation. With this in view, we consider each of the above findings.

(a) Does the onset time of EEM bear any relationship to scintillation? Scintillation has an onset time that varies by about an hour during the course of the year. The monthly mean onset time in October occurs about an hour earlier than at the June solstice. A considerable fraction of the onset time change in scintillation disappears if we use apparent (i.e. sundial) time instead of mean time. The small remaining change in scintillation onset time is in phase with the onset time changes of EEM, but very different from it. It will be remembered that EEM disappears completely at the June solstice. We conclude that EEM cannot be a primary cause of scintillation, since the latter occurs in all months, even those in

which no EEM is visible. The most that our evidence can suggest is that EEM may in some way be associated with an enhancement of scintillation. At Legon the average nightly duration of scintillation as obtained from the monthly means is some 7 hours at the June solstice, around 10 hours in October through December. It is quite possible that EEM is associated with the rise of "bubbles" through the ionosphere, giving rise to very intense scintillation which persists for a longer time, while scintillation occurring in the absence of EEM is due to irregularities confined to the bottom of the F region. These scintillations might well be of lesser intensity and shorter duration.

(b) The annual component in the amplitude of EEM agrees quite well with the annual variation of scintillation. This observation is consistent with the hypothesis that scintillation accompanied by EEM is more than that which occurs during its absence.

(c) The lack of dependence of EEM on sunspot cycle variations does not contradict our hypothesis. If one uses a definition of EEM that measures the absolute change in electron content rather than its relative change, EEM would show a sunspot cycle variation similar to that exhibited by scintillation. The independence of the relative measure of EEM from sunspot cycle variations suggests that EEM depends on some physical parameter of the sun which changes annually relative to the earth, but which does not depend directly on the solar EUV flux, sunspot number or any other parameter which would surely show an 11 year variation. We suggested before (Koster, 1973) and wish to suggest again, that this parameter is the direction of the solar rays relative to the magnetic field lines at Legon.

(d) We next consider the lack of significant correlation of EEM with K_p. During severe magnetic storms, scintillation at Legon is often suppressed. At such times we often have large values of EEM (see curve 1 in Fig. 1). Hence, there is surely no one-to-one relationship between scintillation and EEM. What it does suggest is that, when the conditions for scintillation (whatever they are) are right, the scintillation will be more severe and lasting when a

large EEM is present than when it is absent. When the conditions are not right, there may be no scintillation in spite of the presence of large EEM.

(e) The enhancement of EEM for high elevation satellites is interpreted as meaning that the region of electron depletion (the "bubble") is often of limited extent relative to the total path length of the wave through the ionosphere. If we take a simple case where the vertical E-W section of a "bubble" is circular, the relative depletion along the path to an overhead satellite would be much larger than that to a low elevation satellite, whose total path through the ionosphere may be several times longer. Hence, the higher satellite would display a larger EEM—as is the observed fact.

(f) On the majority of occasions when simultaneous Faraday rotation results have been available from two satellites, the EEM has appeared first on the satellite that is further east, later on the one that is to the west of it. The time differences agree remarkably well with the velocity of the sunset line ($495\,ms^{-1}$ at the equator). This suggests a basic dependence of EEM on the apparent time at the subionospheric point. EEM seems to be triggered by ionospheric sunset, with a time lag that is a function of season.

12. CONCLUSIONS

The evidence found in this investigation seems to be entirely consistent with the picture of a "circulation cell" previously suggested (Koster, 1973), and we shall repeat its essential features here.

A large "circulation cell" moves westward along the equator at the speed of the sunset line. We are thinking here in terms of circulating magnetic field lines which have ionization "frozen" on them. A vertical E-W section of this cell would show an upward velocity on its leading edge, an eastward velocity at the top, a downward velocity on the trailing edge, and a westward velocity at the bottom. These upward and downward velocities are consistent with the measurements of Balsley and Woodman (1971). As the leading edge of the cell passes over an observer at the equator, he observes not only a large upward velocity of the F region ionization

above him, but also a sharp drop in the Faraday angle he is measuring, since the electrons are moving upward and eastward, out of his line of sight. The field lines moving in from below are largely devoid of electrons, since they move in from the E region or lower, where the electron content has fallen drastically due to recombination.

When the trailing edge of the cell passes over the observer sometime later, he measures a large downward velocity of ionization, and his Faraday angle increases sharply due to the movement to electrons into his line of sight from above and from the west.

This circulation can only begin after sunset at the ends of the field lines to which the F region ionization is frozen. The magnetic field lines at Legon have a westward declination of 9°, while those at the subionospheric point of ATS-3 have a declination of 14°. If one adds to this the fact that the dip equator at the longitude of Legon (0°) is some 10° North of the geographic equator, it becomes obvious that the controlling factor will normally be sunset at the northern end of the field lines in question. Circulation should, therefore, be delayed at Legon around the June solstice, when sunset there is very late. This agrees extremely well with the observations reported above.

Our observations force us to conclude that the circulation cell is not the primary cause of the formation of irregularities, and hence of scintillation. We have evidence of a large EEM, and hence a vigorous circulation during magnetic disturbances, when there is no scintillation. And during the June solstice we have quite frequent scintillation, but no evidence of circulation.

But the circulation, of which the EEM is a measure, can easily enhance scintillation in two ways. The circulation cell can lift irregularities, initially formed near the bottom of the F region, into regions where they will persist much longer. It can, in fact, fill the whole region with irregularities, thus enhancing the intensity of the observed scintillation. And the circulation cell can cause scintillation to persist for a much longer time, by lifting irregularities to great heights, where recombination times are much longer.

The 7 hour duration of scintillation during the June solstice, compared to the 10 hour duration in October, could best be explained in this way.

Our picture would suggest that the seasonal behaviour of scintillation at Legon may depend to a large extent on the peculiar orientation of the earth's magnetic field lines at this longitude. Other longitudes might well observe a very different seasonal behaviour.

We conclude that the EEM, though not a primary cause of the production of irregularities in the equatorial ionosphere, is an important contributing factor in increasing the intensity of equatorial scintillation by lifting already formed irregularities to great heights, and in increasing its duration by enabling these same irregularities to persist for a longer time.

It seems quite obvious that the EEM is but another manifestation of the rise of plasma bubbles through the ionosphere as measured *in situ* by the explorer satellites (McClure *et al*, 1977), and appearing as dramatic plumes in the VHF radar range-time-intensity maps produced by the Jicamarca group (Woodman and La Hoz, 1976).

ACKNOWLEDGEMENT

This research has been sponsored in part by Air Force Geophysics Laboratory (AFSC), Hanscom Air Force Base, through the European Office of Aerospace Research and Development, United States Air Force under Grant AFOSR-2628.

REFERENCES

(1) Balsley, B.B. and Woodman, R.F. (1971) Ionospheric drift velocity measurements at Jicamarca, Peru (July 1967-March 1970) Report UAC-17, *World Data Centre A. Upper Atmosphere Geophysics*, NOAA, Boulder, Colorado.

(2) Koster, J.R. (1971) An investigation of the total electron content of the equatorial ionosphere. *Fu Jen Studies*, **4**, 1971.

(3) Koster, J.R. (1972) Equatorial Scintillation. *Planet. Space Sci.* **20**, 1999-2014.

(4) Koster, J.R. (1973) The equatorial evening minimum in ionospheric electron content. *Fu Jen Studies* **7**, 1973.

(5) McClure, J.P., Hanson, W.B. and Hoffma, J.H. (1977) Plasma bubbles and irregularities in the equatorial ionosphere, *J. Geophys. Res.* (In

the press).
(6) Woodman, R. J. and La Hoz, C. (1976) Radar Observations of the F Region equatorial irregularities. *J. Geophys. Res.* **80**, 5447-5466.
(7) Yeboah-Amankwah, D. and Koster, J. R. (1972) Equatorial Faraday rotation measurements on the ionosphere using a geostationary satellite. *Planet. Space Sci.* **20**, 395.

Reference is also made to the following unpublished material:

(8) Koster, J. R., Korfker W. L. and Yeboah-Amankwah, D. (1970) Studies of equatorial ionospheric phenomena using transmissions from active satellites. Final Scientific Report, 26 July, 1970. *Department of Physics, University of Ghana.*
(9) Koster, J. R. and Beer, T. (1972) Ionospheric Research using satellites: An interpretation of Ionospheric Faraday rotation observations at the equator. *Department of Physics, University of Ghana.*
(10) Koster, J. R. (1973b) Ionospheric Research using satellites: The equatorial evening minimum. Interim Scientific Report, 1 February, 1973. *Department of Physics, University of Ghana.*

ATTEMPTED FORMATION OF A STABLE 1,2-DIOXETANE FROM OLEFIN 1

JIH-YUNG CHAO

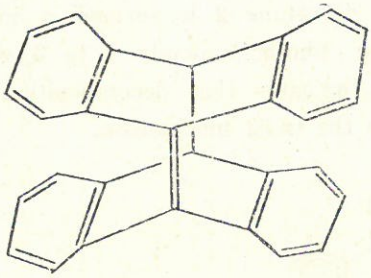

Compound **1**: 1,9-dihydro-bianthracene

Recently, 1,2-dioxetanes and their mode of decomposition have been of interest and a number of stable dioxetanes have been prepared[1-3]. Two major pathways of decomposition are immediately obvious, a process in which both halves of the dioxetane pull away from each other in a simple translational motion as in a suprafacial cycloreversion, or a process in which one half of the dioxetane twists as it moves away from the other as in an antarafacial cycloreversion. It was thought that if the twist mechanism were the only mechanism available to a dioxetane for decomposition, then dioxetane **2** formed from **1** should be stable, since the two halves of the molecule are bonded together at a third point besides the two dioxetane bonds, making the twisting motion impossible.

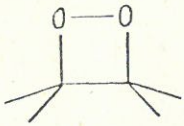

Compound **2**: 1,2-dioxetane

When **1** was irradiated in the presence of oxygen and methylene blue at −78° and warmed to room temperature only **1**, 10,10′-

bianthrone **3**, and anthraquinone **4** were present by tlc. Control experiments showed that **1** was stable to oxygen in the absence of light and that under the same conditions **3** is converted to **4**. Compounds **3** and **4** were separated from unreacted **1** by chromatography and identified by ir and tlc comparison with authentic samples. Thus, if dioxetane **2** is formed it immediately cleaves either thermally or photochemically **1** to **3** which is partially oxidized to **4**. This indicates that decomposition of the dioxetane **2** does not occur via the twist mechanism.

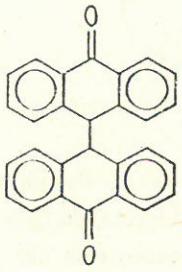

Compound **3**:
10,10-bianthrone

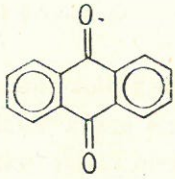

Compound **4**:
anthraquinone

REFERENCES

(1) Bartlett, P.D. and A.P. Schaap, *J. Amer. Chem. Soc.*, **92**, 3223 (1970).
(2) Mazur, S. and C.S. Foote, *J. Amer. Chem. Soc.*, **92**, 3225 (1970).
(3) Wieringa, J.H., J. Strating, H. Wynberg, and W. Adam, *Tetrahedron Lett.*, **169** (1972).

DETAILED STUDIES ON THE GILL FILAMENT OF *CORBICULA FLUMINEA* MÜLLER

CHU-FANG LO and FRANZ HUBER, SVD

ABSTRACT

Photomicroscopy was used to determine the histology and histochemistry of the gill filament of *Corbicula fluminea* Müller.

The main part of the gill filament is covered with various groups of ciliated cells and secretory cells. There are great differences in size, composition, surface specialization and function. Seven ordinary cell types of the frontal part of the filamental epithelium are described.

Photomicroscopy and scanning electron microscopy were used to study the mechanism of food transportation on the gill filament. The functions of the groups of ciliated cells in the transportation of food are demonstrated by feeding the corbiculus with an ovoid-shaped alga, *Chlorella acuminata*. Because of the special shape and green color of these algae, the process of food transportation can be clearly observed and described. The size of food particles which suits *C. fluminea* M. is also discussed.

INTRODUCTION

Studies of the biology of *Corbicula* of a parasite and the minute structure of the gill surface have been reported[1-4]. Lo and Huber (1977) have described the gill of lamellibranch molluscs, *Corbicula fluminea* Müller, as possessing a highly specialized ciliary apparatus that consists of several distinct types of ciliated cells arranged in a regular manner. These ciliated apparatus on the gill filaments are concerned with the movement of water, retention, sorting, and transport of solid materials[4]. The optical and electron microscopic studies on the gill structure and on the movement of cilia of some marine mussels have been illustrated by Atkins (1936, 1937, 1938), Gibbons (1961), Moor (1971) and Owen (1974, 1976)[5-14]. But few papers have been published on the histochemistry of these ciliated cells of gill filament.

In the present study, both optical microscopy and scanning electron microscopy techniques have been used on *C. fluminea* M. to

investigate the histology and histochemistry of the gill filaments and the function of filamental cells in the feeding mechanism.

MATERIAL AND METHOD

The fresh water bivalves, *Corbicula fluminea* Müller, were collected for this study and treated with the following methods for observation.

(A) **The food transportation**

Food transportation was demonstrated by feeding a suspension of algae, *Chlorella acuminata*, for 3 minutes and the details of the process were worked out by removing the gill plate to a slide and observing the motion of the green algae over the surface under the microscope. The cilia were still beating after dissection. The ciliary current of the gill, which transported the food particles, was observed.

(B) **The cells of the gill-filament**

The gills were fixed in Zenker's and Carnoy's fixatives, then embedded in paraffin, and then sectioned 5 μ in thickness. The sections were stained with the following methods: 1. Hemotaxylin-Eosin stain; 2. Periodic acid—Schiff's reagent stain; 3. Mallory's triple stain; 4. Feulgen's stain; and then examined with a bright-field compound microscope.

(C) **The ultrastructure of the gill-filament**

Two different methods were used for this study:

1. For the observation of surface structure: The gills were fixed in 2% glutaldehyde and post-fixed in 1% Osmic acid. After dehydration in the alcohol series, the gills were dried in a CO_2 critical point apparatus.

2. For the observation of internal structure: The gills were fixed in 10% formalin and then embedded in paraffin; sections of 20 μ in thickness were then made and mounted on the coverglass. The specimens were deparaffinized in Xylene twice, then washed in absolute ethyl alcohol twice, and dried in a CO_2 critical point apparatus.

The dried specimens were coated with carbon and gold in that

sequence. Micrographs were taken with JSM–15 at 15 KV.

OBSERVATIONS AND DISCUSSION

(A) Anatomical note

The general gill structure of *Corbicula fluminea* has been described[4]. The following brief note is intended only to introduce the present study.

Two demibranches occur, the outer rather smaller than the inner on each side of the foot. The demibranches are broadly plicate. There are about nine to sixteen filaments to the plica. In the living noncontracted gills the plicae are broad and low, but contraction of the gill occurs during fixation, and the plicae become steep. Usually the filaments are 3.3 μ to 10.3 μ apart in preserved specimens. The ciliary apparatus appears in a regular manner on the gill filament.

(B) Histology and histochemistry of gill filament

The limbs of adjacent filaments are discontinuously connected together by growth of tissue—vascular tissue in general (Fig. 1). So all the gill filaments are joined together to form lamellae. Each demibranch consists of two lamellae.

There are two types of filaments, the larger principal filaments and the smaller ordinary filaments. The principal filament usually lies at the bottom of the crest groove. Between the principal filaments of two lamellae, interlamellar junctions are present (Fig. 1). The interlamellar junctions may be complete or incomplete.

The ostia frequently lie between gill filaments. Water is drawn through the ostia into the intralamellar space. The water in the intralamellar space may be transported to the dorsal excurrent water tube by the contraction of the gill-muscles because the abfrontal surface of the filament of *C. fluminea* is free of cilia.

There are two cords of supporting structures running along the inner surface of the filamental epithelium. These supporting structures stain intensely blue with Mallory's triple stain, and are PAS positive. These reactions indicate that the supporting structure is not chitin, which is common in many species of clams shown by

Atkin (1936, 1937, 1938), but probably is fibrous connective tissue. Chitin is also PAS positive, but it stains red with Mallory's triple stain.

The main part of the gill filament is covered with various cuboidal or cylindrical ciliated cells and secretory cells. There are great differences in size, composition, distribution and in the surface specialization (Figs. 2 and 3). The epithelium of the two opposing surfaces of the outer gill is clearly discernible, as shown in Fig. 4 and Fig. 5, respectively. Figs. 4 and 5 are diagrammatic representations of the cross sections of the gill filaments which are with or without the special large frontal cirri. The filamental epithelium of both surfaces of the inner gill is similar to that of the external surfaces of the outer gill.

As shown in Figs. 4 and 5, six to seven ordinary cell types are found in the frontal part of the filamental epithelium. They will be described in the following paragraph.

(1) *The frontal cells*

There are three or four rows of elongated ciliated cells, $8.5\mu \times 1.3\mu$ in size, at the center of the frontal surface of the gill filament. Each frontal cell contains a slender elongated nucleus, $5.5\mu \times 2.2\mu$, at the base of the cell. The larger diameter is perpendicular to the length of the filament. The chromatins are sparsely deposited in the nucleus (Figs. 6 and 9).

The frontal cells are rich in fine granular cytoplasm which is acidophilic or basophilic. Their reaction to PAS is weak (Fig. 8). They stain deep red with Mallory triple stain (Table 1 and Fig. 7).

The frontal cilia shown in Figs. 4 and 5 are not at their full length because they are generally cut shorter in sections. The number of cilia which arise from a cell is not certain. The frontal cilia tract is about 12μ to 15.3μ in width.

(2) *Special large frontal cells*

There is a row of larger cells present on the posterior side of the frontal surface of each filament of the external lamellae of the outer and of both lamellae of the inner demibranch. These large frontal cells are cylindrical, $8.5\mu \times 5.2\mu$. The ellipsoid nucleus is

Table 1. The histochemical reaction of different cell types in the gill filament of *C. fluminea* M.

	Frontal cell	Special large frontal cell	Pro-latero-frontal cell	Eu-latero-frontal cell	Mucous cell I	Lateral cell	Mucous cell II
Nuclear diameter	5.5–2.2 μ	7.2–3.6 μ	4.3–2.4 μ	7.5–5.3 μ	5 μ	3–1.6 μ	5 μ
Staining reaction:							
Hematoxylin (Cytoplasm)	+	+	+	##	–	–	–
Eosin (Cytoplasm)	+	##	+	##	–	–	–
Mallory triple stain (Cytoplasm)	Red ##	Red +	–	Red ##	Red & Blue + +	Red ##	–
Periodic acid—Schiff's reagent (Cytoplasm)	+	+	+	##	###	##	###
Feulgen's stain (Chromatin)	Sparse	Sparse	Compact	Compact	Sparse	Compact	Sparse

###: Very strong reaction
##: Strong reaction
#: Moderate reaction
+: Weak reaction
–: Negative reaction

also larger than that of the ordinary frontal cell, which is about 7.2 μ × 3.6 μ. Chromatins are loosely distributed. The cell has little cytoplasm and this contains acidophilic and basophilic fine particles. These cells stain with Eosin more intensely than the frontal cells. The cells show weak positive reaction to PAS. The staining characteristic of Mallory's triple stain is similar to that of the frontal cells but less intensive (Figs. 6, 7, 8, 9, and Table 1). There is one special frontal cirrus in one cell (Fig. 3). The cirrus consists of ten to fifteen very long cilia, about 32 μ in length, spaced closely together. The diameter of the base of these cirri is about 0.2 μ. Atkins (1937) suspected that the function of these cirri is to remove sand grains from lamellae. The present studies show that the cirrus is responsible for movement of the mucus sheet which may be with or without food.

(3) *Pro-latero-frontal cells*

There is a single, regular row of small, narrow elongated cells on each side of the frontal surface. Each cell bears a pro-latero-frontal cilium. The sizes of cells and nuclei are 8.5 μ × 2.2 μ and 4.3 μ × 2.4 μ, respectively. The cytoplasm contains fine acidophilic and basophilic particles. These cells give PAS positive reaction, but remain pale with Mallory's triple stain.

(4) *Eu-latero-frontal cells*

The cells from which the large eu-latero-frontal cirri arise are very large and contain one bulky triangular nucleus, 7.5 μ × 5.3 μ. The nuclei of the eu-latero-frontal cells have a stronger affinity to basic dyes than the nuclei of the other cells of the gill. The compact material of the nucleus stains strongly with Feulgen's stain. These results reveal that the eu-latero-frontal cells contain a large amount of DNA. It is possible that an eu-latero-frontal cell is a syncytium.

The cytoplasm is rich in acidophilic and basophilic fine particles, and in PAS positive coarse particles. The cytoplasm also stains deep red with Mallory's triple stain. The histochemical results indicate that the contents of eu-latero-frontal cell are complicated.

(5) *Mucous cell type I*

The nonciliated tract between the lateral and eu-latero-frontal cells is narrow, 9 μ in width. The mucous cell type I usually seems to occur mostly in this region of both the anterior and the posterior side of the gill filament. This triangular cell has a large spherical nucleus. Large granular substances stain but faintly with Eosin. The PAS reaction is strong. The mucous cell type I is the only cell of the gill filament which stains red and blue with Mallory's triple stain (Figs. 6, 7, 8, 9).

(6) *Lateral cells*

The long and very narrow cells bearing the long lateral cilia are in five rows, those nearest to the abfrontal surface being especially narrow. More than seven cilia arise from a cell. The nucleus is similar to that of the pro-latero-frontal cells. The cytoplasm contains PAS positive coarse particles which are sparsely distributed (Figs. 6, 7, 8, 9).

The cilia are very long, 15.5 μ in length. The materials which stick to the lateral cilia show reactions similar to the cytoplasm of mucous cell type II.

Because of the narrow nonciliated tract between the lateral and eu-latero-frontal cells, the tips of the lateral cilia extend upward to the level of the frontal surface, but there still remains a gap.

(7) *Mucous cell type II*

Near the base of the gill filament there are mucous cells type II which may appear frequently on either the anterior or the posterior side. These cells are regular in shape. The nucleus is round, 5 μ in diameter.

The cells contain many very large PAS positive granulae. These granulae remain virtually unstained with the other methods employed (Figs. 6, 7, 8, 9).

(C) **The ciliation and food transportation**

The different functions of the groups of cilia in the transportation of the food are demonstrated by feeding the corbiculus with ovoid shaped algae, *Chlorella acuminata*. Because of the special shape and green color of these algae, the process of transportation can

clearly be observed (Fig. 10). The ciliary current, which is the result of the rapid beating toward the gill surface and ventral end of the gill plate of the lateral cilia, will transport the algae to the frontal surface of the gill filament. The algae are then trapped by eu-latero-frontal-cirri which beat mainly across the length of the filament (Fig. 15). The beating of eu-latero-frontal cirri is not synchronous. They form an undulating tract. This may also be good for food transportation. The trapped algae are limited to the frontal tract and are sent to the ventral end of the gill plate by the frontal cilia which beat toward the ventral direction (Fig. 12). Finally, the algae arrive at the ventral edge of the gill filament (Fig. 13). The food groove at the ventral edge of the inner demibranch is well marked; that of the outer demibranch, however, is very slightly marked.

On each filamental lobe of the marginal groove, on the side facing the groove, is a transversely-oriented semicircular-shaped group of long and coarse cilia, called guarding cilia (Fig. 14). These cilia beat powerfully and quickly so that the large food particles, such as algae, will be sent along the tip of guarding cilia to the direction of the labial palp and mouth.

The bottom of the marginal groove of the inner demibranch is also lined with many fine cilia. When these are closely observed, we can see that the smaller food particles, such as bacteria, are transported along the bottom of the food groove and finally also sent to the mouth.

The mucus which occasionally covers the gill filament often forms a complete sheet on the eu-latero-frontal cirrus. Moore (1971) stated that it is "unlikely that a mucus sheet would cover, and thus put out of action, such a highly specialized filtration system as the latero-frontal cirri provide". On the contrary, the mucus of *C. fluminea* occasionally covers the gill filament and often forms a complete sheet on the eu-latero-frontal cirrus (Fig. 11). The mucus which occasionally covers the gill filament seems to have special meaning in food transportation. Under some conditions, such as when a great number of algae are present on the gill surface at the

same time, the gill will be stimulated and will secrete mucus. The mucus will be mixed with the algae to form a mucus-food sheet. These sheets will move over the surface of the gill ciliary tract to the ventral food groove, propelled by a rapid current which results from a rapid beating of the special large frontal cilia to the ventral end of the gill plate. This mucus-food mass is also sent to the mouth along the food groove.

Usually the size of food particles will influence the transportation rate along the ciliary tract. The food particles which are not larger than 10 μ will be transported quickly through the transport tract (Fig. 15). The net of eu-latero-frontal cirri will retain the smaller food particles. Lo and Huber[4] (1977) have reported that the mesh size of eu-latero-frontal cirri is 0.9 $\mu \times$ 0.2 μ. The small mesh size of eu-latero-frontal cirri will enable them to retain the food particles. Food particles whose diameter is larger than 12 μ are not suitable for feeding. As shown in Fig. 16, a large Phytomastigophora is trapped by eu-latero-frontal cirri, but it cannot move because the frontal cilia are too weak to transport or even to support it. It seems difficult to throw this large unwanted protista out of the tract. The result is a blockage of the transport tract.

REFERENCES

(1) Villadolid, V. and F. G. Del Rosario (1930). Some studies on the biology of tulla (*Corbicula manillensis*), a common food clam of Laguna De Bay and its tributaries. *Philippine Agriculturist, Vol. XIX, No. 6*, 355-381.

(2) Sinclair, R. M. and B. G. Isom (1963). Further studies on the introduced asiatic clam (Corbicula) in Tennessee. *Thesis.*

(3) Huber, F., C. F. Lo and C. H. Wang (1975). A study of *Lophotaspis orientalis* in corbicula (Trematoda: Aspidogastridae). *Bull. Inst. Zool.*, Academia Sinica **14**(1), 1-7.

(4) Lo, C. F. and F. Huber (1977). A study of the gill of *Corbicula fluminea* Müller. I. The minute structure of the gill surface. *Proceedings of National Science Council No. 10.*

(5) Atkins, D. (1936). On the ciliary mechanisms and interrelationships of lamellibranches. I. New observations on sorting mechanism. *Q. J. Microsc. Sci.* **79**, 181-308.

(6) Atkins, D. (1937a). On the ciliary mechanisms and interrelationships of lamellibranches. II. Sorting devices of the gills. *Q. J. Microsc. Sci.* **79**, 339-370.

(7) Atkins, D. (1937b). On the ciliary mechanisms and interrelationships of lamellibranches. III. Types of lamellibranch gills and their food currents. *Q. J. Microsc. Sci.* **79**, 375-419.

(8) Atkins, D. (1938a). On the ciliary mechanisms and interrelationships of lamellibranches. VI. Pattern of the latero-ciliated cells of gill filaments. *Q. J. Microsc. Sci.* **80**, 330-344.

(9) Atkins, D. (1938b). On the ciliary mechanisms and interrelationships of lamellibranches. VII. Latero-frontal cilia of the gill filaments and their phylogenetic value. *Q. J. Microsc. Sci.* **80**, 346-430.

(10) Gibbons, I. R. (1961). The relationship between the fine structure and direction of beat in gill cilia of a lamellibranch mollusc. *J. Biophys. Biochem. Cytol.* **11**, 179-205.

(11) Owen, G. (1974). Studies on the gill of *Mytilus edulis* of the eu-latero-frontal cirri. *Proc. R. Soc. Lond. B.* **187**, 83-91.

(12) Owen, G. and J. M. McCare (1977). Further studies on the latero-frontal tract of bivalves. *Proc. R. Soc. Lond. B.* **194**, 527-544.

(13) Moore, H. J. (1971). The structure of the latero-frontal cirri on the gills of certain lamellibranch mollusca and their role in suspension feeding. *Mar. Biol.* **11**, 23-27.

(14) Morton, B. (1973). Some aspects of the biology and functional morphology of the organs of feeding and digestion of *Limnoperna fortunei* Dunker (Bivalvia: Mytilacea). *Malacologia*, **12**(2), 265-281.

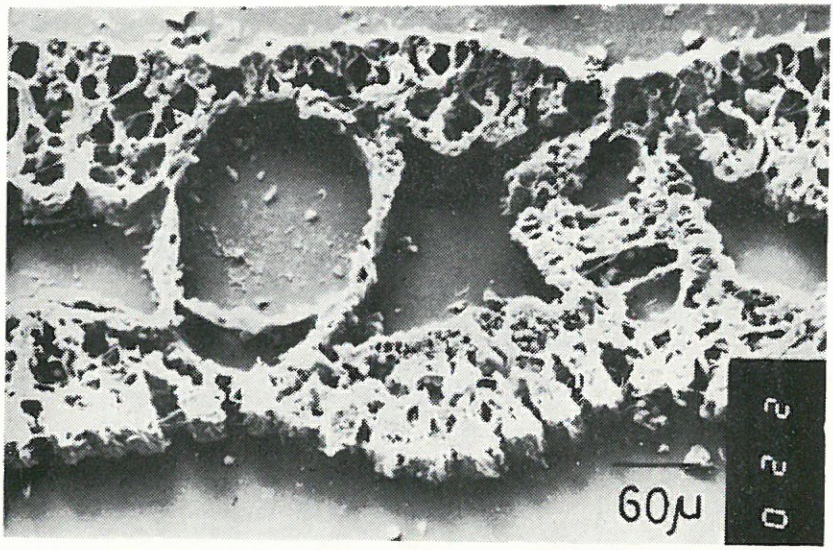

Fig. 1. Scanning electron micrograph of a cross section of the outer gill plate of *C. fluminea* M. showing the interlamellae junctions between principal filaments of opposing lamellae.

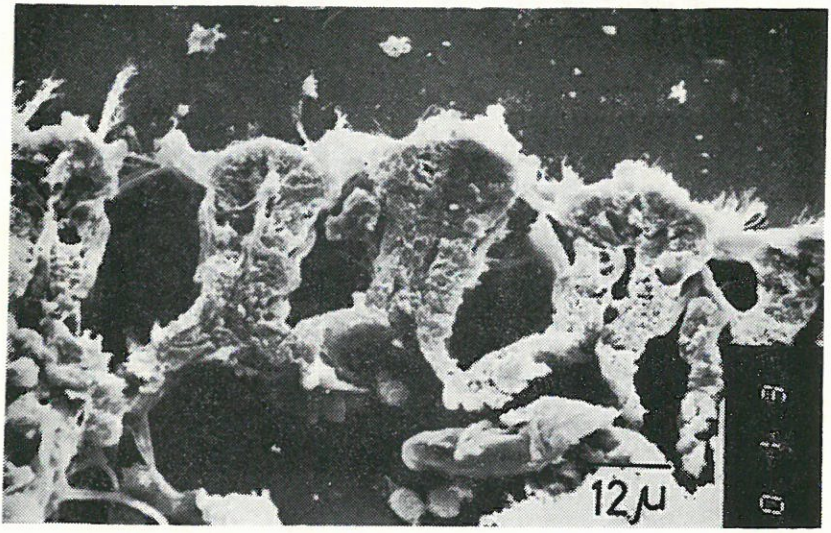

Fig. 2. Scanning electron micrograph of a cross section of four gill filaments showing the ciliation of internal lamella of gill plate.

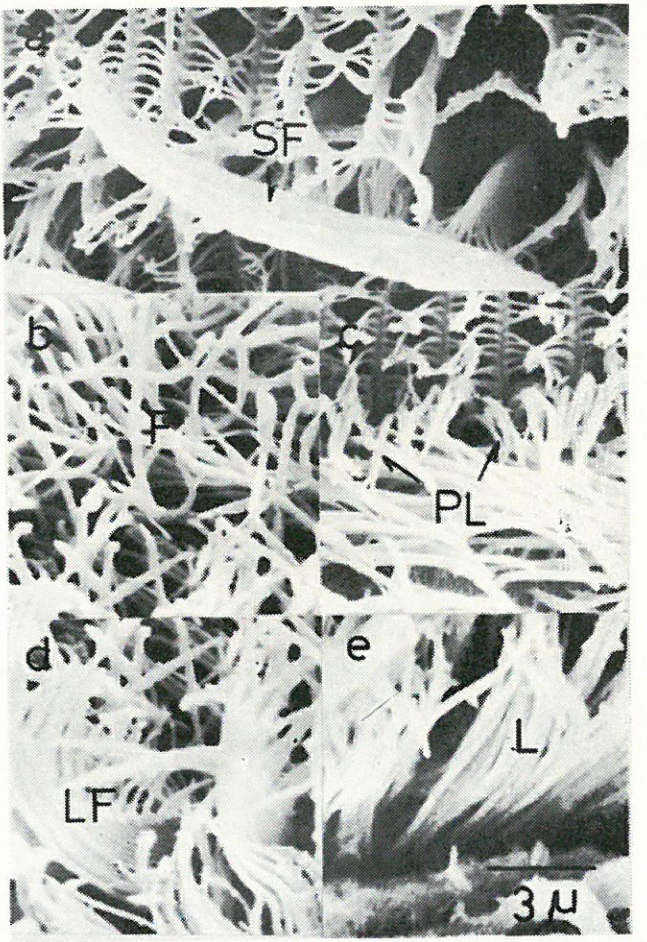

Fig. 3. Scanning electron micrographs of the gill surface showing the cilia or cirri of
a. Special frontal cell
b. Frontal cell
c. Pro-latero-frontal cell
d. Eu-latero-frontal cell
e. Lateral cell

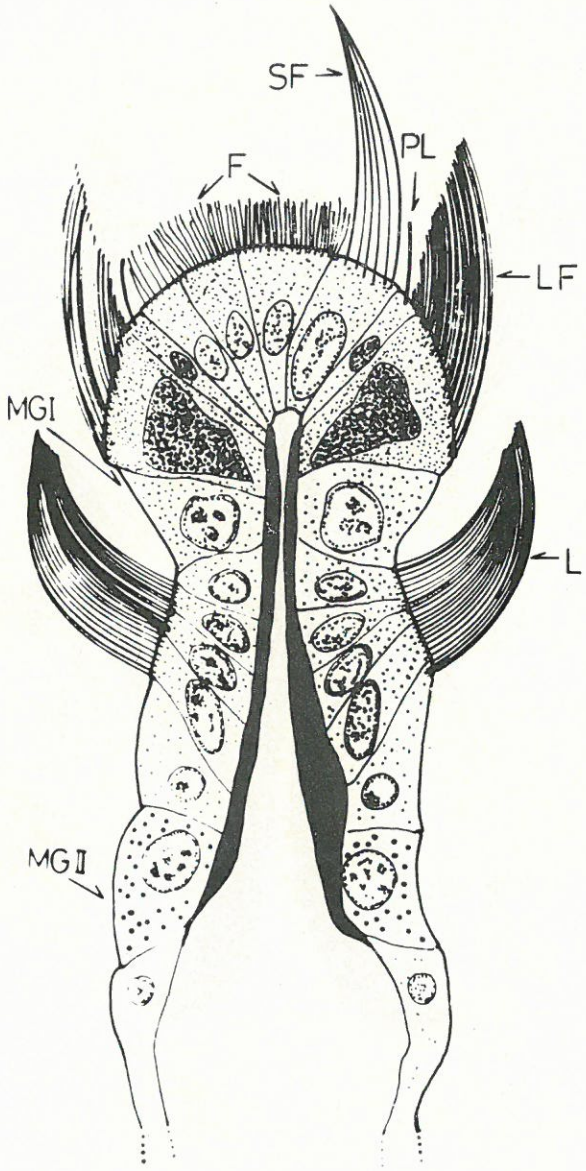

Fig. 4. Diagrammatic drawing of a cross section of external lamella filament showing the arrangement of cells.
F. frontal cilia; L. lateral cilia; LF. eu-latero-frontal cirri; MG I & II. Mucous cell I & II; PL. pro-latero-frontal cilia; SF. special large frontal cirri.

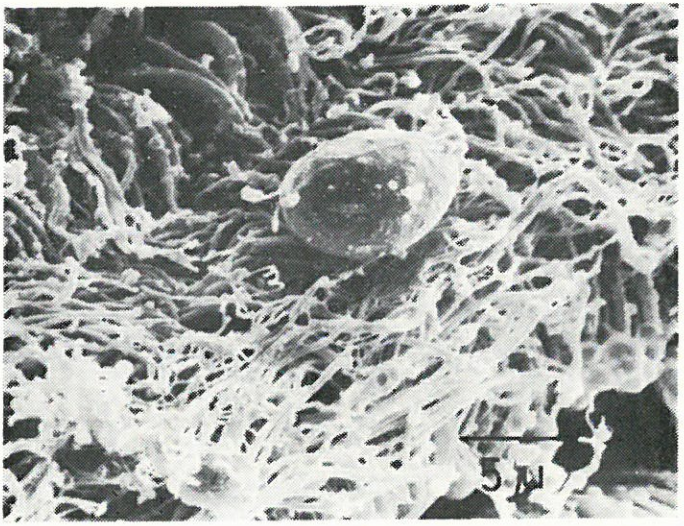

Fig. 10. Scanning electron micrograph of the gill surface showing the ovoid-shaped green alga on the frontal tract.

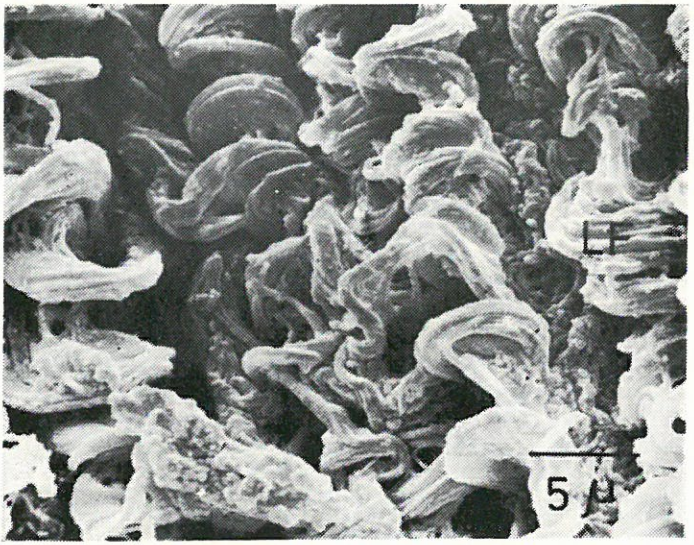

Fig. 11. Complete sheet of mucus covering the eu-latero-frontal cirri. LF. eu-latero-frontal cirrus.

A COMPARISON OF THE EFFECTS OF SOME EDIBLE FATS AND OILS ON SERUM CHOLESTEROL IN GROWING RATS

CHING-MIN TSAI, CHERN-GUANG MING,
JYH-PYNG LEU and JAU-YN WU

ABSTRACT

Diets supplemented with 5% lard, margarine, olive, peanut, salad and corn oils, respectively, caused higher serum cholesterol than a diet without additional fats or oils. It is widely believed that vegetable oils increase cholesterol less than animal fats. The data of this study, however, show that margarine and olive oil increased serum cholesterol levels as much as lard. Comparison of our results with the content of linoleate in the fats and oils shows that increasing the linoleate content decreases serum cholesterol accumulation in the serum. However, the amount of fat intake seems to play a more important role in determining serum cholesterol than linoleate content.

INTRODUCTION

More and more people are becoming aware that the blood lipid level, particularly of cholesterol, is positively associated with the risk of developing coronary heart disease and allied with atherosclerotic disease[1]. Serum cholesterol concentration in population studies is correlated with the proportion of dietary calories derived from fat. Saturated and unsaturated fats appear to be the main dietary components responsible for this relationship. Difference in serum lipid levels and *per capita* fat consumption between the population of the industrially developed and undeveloped countries are very impressive and support the hypothesis that serum cholesterol levels are determined to a large degree by fat consumption[2].

In Taiwan, cardiovascular disease has become a major public health problem in recent years. It ranks first among the ten major causes of death. The cooking oils people consume in Taiwan are somewhat different from those in western countries. Lard, salad and peanut oils are most commonly used in Taiwan. In addition to

lard, salad and peanut oils, margarine, olive and corn oils, mixed respectively with commercial feed, were fed to growing rats in order to study the effects of different edible fats and oils on serum cholesterol content.

MATERIAL AND METHODS

Thirty-five male Wistar rats ranging in body weight from 40–45 g were assigned randomly to 7 dietary treatment groups, 5 replicate for each. Commercial basal diet (Taiwan Sugar Co.) supplemented with 5% lard, margarine (Milk Marrine Far East Margarine Product of Taiwan), olive, peanut, salad, corn oils and blank, respectively, were employed in the study. Each rat was fed 10 g of the assigned diet per day for the first 2 weeks and 12 g for the next 3 weeks with water *ad libitum*.

All rats were housed individually in stainless steel cages and the animal room was maintained at 20–25°C. Animals were sacrificed 24 hours after the last feeding. Blood was collected by cardiac puncture into a vacuum tube for serum cholesterol determination. From the blood sample, serum was obtained by centrifuge at 2500 rpm for 10 minutes, after 2 hours' refrigeration at 4°C. Then serum cholesterol was determined by the Searcy and Bergquist Method[3]. All data were subjected to an analysis of variance and difference between means[4].

RESULTS AND DISCUSSION

Many investigators have shown that the blood cholesterol responds to quantitative alterations in the intake of fats and oils. In general, people agree that animal fats raise the serum cholesterol, whereas vegetable oils lower it[6,7]. Kinsell, Ahrens and Beveridge reported that the polyunsaturated oils produce a decrease in serum cholesterol, while isocaloric amounts of the saturated fats increase levels of serum cholesterol[6].

In this study, it was observed that the levels of serum cholesterol were higher for rats fed lard, margarine and olive oil than those fed peanut, salad and corn oil. The percentage of linoleic acid content

decreases from corn oil to olive oil in the following fashion: corn oil > salad oil > peanut oil > lard > olive oil (Table 1). Comparing this order with the serum cholesterol data of this study, it was found that linoleic acid has the effect on lowering serum cholesterol. But the mechanisms are not clear. Previously, investigators demonstrated the increased excretion of cholesterol and its metabolites[6]. Others reported that linoleate caused a redistribution of cholesterol from plasma into other tissues[6]. Recently, Van Drop *et al.* and Bergstrom *et al.* independently discovered that linoleate is a direct precursor of prostaglandins[8]. The levels of dietary linoleic acid resulting in significant effects on the different criteria ranged from 12 to 22 cal. percent concentration[3].

Table 1. Serum Cholesterol Content[a] in the Growing Rats

Rat No.	Treatment[b]						
	Lard[c]	Magarine	Olive oil[d]	Peanut oil[e]	Salad oil[f]	Corn oil[g]	Blank
1	236	236	275	169	118	170	163
2	180	228	371	163	146	135	79
3	225	236	258	169	191	89	120
4	190	259	135	157	214	158	90
5	202	180	337	281	169	236	143
Mean	207	228	275	188	168	158	120

a. mg cholesterol/100 ml serum.
b. 5% fat or oil added to the basal diet.
c. Iodine number, 66.5; oleic acid, 49.4%; linoleic acid, 12.3%[5].
d. Iodine number, 89.7; oleic acid, 89.5%; linoleic acid, 7.6%[5].
e. Iodine number, 93; oleic acid, 56.5% linoleic acid, 25.8%[5].
f. Iodine number, 135.8; oleic acid, 22.9%; linoleic acid, 55.2%[5].
g. Iodine number, 126.8; oleic acid, 33.5%; linoleic acid, 55.7%[5].

Margarine is made from vegetable oils. However, it increased the serum cholesterol as much as lard. This might be due to the hydrogenation of hardening, which could decrease the cholesterol depressing effect through its saturation[7,9-11].

Olive oil, a vegetable oil, increased serum cholesterol accumulation more than any other vegetable oil ($P<.01$), and even more than lard

($P<.10$). This might be due to the high oleic acid content in olive oil[6,7,11-13].

Peanut oil promoted serum cholesterol slightly higher ($P<.10$) than corn and salad oils. This might be because peanut oil has a lower linoleic acid content than corn and salad oils. Moreover, peanut oil contains a high quantity of long-chain saturated fatty acids, such as arachidic acid and behenic acid[8], which might have a cholesterol-raising effect[6,7,13,14].

It was observed that all fats and oils caused higher serum cholesterol than the blank. These findings suggested that, though linoleic acid has a serum cholesterol depressing effect, fat intake plays a more important role in determining serum cholesterol.

In order to prevent a high cholesterol intake, many people use margarine as a replacement for animal fats. In this study, however, it was observed that margarine caused very high levels of serum cholesterol. Therefore, margarine is not recommended to replace animal fat in cooking. Furthermore, the oils with high linoleate content are recommended to be used in cooking in order to lower serum cholesterol and thereby to prevent atherosclerosis.

REFERENCES

(1) Whyte, H.M. and N. Havenstein. A perspective view of dieting to lower the blood cholesterol. *Amer. J. Clin. Nutr.* **29**, 784, (1976).
(2) Nichols, A.B., C. Ravenscroft, D.E. Lamphiear and L.D. Ostrander. Daily nutritional intake and serum lipid levels; the Tecumseh study. *Amer. J. Clin. Nutr.* **29**, 1384, (1976).
(3) Searcy, R.L. and L.M. Bergquist. A new color reaction for the quantitation of serum cholesterol. *Clin. Chem. Acta* **5**, 192, (1960).
(4) Freund, J.E. *Modern Elementary Statistics*, Ed. 4. Prentice-Hall, Inc., Englewood Cliffs, N.J. pp. 247, (1973).
(5) Dugan, L., Jr. *Principles of Food Science*, Part 1, *Food Chemistry*. Marcel Dekker Inc., N.Y., (1976).
(6) Goodhart, R.S. and M.E. Shils. *Modern Nutrition in Health and Disease; Dietotherapy*, 5th ed. Lea & Febiger, Phila., (1974).
(7) Horlick, L. and B.M. Craig. Effect of long-chain polyunsaturated & saturated fatty acids on the serum-lipids of man. *Lancet* **273**, 566, (1957).
(8) Hwang, D.H., M.M. Mathias, J. Dupont and D.L. Meyer. Linoleate enrichment of diet and prostaglandin metabolism in rats. *J. Nutr.* **105**; 995, (1975).

(9) Anderson, J. T., F. Grande and A. Keys. Independence of the effects of cholesterol and degree of saturation of the fat in the diet on serum cholesterol in man. *Amer. J. Clin. Nutr.* **29**, 1184, (1976).

(10) Beveridge, J. M. R. and W. F. Connell. The effect of commercial margarines on plasma cholesterol levels in man. *Amer. J. Clin. Nutr.* **15**, 391, (1962).

(11) Mattson, F. H., E. J. Hollenbach and A. M. Kligman. Effect of hydrogenated fat on the plasma cholesterol and triglyceride levels of man. *Amer. J. Clin. Nutr.* **28**, 726, (1975).

(12) Chang, S. S. S. *The chemistry of edible fats and oils.* Food Industry Research and Development Institute, Taiwan. (1975).

(13) Malmros, H. and G. Wigand. The effect on serum-cholesterol of diets containing different fats. *Lancet* **273**, 1, (1957).

(14) Grande, F., J. T. Anderson and A. Keys. The influence of chain length of the saturated fatty acids on their effect on serum cholesterol concentration in man. *J. Nutr.* **74**, 420, (1961).

IGNORANCE

This man must be very ignorant, because he answers every question he is asked.

VOLTAIRE

PREPARATION AND EVALUTION OF SOYBEAN CURD*

WEN-LI JWUANG, S. Sp. S.

ABSTRACT

Soybean curd can be prepared from soybean milk by adding either glucano-delta-lactone (G. D. L.) or calcium sulfate as a coagulant. Soybean curd coagulation is temperature and pH dependent. Soybean milk was precipitated by G. D. L. at pH 5.4 and at pH 6.4 to 6.8 by calcium sulfate. The optimum coagulating temperature for both was 70° to 80°C. As the concentration of soy milk increased, a better consistency of soybean curd was obtained. The addition of starch and an increase in the soy-protein concentration in soy milk improved the keeping quality of soybean curd and gave it better water-holding capacity and stronger gel strength.

INTRODUCTION

Soybean milk and soybean curd are widely used as daily foods by people in the Orient. Certain mineral salts and acids are employed to precipitate soybean curd from soybean milk. If the precipitated mass is allowed to drain and is subsequently washed, a sort of white curd is produced which is called by the Chinese name "Tofu".

Miller *et al.*[1] indicate a low retention of thiamine (18%) when soybeans are made into soybean curd and preserved in water by the usual commercial process. They also indicate that the water drained from the soybean curd contains more vitamins than the tofu itself. Storage of the blocks of tofu causes further reduction in the amount of water and water soluble nutrients present. Jackson[2] (1972) prepared soybean cheese using soybeans, skim milk powder, rennet, and lactic starter cultures. He attempted to reduce the beany flavor but was unsuccessful. However, he did manage to improve the keeping quality over that of traditional Chinese soybean curd. Schroder

* The experimental part of this study was done at the Michigan State University, East Lansing, MI, U. S. A.

and Jackson[2] performed a study in which they attempted to improve the flavor of soybean curd by removing the beany taste. The resulting soybean curd was acceptable to American taste panels but not to Oriental panels.

Calcium sulfate precipitation of the soybean milk gives rise to a bland soybean curd that can be varied in texture according to requirements. Glucano-delta-lactone (G.D.L.) has been tested both by Japanese and Chinese food researchers in the production of soybean curd, using G. D. L. to adjust the pH value to approximately 5.4. This yields a firm, smooth, compact mass of curd with a better water-holding capacity than curd precipitated with calcium sulfate ($CaSO_4 \cdot 2H_2O$).

Gelation of the heated soybean protein dispersions give cohesiveness to the molded tofu, helping to form a compact, firm yet soft, body of cold tofu. Meyer *et al.*[3] (1964) state that the rate of gelling and gel firmness are dependent primarily on temperature, duration of heating, and protein concentration.

This present study attempts to improve the consistency and the water-holding capacity of the soybean curd by reviewing traditional methods of production and more recent studies by food researchers. Such an improvement is necessary in order to meet the requirements for the type of fresh, soft curd used in food production.

MATERIALS AND METHODS

The production of soybean curd consists principally of two processes: the production of soybean milk and the production of soybean curd from soybean milk (Diagram 1).

Soybean Milk Production. The basic process for the production of soybean milk employed in this study was as follows: Whole soybeans, (Jack Rabbit brand, distributed by Michigan Bean Division of the Wickes Corp., Saginaw, Michigan 48605) were rinsed in tap water and soaked for 8 to 10 hours at room temperature (25°C). After soaking, the soybeans were drained and rinsed in tap water. Equal amounts of water and soybeans were blended together in a Waring blender for about two minutes. The resulting soybean slurries

Diagram 1. Flow sheet for the production of soybean milk and soybean curd

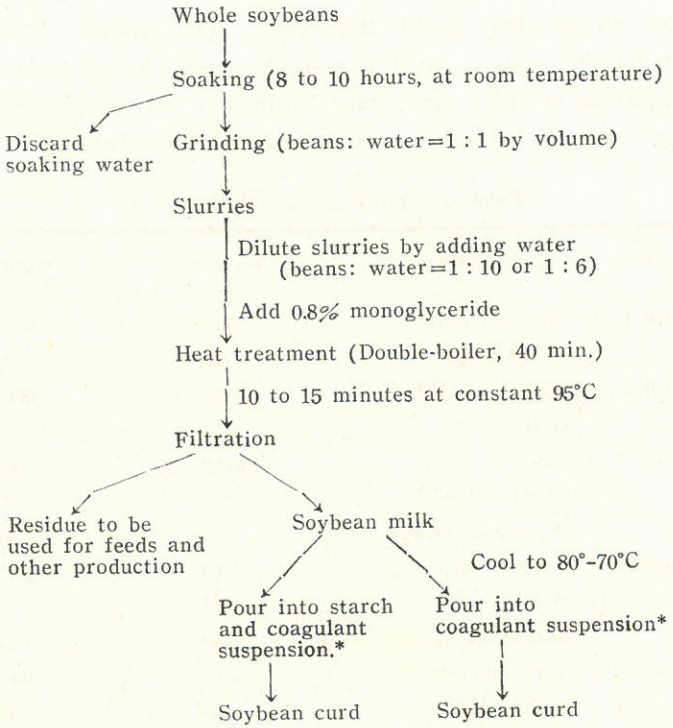

were diluted with water to the desired concentration. Two different concentrations of soybean milk were prepared by adjusting the ratio of water to dry beans to 10:1 and 6:1, respectively. 0.8% monoglyceride as an antifoaming agent was added to the slurries. The diluted slurries were then heated in a double-boiler for forty minutes or heated until the temperature reached 95°C for 10 minutes. The heated slurries were filtered through six layers of cheese cloth to yield two fractions, namely, a coarse residue and a soybean milk.

* Coagulant suspension is prepared by mixing two parts of diluted soybean milk to one part of coagulating agent; this helps to obtain a homogenous mixture of soybean milk and coagulant since the $CaSO_4 \cdot 2H_2O$ is difficult to dissolve in water. G. D. L. easily dissolves in water; therefore it is a very convenient coagulant for producing instant soybean curd.

Soybean Curd Production. The hot soybean milk was cooled to 80°–70°C, and precipitated with 0.5% of $CaSO_4 \cdot 2H_2O$ and 0.3% G. D. L. Agitation was strictly avoided after the soybean milk had been poured into the coagulating agent. The ambient temperature for setting the soybean curd was kept at 80°C for 15 to 20 minutes. Finally, a custard-like curd was obtained. The basic formula for soybean curd and its variations are tabulated in Table 1.

Table 1. Soybean Curd Formulas

Samples	Ingredients	% by weight	Weight (g.)
Control 1	Soybean milk[a]	100.0	400.0
	$CaSO_4 \cdot 2H_2O$	0.5	2.0
Control 2	Soybean milk[a]	100.0	400.0
	G. D. L.	0.3	1.2
Variable 1	Soybean milk[a]	100.0	400.0
	$CaSO_4 \cdot 2H_2O$	0.5	2.0
	Waxy-rice starch	1.0	4.0
Variable 2	Soybean milk[a]	100.0	400.0
	G. D. L.	0.3	1.2
	Waxy-rice starch	1.0	4.0
Variable 3	Soybean milk[b]	100.0	400.0
	$CaSO_4 \cdot 2H_2O$	0.5	2.0
Variable 4	Soybean milk[b]	100.0	400.0
	G. D. L.	0.3	1.2

a Soybean milk concentration, water to bean ratio 10 : 1.
b Soybean milk concentration, water to bean ratio 6 : 1.

When waxy-rice starch was used as a coagulant (cf. variables 1 and 2, Table 1) the procedure of production had to be changed. The very hot soybean milk (above 95°C) was directly mixed with a small amount of waxy-rice starch. Coagulation was completed at 72°C in a short time.

The resulting curd was allowed to cool at room temperature and was stored in the refrigerator overnight. Two samples of each variation were prepared and placed in plastic containers (10×10×8 cm^3). The approximate size of the resulting curd was 10×10×5 cm^3.

One sample of each variation was used for the sensory evaluation by six trained Oriental taste panels; the other samples were used for physical tests such as sheer press value and moisture tests. The collected curd from the sheer press test was used for calculating the percentage yield and the percentage moisture content of the soybean curd. All the undrained samples were put into a miniature tofu mold individually. Each sample was wrapped with a cheese cloth and pressed with a 2 kg weight for 15 minutes. These samples were then used for moisture tests.

All the experimental data were recorded and used for statistical analysis. A pre-test was carried out to give a final basic formula of soybean curd production which is shown in Table 1.

RESULTS: CHARACTERISTICS OF SOYBEAN CURD

Proximate evaluations for the soybean curd are shown in Tables 2, 3, 4, 5, and 6. These data include a total of 24 samples from six variations.

In this study, the undrained curd had a normal light-beany flavor and a firmer custard-like consistency. Table 6 indicates no significant difference ($p<0.05$) in internal color and flavor. All the six trained taste panels gave the same comments—that the soybean curd had a

Table 2. Weight and % yield of soybean curd per 400.0 grams of soybean milk

Variations	Weight of soybean curd (g.)*	% yield of soybean curd*
$CaSO_4 \cdot 2H_2O$, control	149.00 ± 8.41^{c}	37.25 ± 2.10^{c}
G. D. L., control	154.50 ± 24.40^{c}	38.63 ± 6.92^{bc}
$CaSO_4 \cdot 2H_2O$, 1% starch	177.50 ± 30.23^{bc}	44.38 ± 8.67^{abc}
G. D. L., 1% starch	180.25 ± 21.78^{bc}	45.06 ± 6.29^{abc}
$CaSO_4 \cdot 2H_2O$, bean:water=1 : 6	204.25 ± 12.34^{ab}	51.06 ± 5.79^{ab}
G. D. L., bean:water=1 : 6	217.75 ± 25.94^{a}	54.44 ± 7.49^{a}

* a, b, c, ab, bc, *etc.*: If two results in the same column share a common subscript (e.g. A^{ab}, B^{bc} have "*b*" in common) this means that they are not significantly different in a statistical sense ($p<0.05$). Results not sharing a common subscript are significantly different ($p>0.05$).

Table 3. Percent solids in curd and in whey

Variations	% solid in curd*	% solid in whey*
$CaSO_4 \cdot 2H_2O$, control	12.11 ± 0.79^{bc}	2.43 ± 0.09^{c}
G. D. L., control	12.15 ± 0.55^{c}	2.24 ± 0.10^{de}
$CaSO_4 \cdot 2H_2O$, 1% starch	13.24 ± 0.81^{ab}	2.26 ± 0.16^{d}
G. D. L., 1% starch	12.05 ± 0.38^{ab}	2.19 ± 0.13^{e}
$CaSO_4 \cdot 2H_2O$, bean:water=1 : 6	14.33 ± 0.62^{a}	3.71 ± 0.18^{b}
G. D. L., bean:water=1 : 6	13.26 ± 0.98^{ab}	3.71 ± 0.04^{a}

* see footnote of Table 2.

Table 4. pH values of soybean milk and whey

Variations	pH of soybean milk	pH of the whey
$CaSO_4 \cdot 2H_2O$, control	6.8	6.43 ± 0.04
G. D. L., control	6.8	5.44 ± 0.04
$CaSO_4 \cdot 2H_2O$, 1% starch	6.8	6.38 ± 0.04
G. D. L., 1% starch	6.8	5.49 ± 0.07
$CaSO_4 \cdot 2H_2O$, bean:water=1 : 6	6.8	6.40 ± 0.01
G. D. L., bean:water=1 : 6	6.8	5.50 ± 0.01

Table 5. Gel strength—sheer press of soybean curd (lb/force)**

Variations	% solid in soybean milk	sheer press (lb/force)*
$CaSO_4 \cdot 2H_2O$, control	5.26	0.47 ± 0.01^{c}
G. D. L., control	5.26	0.64 ± 0.04^{bc}
$CaSO_4 \cdot 2H_2O$, 1% starch	5.26	0.67 ± 0.03^{bc}
G. D. L., 1% starch	5.26	0.80 ± 0.05^{abc}
$CaSO_4 \cdot 2H_2O$, bean:water=1 : 6	8.96	0.99 ± 0.37^{ab}
G. D. L., bean:water=1 : 6	8.96	1.10 ± 0.09^{a}

* see footnote of Table 2.

** The soybean curd used for sheer press test is not separated from whey.

white color and a bland flavor; an additional comment was made that the G. D. L.-precipitated curd had a slightly sweet flavor. The G. D. L.-precipitated curd possessed a smooth, compact texture and no syneresis; on the other hand, the $CaSO_4$-precipitated curd had a few

Table 6. The sensory scores of soybean curd characteristics

Variations	Internal color*	Texture*	Absence of syneresis*	Flavor*	General acceptance*
$CaSO_4 2H_2O$ control	4.00 ± 0.12^a	3.42 ± 0.19^c	3.08 ± 0.19^c	3.25 ± 0.25^a	3.42 ± 0.42^d
G. D. L. control	4.21 ± 0.22^a	3.88 ± 0.14^{bc}	3.66 ± 0.20^b	3.59 ± 0.09^a	3.79 ± 0.15^b
$CaSO_4 2H_2O$ 1% starch	4.08 ± 0.25^a	3.58 ± 0.45^{abc}	3.75 ± 0.25^{ab}	3.50 ± 0.67^a	3.46 ± 0.46^{cd}
G. D. L. 1% starch	4.37 ± 0.08^a	4.08 ± 0.19^{ab}	3.80 ± 0.39^{ab}	3.33 ± 0.12^a	3.50 ± 0.12^c
$CaSO_4 2H_2O$ bean: water=1:6	3.92 ± 0.45^a	3.88 ± 0.18^{ab}	4.01 ± 0.21^{ab}	3.54 ± 0.24^a	3.75 ± 0.14^b
G. D. L. bean: water=1:6	4.17 ± 0.19^a	4.30 ± 0.27^a	4.14 ± 0.16^a	4.29 ± 0.22^a	4.25 ± 0.34^a

* see footnote of Table 2.

tiny holes that gave a loosely-bond texture and caused a moderate degree of syneresis. As the concentration of soybean milk increased, the degree of syneresis present in the $CaSO_4$-precipitated curd decreased. This fact is illustrated by the findings recorded in Table 6. Therefore in general acceptance, the G. D. L.-precipitated curd received higher scores than those of the $CaSO_4$-precipitated curd. Soybean curd prepared from a higher concentration of soybean milk was more acceptable than that from the less concentrated.

It is interesting to mention that, besides the six trained taste panels, there were twelve untrained taste panels who preferred the curd precipitated from calcium sulfate to that of G. D. L., because the calcium sulfate precipitated curd tasted similar to their homemade tofu. They complained that curd precipitated from G. D. L. contained certain unknown additives which gave a sweet flavor; but they also admitted that the curd prepared from G. D. L. had a finer texture than that of calcium sulfate curd.

The texture of the pressed curd can be modified according to the amount of water pressed out. In this study, a 2 kg weight was applied to each sample for fifteen minutes; the resulting curd had a smooth rubbery texture. In comparison, G. D. L.-precipitated curd had a firmer consistency than that of $CaSO_4$-precipitated curd. The

amount of the resulting curd was slightly higher after G.D.L. precipitation than after $CaSO_4$ precipitation. This was due to the fact that the G.D.L. resulting curd had a better water-holding capacity, and that the pH value of the G.D.L. final product was relatively close to the isoelectric point of soy protein. This fact is illustrated clearly in Table 4.

Table 3 indicates that the percent solid in whey increased as the concentration of soybean milk was increased. The percent solid content in whey separated from the G.D.L. precipitation was slightly less than that of the $CaSO_4$ precipitation, except for variables 3 and 4, which showed the opposite result (Table 3). These two variations were prepared from soybean milk of higher concentration (bean: water=1:6). Variables 1 and 2 with addition of 1% waxy-rice starch showed significant difference ($p>0.05$) in decreasing amount of solid content in whey. This was due to the fact that the thickening power of starch made it a very valuable agent in changing a predominantly liquid mixture into a solid form, thereby helping to minimize the loss of solid content in whey. The loss of soluble solid in whey was considered by Miller[1] in a previous study. But since then, there has been no attention paid to minimizing the loss of nutrients in the discarded whey. It is hoped that a further study on whey composition will help to decide whether it is worthwhile or not to retain the nutrients present in whey.

The acceptance of a beany flavor is a matter of dietary adaptation. This conclusion was indirectly mentioned by Schroder and Jackson[2] in their studies on improving soybean flavor. They wrote: "Three samples of curd (2 tested portions of soybean cheese and one sample of Chinese soybean curd) were given to the panel members; 19 of 23 ranked the tested soybean cheese as the best, and only 4 ranked the Chinese sample as the best. All panel members of Oriental origin preferred the Chinese curd to the tested soybean cheese". The beany flavor can be masked by strong flavorings such as cinnamon, cocoa, vanilla, almond, etc., in sweet desserts, and by garlic, onion, dried shrimp, hot pepper, curry powder, celery, ginger, tomato sauce, etc. which are popular spices used in preparing tofu dishes.

DISCUSSION AND CONCLUSIONS

The factors that affect the soybean curd characteristics can be summarized as follows:

1. The varieties of soybeans and the concentration of soybean milk.
2. The pH value of the curd.
3. Temperature and heat duration.
4. Chemical and mechanical treatment of the soybean milk.
5. Ionic strength.
6. Presence of electrolytes, non-electrolytes or other substances.
7. Degree of hydration and dispersion of the protein.

Varieties of Soybeans and the Concentration of Soybean Milk.

The higher the concentration of soybean milk the stronger is the beany taste. This was detected by all six taste panels as indicated in the sensory score sheet (Table 6), although Table 5 does not show any significant difference. A plain curd was served for sensory evaluation, since this study was attempting to find the different characteristics between the two resulting curds which were prepared from G. D. L. and $CaSO_4$ precipitation. The varieties of soybeans and their composition had an effect on the qualities of soybean milk such as color, flavoring, solid matter, etc. Since the soybean milk is directly involved in soybean curd manufacturing, the varieties of soybeans can influence the quality of the soybean curd.

Markley[4] states that the major protein fractions of soybean protein are glycinin (78%), legumelin (1.5%), glutilin (7%), copper derivative of casein, lipoprotein and prolamin. Glycinin, a globulin-like protein, has an isoelectric point at pH 5.2, and can be precipitated by dilute acid at pH values from 5.2 to 5.7. His statement supports this study's use of G. D. L. as an acid coagulant.

Glycinin contains 5.1% carbohydrates which give viscosity upon heating and also contribute to the turbidity characteristic of soybean milk. Glycinin does not coagulate at the boiling point in a short period of heating. Legumelin and glutilin are heat-coagulable proteins; therefore both of them contribute to the gel formation of heated milk. It was suspected that the copper derivative of casein

could be precipitated by Ca^{++}, since calcium is more active than copper. Lipoprotein plays an important role in the formation of the protein-lipid complex of the three dimensional network of soybean curd, due to the surface-active function of lecithin present in lipoprotein. Prolamin contributes to the foaming characteristic of soybean milk during grinding and heating. In soybean milk processing, about 0.8% monoglyceride is used as antifoaming agent. Chen[5] (1975) reports that monoglyceride is a hydrophobic emulsifier which does not cause protein denaturation; the addition of 0.4% to 0.8% monoglyceride can inhibit the foaming which occurs in soybean milk; it can also increase the firmness of soybean curd.

Table 5 shows significant differences as the concentration of soluble solid in soybean milk increases. The dispersions tend to change from sol to gel upon heating; and therefore they give a stronger gel strength to the product. Table 2 and Table 3 also show the correlation that a more concentrated soy milk yields a greater amount of curd. Analysis of variance indicates that there are significant differences among both variables and replications ($F > 0.05$) of the yielding curd and the solid content in curd. The replication differences might be due to the error of using the volumetric method instead of the weighing method in measuring soy milk. Since the control of soy milk temperature is very important in the formation of soybean curd, the volumetric method of measuring soy milk would be a more efficient way of carrying out this study.

The pH Value

Table 4 indicates that the whey separated from G. D. L. precipitation has a lower pH value than that of the calcium sulfate precipitation. The result is coincident with Chen's experiment on soybean curd production[5]. The soybean milk prepared in this study had a pH of 6.8. Markley[4] states that the pH of soybean milk ranges from 6.7 to 7.0, depending much on the pH of the extracting water. He also points out that soybean protein at pH 5.4 has a higher N-content than that precipitated at pH 4.0. From previous studies he concludes that the isoelectric point of soy-protein is approximately 5.2. Acid-

precipitated soybean curd has its best quality at pH values from 5.4 to 5.6. Outside this range, a soft curd with poor water-holding capacity is produced. Calcium sulfate-precipitated curd has an optimum pH ranging from 6.4 to 6.8.

Different coagulants precipitate soybean milk in different pH ranges. Table 4 indicates that G. D. L. changes the pH of soybean milk from 6.8 to 5.4. Therefore one can conclude that the changing of pH brings about the precipitation of soybean milk. Calcium sulfate has very little effect on changing the pH value. On the contrary, it precipitates soybean milk by the chelating effect of metallic salts. Circle *et al.*[3] state, "Ca^{++} ions having amphoteric properties were better glutinizing agents than those of the strongly basic metals, the corresponding SO_4^{--} tending to exert an insolubilizing action on the protein." Since calcium sulfate is insoluble in water, it has to be mixed with 0.1% diluted soybean milk which acts as a nucleic coagulating agent. Circle[3] also comments: "Since the salt solutions themselves are neutral, the decrease in pH that follows the addition of soymilk to them must be the result of some interaction between the milk and the salt cation, leading to the liberation of H^+." Loeb[6] claims that at any given pH value the reaction between salts and proteins is stoichiometric, and is governed only by the valence of the ion having a charge opposite to that of the protein.

Therefore the concentration and the amount of the coagulant are determined by the pH value of soybean milk, by the pH value of the precipitant, and by the kind of coagulant.

Temperature and Heat Duration.

Previous studies indicate that heating causes a significant decrease in the beany flavor and inactivates the enzymatic reaction of native soybeans. Heating at a temperature above 75°C causes gelation of soy protein, which is related not only to the degree of hydration of the protein molecules, but also to an unfolding of the protein structure as it changes from globular to fibrous form. Disulfide bonds are an important factor in heat gelation. Intermolecular crosslinks formed by sulfhydryl-disulfide interchange may help stabilize the protein

network, thereby favoring other interactions required for gelation.

Circle[3] reports that the extent of denaturation of glycinin increased with the time of heating and the temperature, when glycinin was heated in water up to 100°C for periods up to 120 minutes. Nakamura[7] states "7-S protein (glycoprotein) of soy protein is sensitive to heating at higher ionic strengths, forming aggregates directly; whereas 11-S protein (pure globulin of soybean) is sensitive at lower ionic strengths, dissociating to subunits which partly form aggregates." The fact that 7-S protein cannot form a firm gel by G. D. L. after heating, and that 11-S protein can form a firm gel under reasonable heating, can probably explain why the optimum coagulating temperature for G. D. L. and $CaSO_4$ was 70°C to 80°C instead of the boiling temperature. This also can explain the differences between these two resulting curds.

The fragile body of soybean curd in this study was extremely sensitive to agitation. This characteristic facilitated the separation of the hot whey and hot curd. Pressing the curd while hot gave a curd with higher cohesiveness and a better compact texture, which is desired by the consumer. The high water content of the soybean curd provides a suitable environment for the growth of microorganisms, and hence becomes a nutritional health problem to be considered urgently in soybean curd production. It is hoped that further studies will deal with these problems.

REFERENCES

(1) Miller, Carey D., H. Denning, and A. Bauer, Retention of Nutrients in Commercially prepared Soybean Curd, *J. Am. Dietetics Association* (1952).

(2) Schroder, P. D. J., and H. Jackson, Preparation and Evaluation of Soybean Curd with Reduced Beany Flavor, *J. Food Science*, **37**, 450 (1972).

(3) Circle, S. J., E. W. Meyer, and R. W. Whitney, Effect of Heat and other Factors on Gelatin, *J. Am. Cereal Chem.*, **41**, 151-171 (1964).

(4) Circle, S. J., *Soybean and Soybean Products, Vol. I*, edited by K. S. Markley. Chapter VII Proteins and other Nitrogenous Constituents. (1952).

(5) Chen Gin-Mo, *Study on Manufacture of Instant Soybean Milk*, Food Industry Research Institute, Hsinchu, Taiwan, (1975).

(6) Loeb, J., *Proteins and the Theory of Colloidal Behavior*, Mc Graw-Hill, New York, (1922).

(7) Hashizume K., N. Nakamura, T. Watanabe, Influence of Ionic Strength on Conformation Changes of Soybean Protein Caused by Heating, *Agr. Biol. Chem.*, **39**(7), 1339-1347, (1975).

TEACHING

Perhaps teaching should be compared with the most difficult and unrewarding of all occupations, politics. In Winston Churchill's memoirs one of the most noteworthy points is that, in spite of half a century's experience and vast knowledge of history, Churchill never felt he could find a permanent answer to any problem. He could only produce temporary solutions; and hope for the best. That is true for teachers also. No solutions to any of our problem are permanent. Change and renewal are constantly necessary. We must incessantly re-examine our job and ourselves.

GILBERT HIGHET

EFFECTIVENESS OF FIVE LOCAL DETERGENTS: *A COMPARATIVE STUDY*

MARYTA LAUMANN, S. Sp. S.

ABSTRACT

Information on local detergent consumption patterns and laundry practices was obtained from 178 Taiwan households by means of a questionnaire consisting of 25 multiple-choice statements.

Based on the survey results as well as on pre-test experiments, relevant conditions for the experimental part of the study were determined. The factorial experimental design consisted of 120 different wash treatments with five replicates for each treatment. Factors investigated were: five detergent brands, four detergent concentrations, three water temperatures and two substrates. Tests were conducted with a standard Launder-Ometer and reflectance values on the two dependent variables, soil removal and whiteness retention, were obtained by means of a spectrophotometer. A complete analysis of variance by computer using a linear, additive, fixed effect model was made on each of the dependent variables for each of the substrates, proving all F-values to be significant at the 0.01 level.

Results indicated considerable differences in the effectiveness of some of the detergent brands on the two substrates. Detergency was best at the 2 g/l or 3 g/l, detergent concentration levels while the 1 g/l and 4 g/l levels proved highly inefficient. Twice as much and more soil was removed when washing the cotton substrate in warm and hot water as compared to cold water. The Dacron/cotton substrate also yielded significantly better performance results at warm and hot wash temperatures.

On the basis of the survey as well as the experimental results it was concluded—in the interest of economy and consumer satisfaction—that more adequate labeling of local laundry detergents should be provided, particularly as regards specific usage directions. Instead of "all-purpose detergents" only, the manufacture of differentiated laundry products was recommended.

INTRODUCTION

A brief tour through Taipei supermarkets and retail stores by the writer resulted in the discovery of fourteen available laundry detergents marketed under different brand names by eight local

manufacturers. All of them claimed directly or indirectly to be all-purpose detergents. Detergent package labels were found to be either totally absent or void of vital information. Ten of the plastic packages were not even labeled as to weight of content, thereby preventing the consumer from making any meaningful price comparisons. None of the plastic containers provided directions as regards proper quantity of detergent to be applied to a specified washload. The choice of appropriate water temperature in laundering was also generally ignored with the exception of one brand which stated that better results would be obtained when using warm water.

This fact-finding study tour, instigated by the complaints and inquiries about local laundry detergents from housewives, full-time laundry women, colleagues, students and friends, over many years, marked the beginning of a primary study on the problem in greater depth. Phase A of this study was to consist of a survey on detergent consumption patterns and laundry practices of Taiwan households. Phase B would make use of experimental procedures to compare the effectiveness of popular local detergent brands under varying conditions. The aim of the study would be to promote the rights of the local consumer — especially the right to information and to selection — and to raise the level of consumer satisfaction by providing factual knowledge on the performance of Taiwan-produced detergents.

The study presented here was initiated in the summer of 1976 and completed in April 1977.

PHASE A: SURVEY ON CONSUMPTION OF LOCAL DETERGENTS AND LAUNDRY PRACTICES

MATERIALS AND METHODS

A questionnaire consisting of a total of 25 multiple-choice questions was distributed to 300 students from three departments of Fu Jen University. Questions were aimed at giving insight into conditions such as households' consumption patterns, brand preferences, quantity of detergent used on a specified washload, temperature conditions, frequency of laundering, degree of satisfaction

with detergent in use, ownership of laundry equipment, etc. In addition, information on the general socio-economic standing of the 300 households was requested. To insure maximum standardization in the measurement of detergent amount a household would apply to a given washload, cooperating students were provided with a standardized measuring cup.

After a period of three weeks 178 questionnaires (59.5%) were returned. Responses were processed by the IMB 1130 computer at Fu Jen University for statistical treatment. Data were summarized, expressed in percentages and subjected to cross-table analysis.

RESULTS AND DISCUSSION

As many as 98.3% of the responding families indicated that they use laundry detergents. Among the 14 detergents listed in the questionnaire Bai-Lan (白蘭) was identified as the most popular brand with a market share of 56.9%, followed by Lan-Bao (藍寶) with 13.8%, Shr-Ba (世霸) 7.5%, Tai-Yang (太陽) 4.0% and Hsui-Jing (水晶) 3.4%. The market share of the remaining nine detergents, with the exception of Hwa-Su (花束), amounted to less than 2%.

Of the detergent-using households 62.1% admitted having "no real reason" for their particular choice of brand. They felt that available products were about the same in terms of cleaning efficiency and cost to the consumer. Inasmuch as all local laundry detergents are all-purpose detergents, are in most instances unlabeled as regards weight of content and fail to provide the consumer with product usage information, the above expressed attitude can hardly be surprising, for there is no factual basis on which to select or compare products.

Actual amounts of detergents used by local households for specified washloads and medium-sized washing machine capacity were determined on a volume as well as gram per liter basis. Results indicated remarkable differences. In terms of volume some families would use less than one cup while others would use as much as three or more cups for one and the same washload laundered under identical

conditions. In terms of detergent weight this variation ranges from 0.66 to 4.59 grams per liter of water. In short, the local detergent consumer seems highly uncertain as to the proper amount of detergent to use.

Moreover, considerable arbitrariness as regards adjustment of detergent amount to the composition of different types of washloads was observed. On the average, instead of decreasing the amount of detergent for washloads consisting of colored or wool-like articles as compared to the amount used for a washload consisting of pillow-cases, underwear and towels, the opposite behavior was followed. This arbitrariness on the part of local detergent users indicates that many consumers, in addition to being uncertain about the proper amount to be used for a given washload, also seem to lack basic knowledge of clothing care. The latter is the more serious inasmuch as locally sold textile and clothing articles frequently are unidentified as to fiber content and fabric finish and hardly ever carry labels giving instructions pertaining to laundry care.

Of the 124 households owning washing machines 83.9% also owned electric water heaters. Ownership of a water heater, however, had no effect on the water temperature used for laundering. As many as 88.1% of the 178 households did all their wash in cold water including washloads consisting of cotton underwear, bath towels and bedlinens. The following are some reasons that may be forwarded to explain this unexpected finding. (1) Traditionally, laundering was done along the riverside in cold, running water. (2) In general, people in Taiwan seem to be unaware of the benefits of improved cleanliness and sanitation derived from washing at warm or hot temperatures, particularly with clothing articles directly in contact with the human body. (3) Local detergent manufacturers neglect to provide detergent packages with instruction as to what temperature will yield best results under specified conditions.

Fifty-two families (30%) expressed dissatisfaction with the detergent in use. Lack of cleaning efficiency constituted the main complaint. Other complaints centered around fast deterioration of fabric, color loss, and inadequate labeling.

PHASE B: EXPERIMENTAL STUDY ON SOIL REMOVAL AND WHITENESS RETENTION ON COTTON AND DACRON/ COTTON AS A FUNCTION OF TEMPERATURE AND CONCENTRATION

MATERIALS AND METHODS

Based on the information and insights gained through the "Survey on the Consumption of Local Detergents and Laundry Practices" (Phase A of this study) as well as on results obtained from pretesting experiments (following directions of relevant test methods[1,2]) ex-experimental conditions and procedures for Phase B of this study were determined as outlined below.

The number of detergent brands to be subjected to instrumental testing was limited to the five with highest popularity scores: Bai-Lan, Lan-Bao, Shr-Ba, Tai-Yang and Hsui-Jing. In the absence of manufacturers' recommended detergent amounts to be used for a given washload, the following four experimental detergent concentrations were decided upon: 1 g/l, 2 g/l, 3 g/l and 4 g/l. The choice of these concentrations was considered realistic inasmuch as they represented the range of actual quantities used by local consumers. To adequately reveal the effect of temperature on cleaning efficiency of the chosen brands, three experimental temperature levels were employed: cold (21°C), warm (49°C) and hot (71°C). Two kinds of standardized carbon/oil soiled substrates, a 100% cotton percale test fabric and a Dacron 54 W/cotton shirting test fabric with a durable press finish, were used to reveal possible differences of brand effectiveness in relation to fabric composition. These two substrates were given preference because they represent the two most commonly used local fabrics and their soilings.

Each sample unit consisted of two parts of the same fabric: the soiled portion on which to measure detergent effectiveness in terms of soil removal* and the unsoiled portion (white) on which

* Soil removal is defined as the ability of a detergent to increase the reflectance of a soiled fabric through laundering.

to measure detergent effectiveness in terms of whiteness retention*. The size of each sample unit measured $4\frac{1}{2} \times 8\frac{1}{2}$ inches. Five replicas of each unit were considered sufficient. Accordingly, a total of 1200 test specimens (600 for each of the two fabrics) were subjected to testing procedures.

A standard Atlas Launder-Ometer, Model LHTP, was used to test-launder the properly prepared and identified fabric specimen. The apparatus rotates closed stainless steel cylinders in a thermostatically controlled water bath at 42 revolutions per minute. Sufficient abrasive action is obtained through the use of standard steel balls and minimum volume of wash solution. After proper temperature adjustment the test machine was loaded with twenty closed, 1200 ml steel cylinders, each filled with 50 ml test wash solution plus 100 steel balls and a single well-crumpled specimen. Using the program mode of operation, providing maximum control of temperature and time, the Launder-Ometer was activated for a duration of 12 minutes. This time span approximately equals that of one home or commercial machine wash cycle.

The test laundering cycle was followed by two 1-minute rinse cycles in the Launder-Ometer, each time using 500 ml of fresh 21°C $\pm$ 2°C tap water and 100 steel balls per specimen. After rinsing, specimens were properly dehydrated and air-dried at room temperature. Throughout the entire laundering period the degree of water hardness could be controlled between 148–150 ppm (considered moderately hard water) and the pH between 7.12 and 7.50.

The efficiency of the five detergent brands in removing soil from fabrics and retaining original fabric whiteness was determined on the basis of reflectance values obtained by means of a filter spectrophotometer (Kollmorgen Model KCS 11). A wave length of 560 millimicrons was employed, corresponding to the Y-filter of the instrument.

In setting up the experimental study and analysis of data,

* Whiteness retention is the ability of a detergent to maintain or restore the original reflectance of white textiles by preventing the redeposition of soil particles suspended in the wash or rinse water.

statistical procedures as outlined by Steel and Torrie[3] were followed. To permit comparison of several factors simultaneously, a completely random factorial design was used on each of the two substrates. Specifically, the design was a $5 \times 4 \times 3$ factorial with five replicates for each experimental unit. Reflectance readings taken by means of the filter spectrophotometer were converted into soil removal and whiteness retention values using appropriate formulas. Statistical computation was made by computer (Varian V 76) at Fu Jen University). A complete analysis of variance using a linear, additive, fixed effect model was made on each of the dependent variables and each substrate. F-values of the main effect of each single factor and of their interactions were all found to be significant at the 0.01 level.

RESULTS AND DISCUSSION

Overall Effect on Substrate

On the average, the soil removal achieved on the polyester/cotton fabric exceeds that obtained on the 100% cotton fabric by 13.53%. The comparatively higher degree of overall soil removal on the fabric blend may be explained by the differences in the physical structure of the two fibers involved. Cotton fiber with its hydrophilic surface and its flattened, twisted longitudinal structure provides comparatively better opportunity for soil particles to penetrate the interior of the fiber or hide in its configurations (Figs. 1–3).* According to Korella[4] the latter possibility is enlarged when fiber swelling due to absorbency of wash water occurs. The Dacron fiber with its smooth, hydrophobic surface and its rounded, even, straight longitudinal structure offers considerably less chance for soily substances to attach themselves intimately to the fiber (Figs. 4–6).* The permanent press finish applied to the Dacron/cotton blend, moreover, renders the 35% content of cotton fiber more soil resistant due to the resinous coating provided by the so-called "easy care" finish.

* Micrographs were taken with the scanning electron microscope of the Biology Department at Fu Jen University.

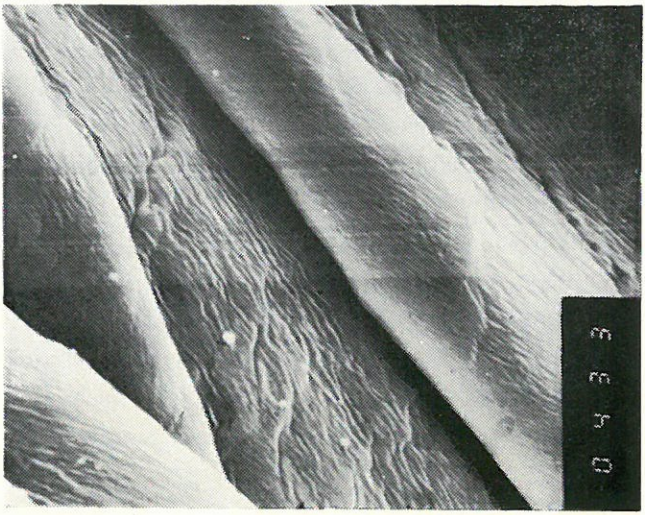

Fig. 1. Cotton Fiber (3000×): Scanning electron micrograph shows original i.e. unsoiled and unwashed fibers. Fiber surface indicates wrinkles and roughness; fiber structure is flattened, twisted and generally uneven.

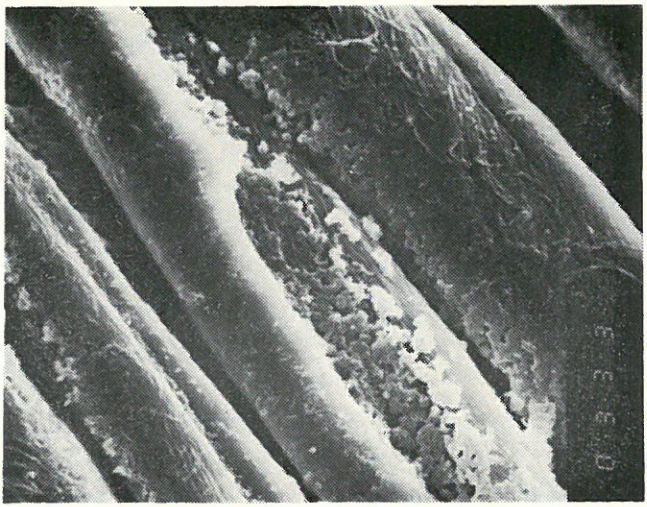

Fig. 2. Cotton Fiber (3000×): Scanning electron micrograph presents unwashed fiber, soiled with a carbon/oil mixture. Soil particles are seen to deposit preferably within the surface grooves and between fibers.

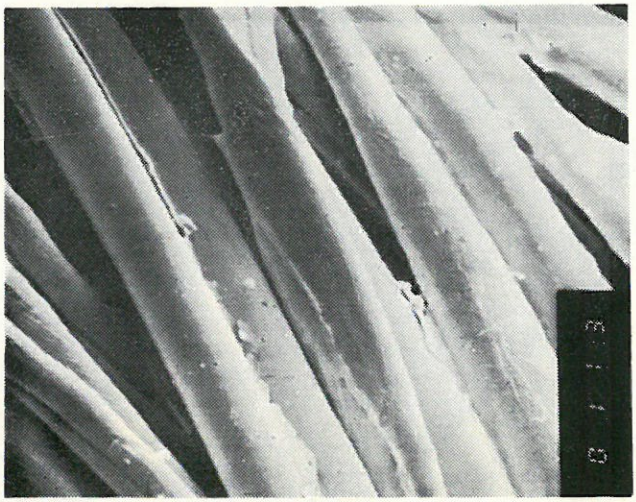

Fig. 3. Cotton Fiber (1000×): Scanning electron micrograph illustrates carbon/oil-soiled specimen after laundering. Fine soil particles still hide at places least exposed to the attack of detergents and the action of mechanical forces during the laundering process.

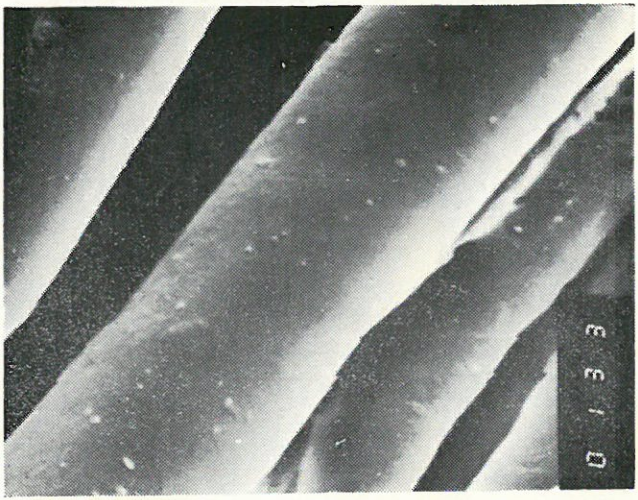

Fig. 4. Dacron Polyester Fiber (3000×): Scanning electron micrograph shows original i.e. unsoiled and unwashed fibers. Fiber surface is free from wrinkles; fiber structure is rounded, smooth and even.

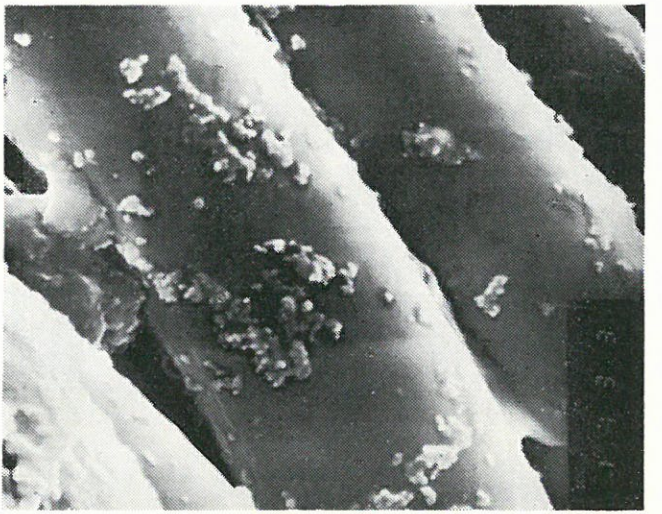

Fig. 5. Dacron Polyester Fiber (3000×): Scanning electron micrograph depicts unwashed fiber, soiled with a carbon/oil mixture. Soil particles are seen to attach themselves more superficially to the fiber in comparison to the cotton fiber (Figure 2).

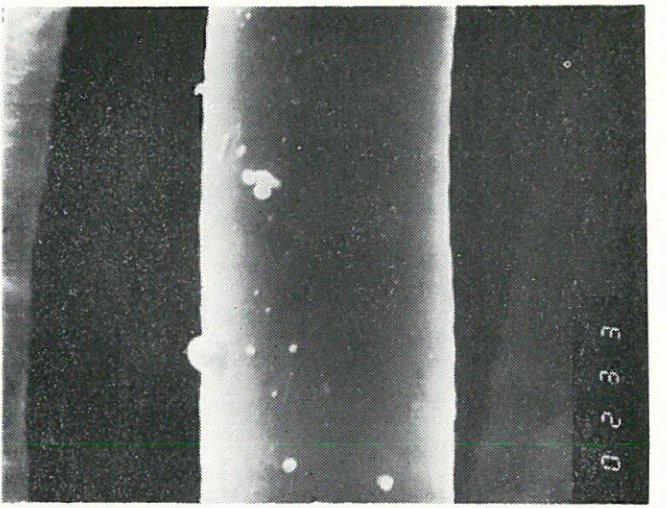

Fig. 6. Dacron/Cotton Blend (3000×): Scanning electron micrograph presents carbon/oil-soiled specimen after laundering. Oily soil particles are still visible on the fiber surface.

Effect of Detergent Brand

Comparative overall soil removal differences among the five detergent brands ranged from 0.2% to 3.3% for cotton and from 1.0% to 6.4% for Dacron/cotton, while overall whiteness retention differences ranged from 1.6% to 2.5% for cotton and 0.3% to 1.4% for the synthetic blend. Since the choice of detergents was based on popularity ranking, which in itself constitutes a kind of performance evaluation relying on experience, no extreme differences in effectiveness between the five detergents were expected. Differences in soil removal of $\pm 1\%$ were judged discernible in daylight with the unaided human eye. However, even differences amounting to less than 1% should not be easily dismissed as unimportant inasmuch as laundering is a process to be repeated many times and differences initially judged undiscernible eventually accumulate into noticeable effects.

As regards the comparative effectiveness of individual detergents in relation to the two substrates, some of the brands were seen to perform considerably better on the 100% cotton fabric while others were more effective on the synthetic blend (Fig. 7). Bai-Lan was found to have best overall effectiveness in terms of soil removal as well as whiteness retention on both kinds of test fabric. Lan-Bao, poorest performer on cotton, took a clear second rank as regards performance on Dacron/cotton, thereby supporting the popularity ranking it had received based on survey results. Bai-Lan maintained its leading position at each of the practically conclusive three-factor interactions — except for soil removal on cotton on which Shr-Ba took the lead (Fig. 8, 9).

Although all of the five detergents claim to be all-purpose detergents, it is evident from the findings expressed in the preceding paragraphs that detergent effectiveness is related to fabric composition. There is a need, therefore, for more explicit detergent labeling indicating on which type of fabric a given detergent will perform most successfully. The findings also indicate the desirability of the manufacture of other than all-purpose detergents which so far are practically non-existent in Taiwan.

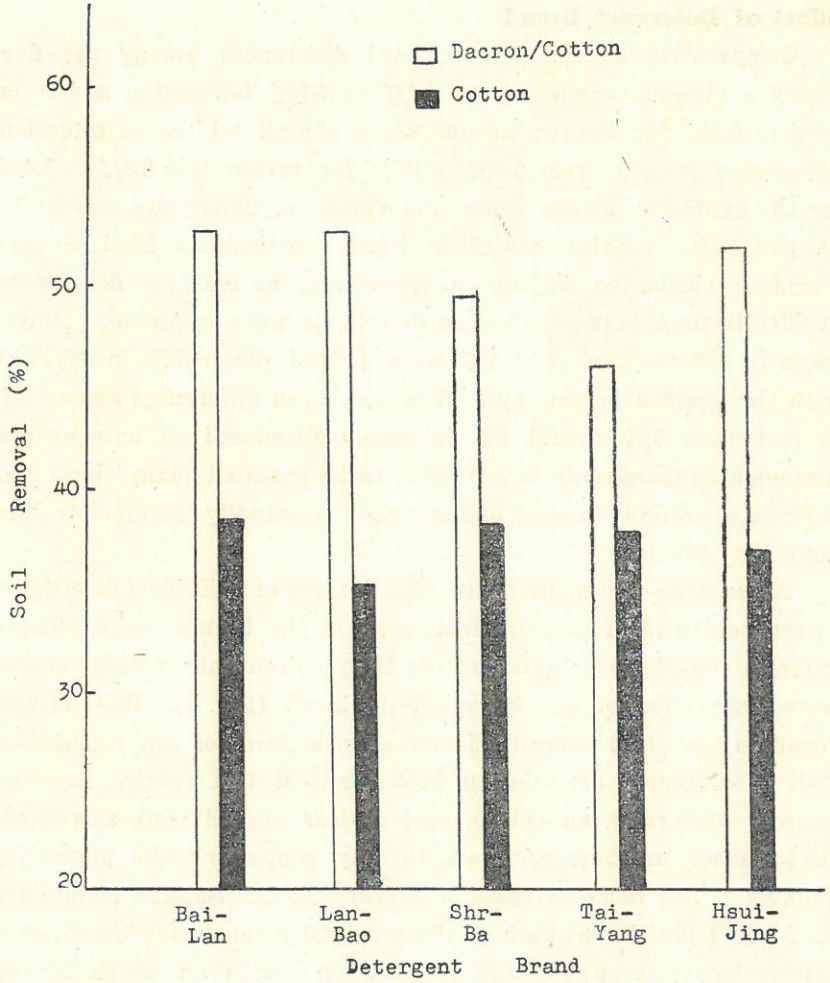

Fig. 7. Overall Effect of Detergent Brand on Soil Removal from Dacron/Cotton as Compared to Soil Removal from 100% Cotton at Average Detergent Concentration and Temperature.

Effect of Detergent Concentration

Best overall detergency in terms of soil removal as well as whiteness retention was achieved when using a 2 g/l detergent concentration both on cotton and on Dacron/cotton (Fig. 10). The 1 g/l concentration level resulted in an overall soil removal decrease

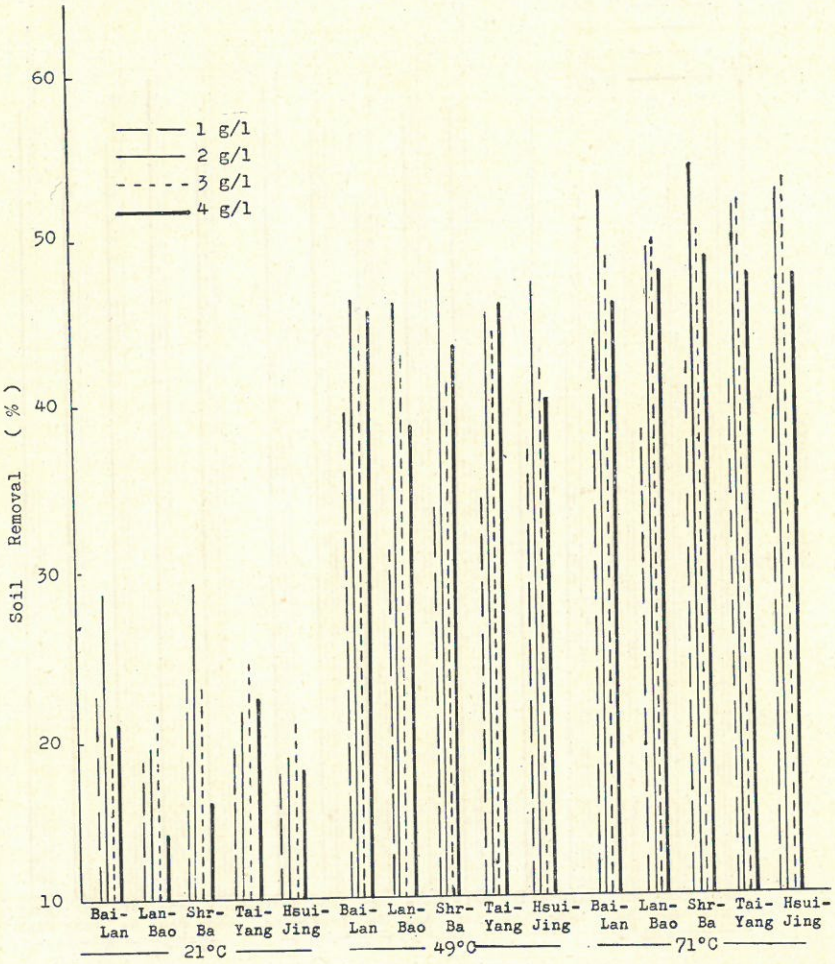

Fig. 8. Percent Soil Removal on Cotton Fabric by Individual Detergents at Specific Levels of Detergent Concentration and Temperature.

of as much as 9.2% on cotton and 20.7% on Dacron/cotton. Contrary to the assumption of many a local detergent user that better soil removal results are guaranteed with the use of more detergent, a soil removal decrease, as much as 5.3%, was registered for both test fabrics at the 4 g/l level as compared to soil removal at the 2 g/l level—a striking indication of the wastefulness and counter-productivity involved in the use of excessive amounts of detergent. On

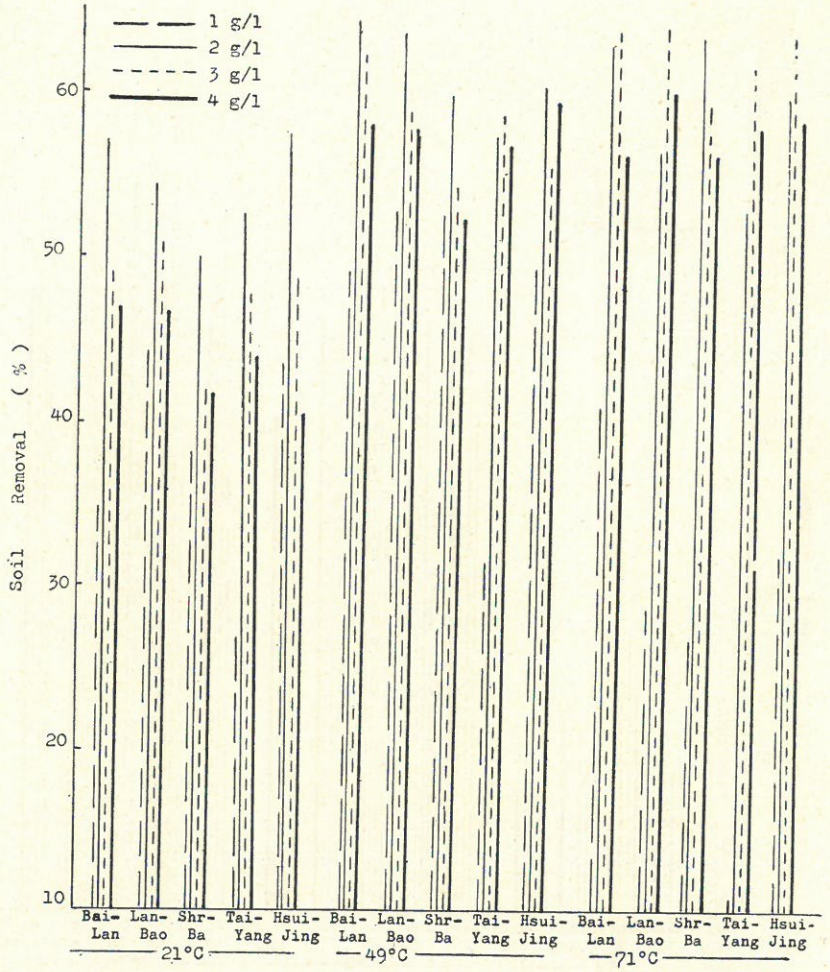

Fig. 9. Percent Soil Removal on Dacron/Cotton Fabric by Individual Detergents at Specific Levels of Detergent Concentration and Temperature.

the specific, practically interesting three-factor interaction level, Tai-Yang and Hsui-Jing yielded best results at the 3 g/l concentration level, while Bai-Lan and Shr-Ba produced considerably better results at the more economical 2 g/l level on both substrates. Lan-Bao slightly excelled at the 3 g/l level (Fig. 8, 9).

On the average, whiteness retention on cotton and Dacron/cotton increased with increasing detergent concentration. Since, however,

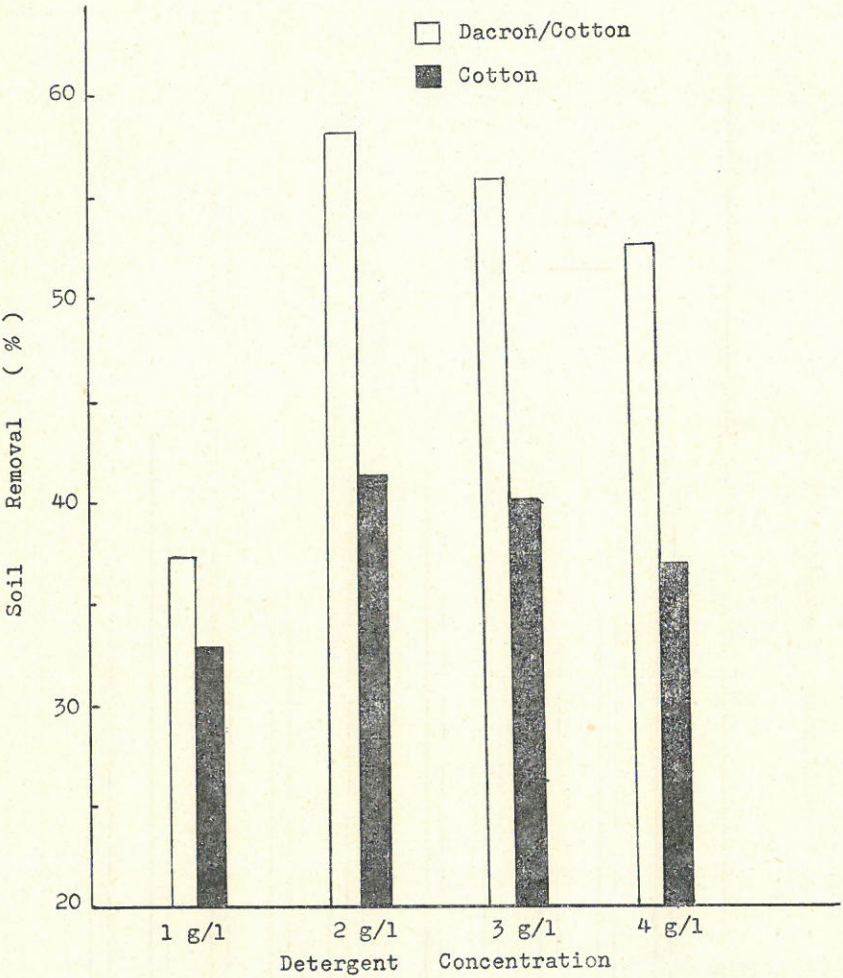

Fig. 10. Overall Effect of Detergent Concentration on Soil Removal from Dacron/Cotton as Compared to Soil Removal from 100% Cotton by the Average, Popular Detergent at Average Temperature.

soil removal at the 1 g/l and 4 g/l was found unsatisfactory, these two levels were considered of no further interest in relation to results obtained on whiteness retention. The three-factor interaction revealed that on cotton best whiteness retention was achieved at the 3 g/l level while on Dacron/cotton best results were observed at the 2 g/l level, except for Bai-Lan (Fig. 11, 12).

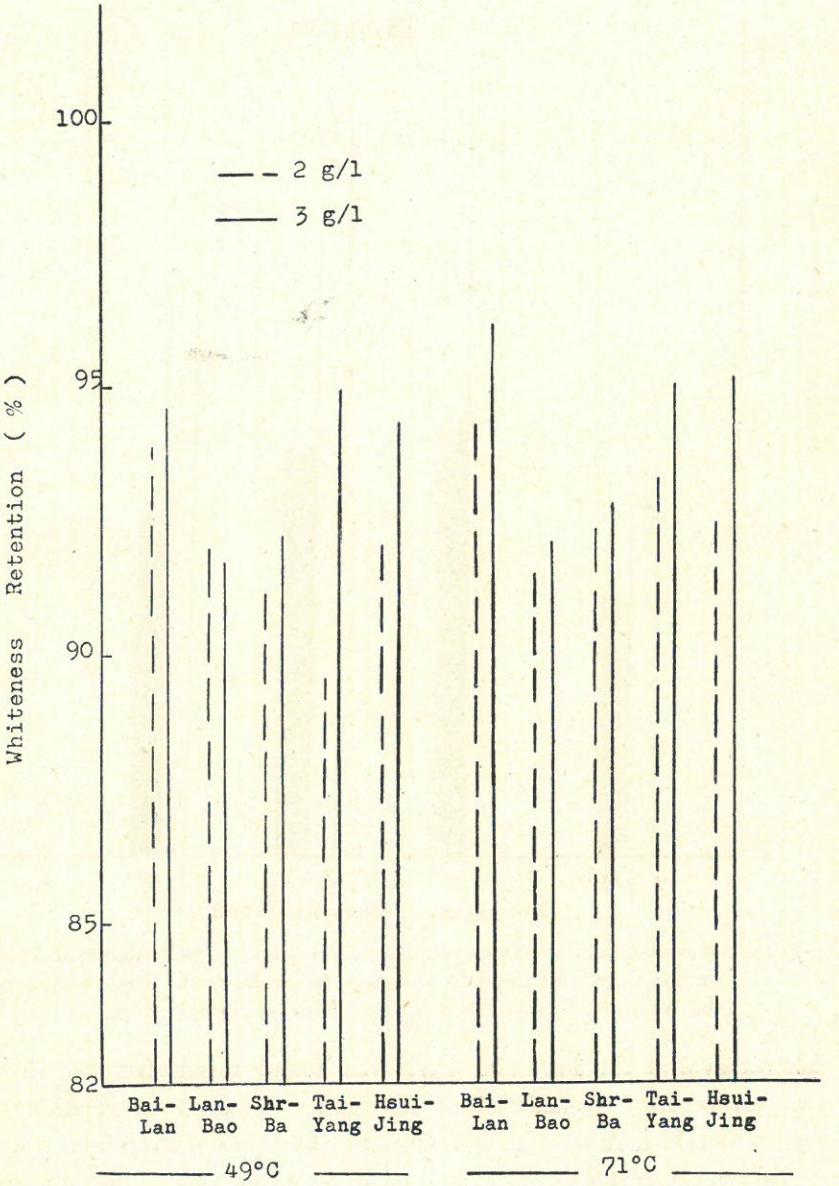

Fig. 11. Percent Whiteness Retention on Cotton Fabric by Five Detergents at Specific Levels of Detergent Concentration and Temperature.

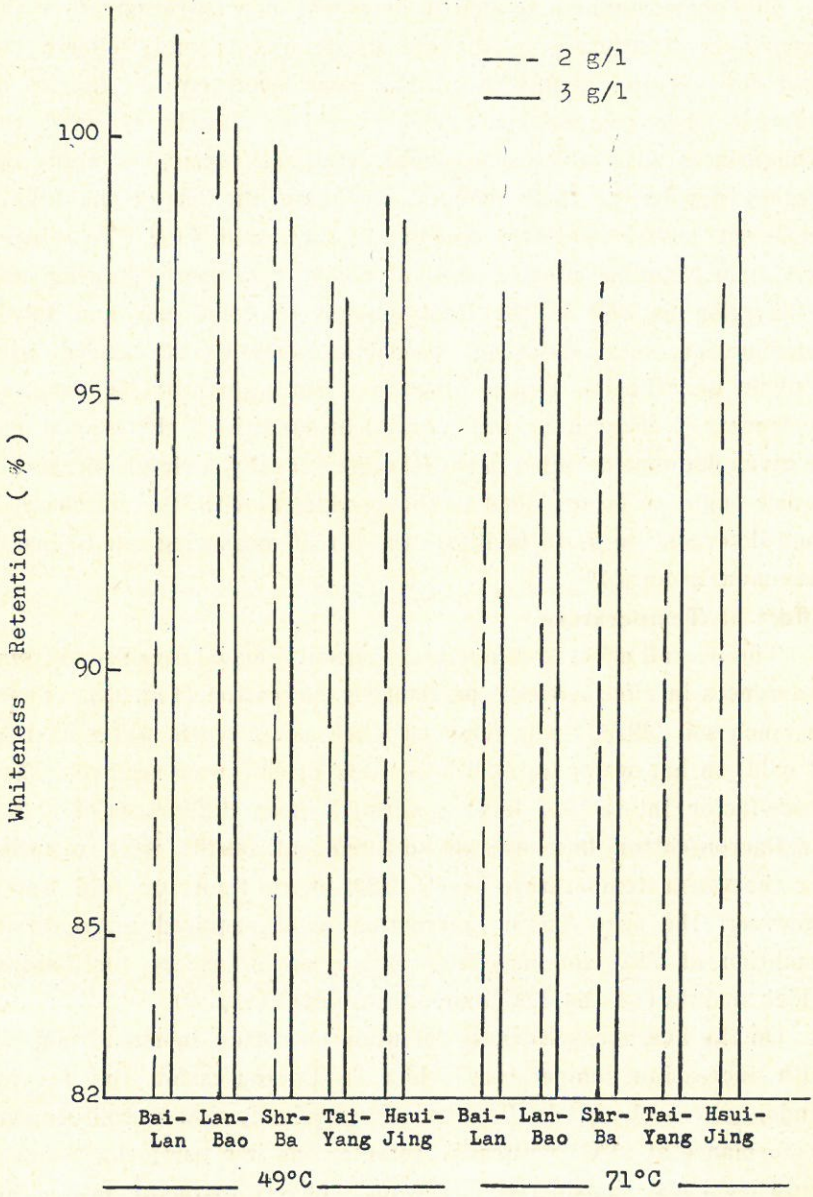

Fig. 12. Percent Whiteness Retention on Dacron/Cotton Fabric by Five Detergents at Specific Levels of Detergent Concentration and Temperature.

The above findings related to detergent concentration prove the importance of accuracy in the use of detergents and indicate the need for varying quantities of the same detergent on fabrics of different fiber composition. Survey results clearly revealed the arbitrariness with which many local detergent consumers apply detergent powder to their laundry, including the use of the highly inefficient and/or wasteful amounts of 1 g/l and 4 g/l. To achieve maximum cleaning effectiveness, economy, consumer education and satisfaction as well as the least amount of color loss and fabric deterioration, local detergent products ought to be labeled with explicit quantitative usage directions. Since quantitative usage of detergents is affected by water hardness conditions, this should also be given due consideration in the labeling. Ideally, a simple measuring device ought to be provided to the consumer with the purchase of each detergent so as to facilitate the act of measuring and to insure maximum accuracy.

Effect of Temperature

The overall effect of temperature on soil removal revealed extreme differences in effectiveness, particularly on cotton (Fig. 13). Twice as much soil (42.3%) was removed when using warm water instead of cold; in hot water an additional 6.9% of soil was removed. The three-factor interaction level confirmed these differences (Fig. 11). On Dacron/cotton best overall soil removal results were recorded for the warm temperature level; 9.2% more than for cold water. However, the three-factor interaction level required an optimum condition of 71°C for maximum soil removal, except for Bai-Lan which maintained the 49°C temperature level (Fig. 9).

On the average, whiteness retention on cotton increased slightly with increasing temperature while on Dacron/cotton the reverse tendency was observed. Because of remarkably lower soil removal performance at 21°C, whiteness retention at this particular temperature level was considered irrelevant. The three-factor interaction more specifically confirmed that on cotton best whiteness retention results were achieved at 71°C — except for Lan-Bao which at the 2 g/l performed better at 49°C. Results on Dacron/cotton also con-

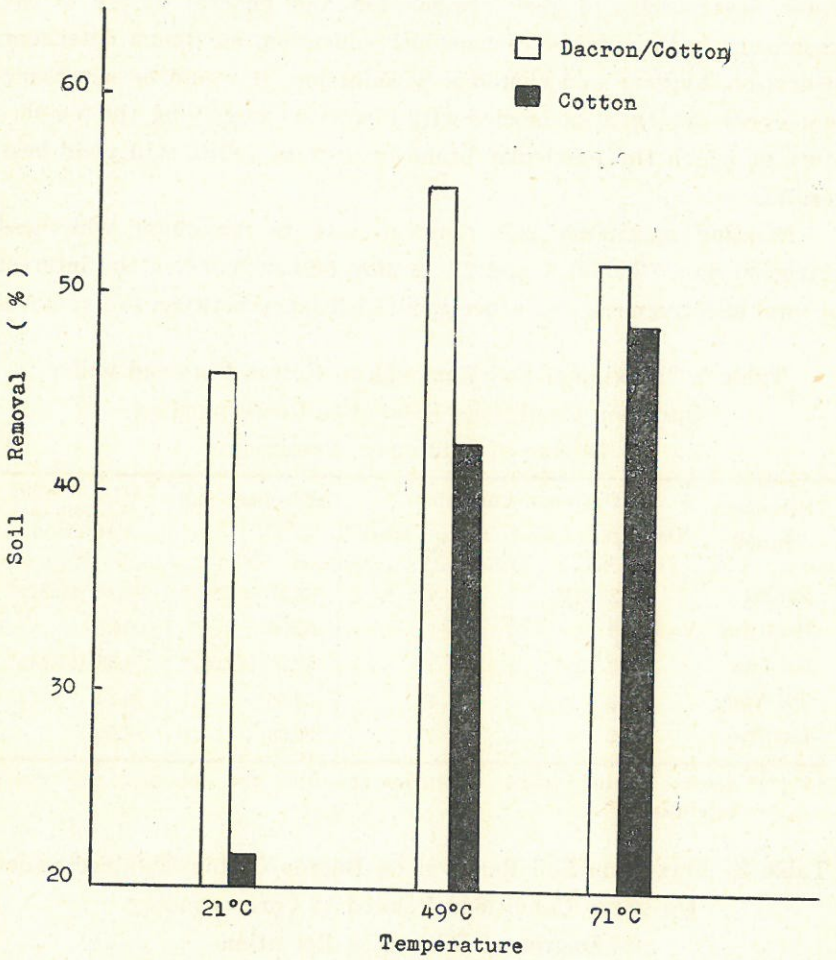

Fig. 13. Overall Effect of Temperature on Soil Removal from Dacron/Cotton as Compared to Soil Removal from 100% Cotton by the Average, Popular Detergent at Average Detergent Concentration.

firmed the general tendency of best whiteness retention at 49°C with the exception of Tai-Yang, which at the 3 g/l level performed better at 71°C (Fig. 12).

The experimental results on temperature constitute a very significant finding in the local context inasmuch as survey results indicated that as many as 82.1% of local households wash in cold

water, irrespective of fiber composition and general nature of the washload. In the interest of consumer education, maximum detergent utilization, hygiene and customer satisfaction, it would be necessary that every detergent be labeled with directions specifying the temperature at which the particular brand on a given fabric will yield best results.

Relating maximum soil removal data to maximum whiteness retention data (Tables 1 and 2), it may be concluded in the interest of total effectiveness, i. e., a preferential balance between soil removal

Table 1. Maximum Soil Removal on Cotton Obtained under Optimum Conditions Related to Corresponding Degree of Whiteness Retention

Detergent Brand	Optimum Conditions		Maximum Soil Removal %	Corresponding Whiteness Retention %
	Detergent Conc. g/l	Temperature °C		
Shr-Ba	2 (3)*	71	54.41 (52.36)*	92.33 (92.93)*
Hsui-Jing	3	71	53.90	95.27
Bai-Lan	2 (3)*	71	52.74 (49.09)*	94.35 (96.24)*
Tai-Yang	3	71	52.36	95.23
Lan-Bao	3	71	50.08	92.05

( )* values obtained under optimum condition for maximum whiteness retention

Table 2. Maximum Soil Removal on Dacron/Cotton Obtained under Optimum Conditions Related to Corresponding Degree of Whiteness Retention

Detergent Brand	Optimum Conditions		Maximum Soil Removal %	Corresponding Whiteness Retention %
	Detergent Conc. g/l	Temperature °C		
Bai-Lan	2 (3)*	49	64.97 (61.48)*	101.51 (101.77)*
Lan-Bao	3 (2)*	71 (49)*	64.01 (63.07)*	97.88 (100.56)*
Shr-Ba	2	71 (49)*	63.15 (59.71)*	97.15 (99.83)*
Hsui-Jing	3 (2)*	71 (49)*	62.66 (59.90)*	98.41 (98.92)*
Tai-Yang	3	71	61.45	97.65

( )* values obtained under optimum condition for maximum whiteness retention

and whiteness retention, that on cotton 71°C constitutes the optimum temperature condition for all five detergent brands. On Dacron/cotton the optimum temperature is 49°C for Bai-Lan, Lan-Bao and Hsui-Jing. Tai-Yang needs 71°C and Shr-Ba a temperature between 49°C and 71°C, probably close to 60°C.

As regards optimum detergent concentration on cotton, Lan-Bao, Tai-Yang and Hsui-Jing achieved highest total effectiveness at 3 g/l. Bai-Lan seems to require slightly more than 2 g/l and Shr-Ba about 2.5 g/l. On Dacron/cotton the 2 g/l level is considered the preferable condition for four of the tested detergent brands while Tai-Yang requires 3 g/l for maximum total effectiveness.

RECOMMENDATIONS FOR FURTHER RESEARCH

Since this paper reports the findings of a primary experimental investigation on the effectiveness of local detergents, it can only provide an initial contribution to the improvement of local detergent consumption and labeling. Following are some examples of further studies that need to be undertaken.

Experiments in this study utilized water of medium hardness. In order to provide precise and adequate quantitative detergent labeling for the entire range of water hardness degrees in Taiwan, further experimentation with soft and hard water is to be done.

In order to translate the findings of this study into locally relevant label directions, it is necessary to determine the relationship between the Launder-Ometer used in this study and the actual local washing machine.

The study of redeposition or whiteness retention requires that the contribution of optical brighteners to whiteness be excluded in the measurement of reflectance. Since, however, detergent users judge white fabrics in terms of total brightness, further studies ought to give consideration to this factor. Some of the five brands claimed to contain optical brighteners.

Soil removal and whiteness retention values provide but a limited measure of detergent effectiveness. Further research needs to be done on the damaging effects of local detergents such as fiber

deterioration, color loss and shrinkage after repeated launderings and under the influence of varying conditions of temperature and detergent concentration.

Experimental studies on substrates of fiber composition and soilings different from those used in this study would be desirable.

To more objectively evaluate the comparative effectiveness of local detergents, it would be necessary to include well-known foreign products and/or a standard detergent such as the AATCC standard detergent in the experimental comparison.

REFERENCES

(1) American Association of Textile Chemists and Colorists (AATCC), Test Method 61-1975, *Technical Manual*, 153-154, (1975)
(2) Brüschweiler, Methods of Testing the Performance of Washing Machines and Detergents, *Tenside* **5**, 229-237, (1973)
(3) Steel, R.G. and J.H. Torrie, *Principles and Procedures of Statistics*, 194-230, (1960)
(4) Korella, K., *ABC der Wäschepflege*, **15**, (1967)

CONTRIBUTORS TO THIS NUMBER

Yi-Ching Yen 顏一清 is professor of mathematics at Fu Jen University.

Tsing-Jen Ho 何清人 is associate professor of mathematics at Fu Jen University.

Fong-Jen Lin 林豐仁 is associate professor of physics and acting chairman of the Department of Electronic Engineering at Fu Jen University.

John R. Koster, SVD, is professor of physics at the University of Ghana, West Africa, and visiting professor of physics at Fu Jen University.

Jih-Yung Chao 趙寄蓉 is associate professor of chemistry at Fu Jen University.

Chu-Fang Lo 羅竹芳 is associate professor of biology at Fu Jen University.

Franz Huber, SVD, 扈伯爾 is professor and head of the Department of Biology at Fu Jen University.

Ching-Min Tsai 蔡敬民 is associate professor of nutrition and food science at Fu Jen University.

Wen-Li Jwuang, SSPS, 莊文孋 is lecturer in home-economics at Fu Jen University.

Maryta Laumann, SSPS, 羅麥瑞 is associate professor and head of the Department of Textiles and Clothing at Fu Jen University.

PRINTED BY

Ching Hua Press Co., LTD., Taipei